An investigation of some scanner and film characteristics to improve the effective use of radiochromic film for radiotherapy dosimetry

Tarafder Jahangir Shameem

A thesis submitted in
fulfillment of the
requirements of the degree of

Doctor of Philosophy

THE UNIVERSITY OF SYDNEY

Faculty of Science

The University of Sydney

2025

Statement of Originality

I hereby declare that this submission is my own work and that, to the best of my knowledge and belief, it contains no material previously published or written by another person nor material which to a substantial extent has been accepted for the award of any other degree or diploma of the University or other institute of higher learning, except where due acknowledgement has been made in the text.

Tarafder Jahangir Shameem

Date : 15 August 2025

Statement of using generative AI

No content produced by generative AI tools has been used in the preparation of this thesis

Tarafder Jahangir Shameem

Date : 15 August 2025

Abstract

Radiochromic film as a radiotherapy dosimeter offers some distinct advantages such as high resolution, near tissue equivalence and weak energy dependence. In addition, its small thickness and planar resolution make it very suitable for measuring complex radiation dose distributions, such as IMRT and VMAT plan verification, which requires dose distribution information in different planes. However, the read-out process, which is normally done by optical scanning of the films is not straight-forward, which limits the use in clinical practice. The main problem with scanning radiochromic film for dosimetry is the systematic artefacts, which result from two sources. The first is associated with the film itself, which results from the active ingredient shape, size and orientation. The other is from the flatbed scanners, which are used widely for digitising the irradiated film.

The active ingredient of the most widely used radiochromic film, known as Gafchromic film, is LiPCDA, which traditionally forms crystals of 15 μm in length and 2 μm in diameter. These rod-like crystals induce anisotropic scattering and light polarisation which in turn are partly responsible for the two major artefacts, the orientation effect and the lateral response artefact (LRA) effect. Upon irradiation the active ingredient bonds with other neighbouring monomers to form polymers which increases these effects. As part of the continuous improvement of the range of Gafchromic films, their designs have variously reduced the crystal size to 4 μm x 2 μm, changed the emulsion to reduce signal to noise ratio and added an inhibitor to reduce the size of polymer upon irradiation. Two novel films (EBT-4 and MD-V3) have been comparatively characterised in this work against two established films (EBT-3 and EBT-XD), to provide quantitative data on their performance and on selection for different applications. Smaller crystal size is shown to reduce the LRA effect and adding bonding inhibitor made LRA independent of dose given to the film. Based on the findings, recommendations are made on optimal choice of films for different radiotherapy dose ranges. EBT4, with improved signal to noise ratio over EBT3, is a better choice for standard dose ranges, with extra care to be taken on maintaining the same post irradiation time gap between irradiation and scanning for both calibration film and experimental verification or QA films. MD-V3 showed improvement over EBT-XD films, especially in terms of reduced dose dependence of LRA compared to other radiochromic films.

The construction and components of the digitising flatbed scanners also contribute towards the artefacts, requiring strict read-out protocols and corrections. Different scanner makes and models have different degrees of such contributions. Epson scanners are the most popular and widely used for radiotherapy film dosimetry. Different models use different light sources, different lenses and different mirror systems. Two A4 Epson scanner models, V700 and V800,

were compared for several characteristics, which were shown to be different, making these not interchangeable. The contribution of three scanner components, the lens system, mirror system and scanner bed, to LRA effect and light polarisation were investigated, using films irradiated mainly with 6 MV X-rays. Firstly, the scanner bed contribution was found to be negligible if the refractive index of the material is similar to that of film. Secondly, Epson V700 scanners use a wide-angle lens, having a focal length of 38 mm, to keep the lens close to the mirror system, to keep the dimensions of the scanner small. Because of this, the lens cannot capture all the light from the furthest ends of the mirror, which contributes to the LRA effect. Lenses with different focal lengths were investigated, using a direct digital camera approach, and a lens with 50 mm focal length was found to be a good compromise between reducing the LRA effect and distance needed to place the lens from the film and/or mirror. For example, LRA was reduced from about 8% to about 2% for a film irradiated by 5.6 Gy. The distance needed from film to lens was 500 mm for this lens. Thirdly, the mirror system introduces light polarisation which in turn contributes to the LRA effect. Depending on model, Epson scanners use four or five mirrors to guide the light from the source passing through the film to the lens and sensor. The number and orientation of mirrors was investigated to consider whether reducing the number of mirrors would reduce the light polarisation. Using only one mirror or no mirrors (direct digital camera only) reduces the light polarisation from about 10% to about 2% for a film irradiated with 5.6 Gy.

This work has demonstrated that a modified scanner with one mirror or no mirrors and a direct digital camera read-out system with lens of 50 mm focal length would improve the film dosimetry significantly, reducing the artefact corrections and associated film dosimetry uncertainties, but would be likely to make the scanner bulkier. Future work on development of films and modified scanner designs could aim to take this further to give LRA levels that need no correction factors.

Contribution of Collaborators

This thesis contains 3 published papers and one accepted paper. Each of these studies was originated, designed, performed and written by the candidate Tarafder Jahangir Shameem.

The candidate performed all the experimental works, collection and analysis of data, wrote the manuscripts and was the primary author through the review process for all four papers.

David Thwaites, Martin Butson and Nick Bennie were the supervisors and they reviewed and provided constructive feedback for all four papers.

Tarafder Jahangir Shameem

As supervisor for the candidature upon which this thesis is based, I can confirm that the authorship attribution statements above are correct.

Professor David Thwaites

Acknowledgment

Undertaking this thesis has been a long process and could not have been completed without support from many people around me. My sincerest thanks to my supervisors David Thwaites, Martin Butson and Nick Bennie. They have been very supportive, understanding and encouraging, as needed to keep me on track. Their mentorship and guidance made it possible to undertake part-time study with clinical medical physicist duties and helped me focus to complete the thesis.

Thanks to my wife for supporting, encouraging and appreciating the whole process from starting the project up to the finishing the thesis.

Thanks to my parents without whom I would not be in the position I am right now. My late father and my mother, who now has dementia, would be so proud. They always had faith in me, maybe more than I have for myself.

Thanks to my uncle Mahbubur Rahman who always encouraged me and enquired about progress all the time.

My special thanks to Elekta engineer Adam Kerr who went above and beyond to help me make some equipment needed for some experimental work for the thesis.

I also acknowledge that “This research was supported by an Australian Government Research Training Program (RTP) Scholarship”

Table of Content

List of Figures

List of Tables

List of Abbreviations

AAARA	As Accurately As Reasonably Achievable
AAPM	American Association of Physicists in Medicine
CCFL	Cold Cathode Fluorescent Light
CMOS	Complementary Metal-Oxide Semiconductor
CT	Computer Tomography
DET	Double Exposure Technique
DNA	Deoxyribonucleic Acid
DSLR	Digital Single Lens Reflex
DVH	Dose Volume Histogram
EPA	Environment Protection Authority
EPID	Electronic Portal Imaging Device
EVA	Ethylene-Vinyl Acetate
FFF	Flattening Filter Free
HDR	High Dose Rate
IAEA	International Atomic Energy Agency
ICRU	International Commission on Radiation Units and measurements
IMRT	Intensity Modulated Radiotherapy
JPEG	Joint Photography Experts Group
KV	Kilo Voltage
LED	Light Emitting Diode

LINAC	Linear Accelerator
LP	Laminating Pouch
LRA	Lateral Response Artefacts
MET	Multiple Exposure Technique
MLC	Multi-Leaf Collimator
MU	Monitor Unit
MV	Mega Voltage
OAR	Organ At Risk
LiPCDA	Lithium Pentacosa Diynoic Acid
PMMA	Polymethyl Methacrylate
PMT	Photo Multiplier Tube
PV	Pixel Value
QA	Quality Assurance
RGB	Red, Green, Blue
ROI	Region Of Interest
RT	Radiotherapy
SABR	Stereotactic Ablative Body Radiotherapy
SBRT	Stereotactic Body Radiotherapy
SD	Standard Deviation
SGRT	Surface Guided Radiotherapy
SNR	Signal to Noise Ratio
SRS	Stereotactic Radio Surgery

SSD	Source to Surface Distance
TIFF	Tagged Image File Format
TPS	Treatment Planning System
VMAT	Volumetric Modulated Arc Therapy

Research Publication

1. Shameem, T., Bennie, N., Butson, M. and D. Thwaites. Comparative characterisation of different types of Gafchromic films for radiotherapy use. *Phys Eng Sci Med* (2025). https://doi.org/10.1007/s13246-025-01596-0

2. T. Shameem, N. Bennie, M. Butson, and D. Thwaites, "A comparison between EPSON V700 and EPSON V800 scanners for film dosimetry," *Phys Eng Sci Med*, vol. 43, no. 1, pp. 205–212, 2020. https://doi.org/10.1007/s13246-022-01136-0

3. T. Shameem, N. Bennie, M. Butson, and D. Thwaites, "Effect of scanner lens on lateral response artefact in radiochromic film dosimetry," *Physical and Engineering Sciences in Medicine*, vol. 45, pp. 721–727, 2022. https://doi.org/10.1007/s13246-022-01136-0

4. T. Shameem, N. Bennie, M. Butson, and D. Thwaites, "Effect of mirror system and scanner bed of a flatbed scanner on lateral response artefact in radiochromic film dosimetry," *Physical and Engineering Sciences in Medicine*, vol. 47, pp. 1651–1663, 2024 https://doi.org/10.1007/s13246-024-01478-x.

1 Introduction

1.1 What is radiotherapy trying to achieve

Ionizing radiations, i.e. those with sufficient energy interactions to enable removal of electrons from an atom or molecule, are used in radiation therapy for cancer patients for identifying, localising and treating tumours. Both low and high energy photons are used for imaging and treatment, high energy electrons are used for treatment only, and other particles are also used for treatment, with most treatments being carried out with high energy photons. More than 50% of cancer patients undergo radiation therapy [1], for eradication or control of cancer or palliation of symptoms. The technical aim of the radiation therapy process is to deliver a very accurate dose to a well-defined target, i.e. cancerous tumour, while sparing or giving minimum dose to the surrounding normal tissues. This results in control or removal of disease, longer life and/or improved quality of life [2].

Ionizing radiation specifically induces damage in critical molecules within the cells, such as DNA (deoxyribonucleic acid), makings those molecules unstable. These in turn react in ways that prevent them functioning and dividing properly and eventually causes cell death. There are three possible outcomes that may result from an interaction of ionising radiation with a cell. The cell may repair the damage, the cell may survive with a mutation, or the cell may die [3] Normal tissue repair capability is greater than that of tumour cells [3], which results in the higher probability of death of tumour cells than that of normal tissue. The probability of biological effects versus dose is generally described by dose response curves having a sigmoid shape (Figure 1-1), where there is no effect below a threshold dose, then a gradually increasing effect with increasing dose, followed by the effect rising sharply and finally levelling off to a plateau, often of full (100%) effect at high enough doses. Because of having greater repair capability and because radiotherapy targeting of the tumour aims to spare normal tissue as much as possible, normal tissue damage is typically less than that of tumour cells for the same dose delivered, which results in the dose response curve of tumours being to the left (lower dose) of that for normal tissue. The general aim of radiotherapy is to exploit this for an optimum dose that maximises tumour control with minimum normal tissue damage. Figure 1-1 shows schematic dose response curves, which are different for different tissues, where in this example a dose of 50 Gy will cause 95% probability of tumour control and 5% probability of normal tissue damage. Optimising treatment planning for individual patients, and also many advances in radiotherapy treatments and methods, aims to maximise eradication of tumour cells and minimise the normal tissue damage.

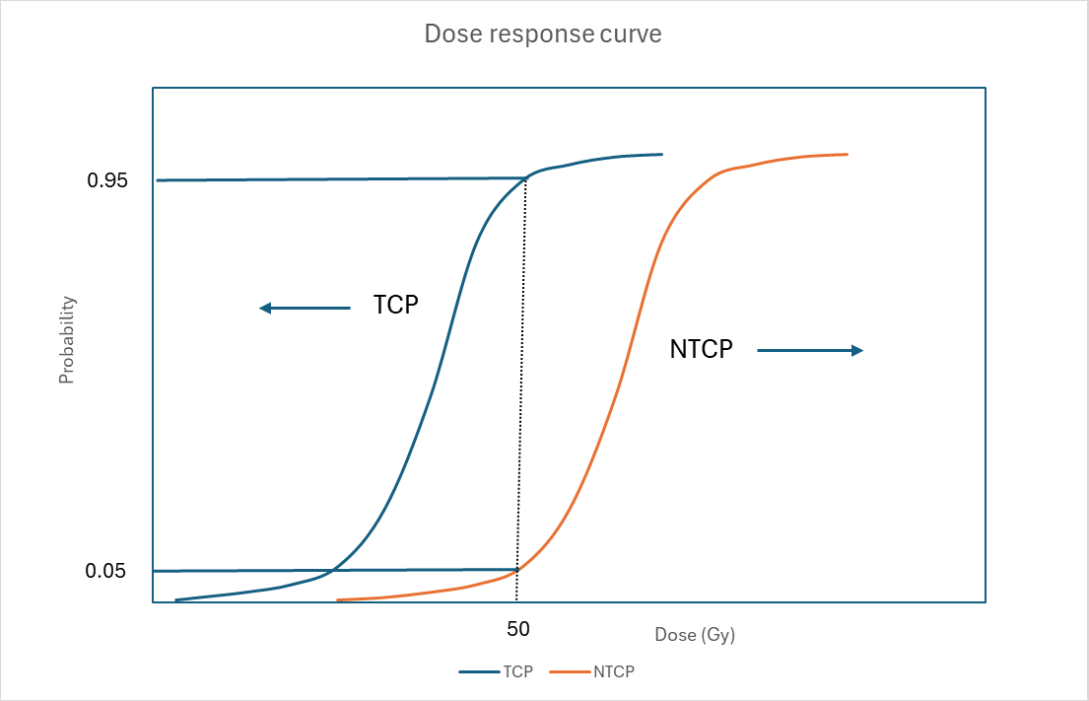

Figure 1-1: A typical dose response curve of tumour cell and normal tissue

1.2 Accuracy and precision required

Radiation therapy is a complex process involving many inter-connected steps, shown in broad higher-level terms in Figure 1-2. The accuracy of each step contributes to the overall accuracy of treatment outcome. Since the dose response curves are typically steep, as seen in Figure 1-1, a small deviation from intended dose delivery can cause a big change in treatment outcome. Conventionally, a 5% change in dose delivered may cause a 10-20% change in response depending on the region of the dose response curve involved [2].

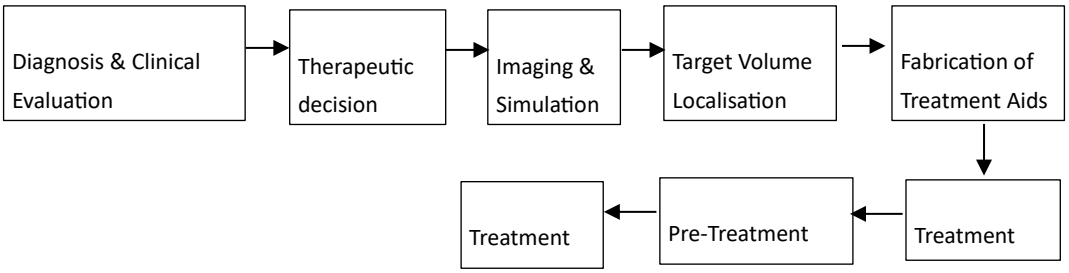

Figure 1-2: Radiation therapy process

Statements about the required accuracy must also take into consideration what is practically achievable. A number of studies [4–8] have described the levels of accuracy that are desirable and evaluated those that are practically achievable. The major sources of uncertainty, described by these studies are

i. Absorbed dose to reference point in water phantom and hence to patient

ii. Determination of relative dose distributions to characterise the beams used

iii. Relative dose calculation (treatment planning for the individual patient, including imaging, delineation of structures, and treatment plan design/optimisation)

iv. Patient irradiation (dose delivery)

Acceptable levels of combined accuracy in the dose delivered to the dose specification point in a patient irradiation have been broadly quoted as 5% for many years[4,6,8,9], often taken as a 2 standard deviation level. However, the radiotherapy process is increasingly complicated with time as processes and methods advance. According to IAEA Human Health Series No. 31 [8] the stated value of accuracy of 5% is an over-simplification for a wide range of procedure which use a wide range of technologies. Radiotherapy should be applied as accurately as reasonably achievable (AAARA) within biological and technological considerations. Thwaites [7] evaluated a wide range of experimental data on accuracy of different levels of procedures and stated that 3 - 3.5% overall accuracy (one standard deviation) is achievable by following modern dosimetric methods and procedures. In addition, geometric accuracy is as important, since this also translates into dosimetric impacts; this is partly in terms of coverage of target or overlap onto normal tissues, but also since modern radiotherapy delivery methods use intensity variations across the irradiated structures to build the required dose distributions (see section 1.4) and these must also align geometrically with their required positions [7].

1.3 How accuracy is ensured, leading to commissioning, QA and verification as three measurement-based parts of the radiotherapy process

Precision and accuracy in radiotherapy are dependent on many factors, including adequate staffing with proper training, proper QA (quality assurance) tools and technologies and clear and well-designed procedures. Quality assurance includes all procedures that ensure the safe administration of prescribed dose to the target, minimal dose to normal tissue, minimal exposure of radiation workers and public and adequate patient monitoring aimed at determining the end result of the treatment [10,11]. Increasing complexity in treatment equipment and procedures demands similarly increasing complexity in QA procedures to match. A well-designed quality assurance program reduces uncertainty in every step of the radiotherapy process, which in turn improves dosimetric and geometric accuracy and precision in dose delivery. This improves treatment outcome of increasing tumour control and reducing normal tissue complications. A prerequisite for managing uncertainties is the presence of a comprehensive quality assurance programme [10–13]. This includes

i. Acceptance testing of equipment: The purpose of acceptance tests is to verify that the equipment satisfies the specifications stated in the contract with the supplier. It ensures the basic performance of the equipment.

ii. Commissioning: Following acceptance of equipment, a full range of measurements are done, covering the whole range of possible operation scenarios, for characterisation of its performance. In this step, a set of baseline measurements is also performed for reference for future periodic QA tests.

iii. Periodic QA tests: There are several published guidelines, which describe different tests recommended with different time intervals to ensure performance remains within recommended tolerances of the original commissioning [10, 12-15].

iv. Preventive maintenance: Usually the supplier performs periodic preventive maintenance investigations and actions to keep the equipment operating smoothly at the machine level to support the continued performance requirements.

v. QA tests following any repair or upgrade of any equipment: sufficient tests need to be done to make sure the equipment continues to function as per specification.

The QA programme should encompass all systems that impact on the overall delivery of radiotherapy [12,13], with the main systems being:

i. Radiation therapy delivery equipment, which includes linear accelerators (linacs) and their onboard imaging systems, and any other in-room patient-related systems, such as SGRT (surface guided radiation therapy) equipment.

ii. CT simulators for taking the pre-treatment images that treatment planning is based on

iii. Treatment planning computer systems, which includes beam data library, dose calculation models, data I/O, etc.

iv. Individual treatment plans, which includes the treatment planning process and treatment plan QA for individual patients

v. Measurement equipment used for any steps in the radiotherapy process, e.g. in acceptance and commissioning, in QA, in patient dosimetry, in development of new techniques, in verification of methods or individual patient dose verification, etc.

1.4 Evolution of RT methods to more advanced approaches; problem with point dose measuring systems for advanced methods

Historically, most dosimetry measurements in radiotherapy were done with point dose measurement methods. In addition, part of the treatment plan QA was based on independent calculation and verification of dose at one point in the plan preferably at the isocentre or at the centre of the target [12]. Since the introduction from the early 1990s of intensity modulated radiation therapy (IMRT), with dynamically varying multi-leaf collimator (MLC) leaves shape

and position throughout a treatment delivery, and volumetric modulated arc therapy (VMAT), with dynamically changing leaves and gantry positions throughout treatment delivery, the whole radiation therapy process became more complex [16,17]. Such treatments create complex dose distributions with steep dose gradients near organs at risk (OAR). Fluence modulation allows radiation beams to be directed to the target through critical structures by differentially shielding the latter. A single point dose verification alone for patient specific treatment plan QA is not enough for treatment plans with IMRT dose distributions, which are much more heterogeneous with different degrees of modulation. IMRT plan QA demands more complex multi-point/multi-dimensional measurement-based QA along with independent verification of monitor units (MU) [18]. IMRT treatment delivery has many more sources of uncertainties. Some of those result from modelling of different aspects of the MLC, selection of calculation grid size and modelling of tissue heterogeneity correction in the treatment planning system (TPS); and also from uncertainty in positioning of different parts of the linac, e.g. MLC, gantry, collimator, table etc, as well as different aspects of the beams themselves. IMRT QA needs to include the spatial location of dose gradients. Thus, modern complex radiotherapy dose distributions require at least 2D, and ideally 3D, measurement systems and methods, with sufficient accuracy in practical use to meet the overall demands of ensuring radiotherapy dose accuracy and spatial/geometric resolution and accuracy [13,18]. As a general comment on dosimetry methods, it is desirable to have the best possible accuracy and precision possible in a measuring system.

1.5 Measurement methods for complex dose distributions, including film dosimetry

As outlined in section 1.4, with the advent of IMRT and VMAT, modern radiotherapy has required increasingly sophisticated verification of complex three-dimensional dose distributions. A dose distribution is represented as an array of points, which are defined by location and dose value. The spacing between the points is the spatial resolution of the distribution, which plays a vital role in displaying and evaluating the IMRT plan. The resolution in a planned distribution relates to calculation grid size in the treatment planning system, whilst in a measured distribution it relates to size and spacing of detector elements if discrete detectors are used, or other characteristics of the measuring and readout system if continuous (or quasi-continuous) detectors are used.

Measurement systems used for IMRT plan QA (patient specific QA) and other relative dosimetry of complex dose distributions include 2D and 3D diode arrays, 2D ionisation chamber arrays, electronic portal imaging devices (EPIDs), and radiochromic film dosimetry [18–21].

Detector arrays (using either diodes or ionisation chambers) offer rapid readout and convenient setup for IMRT QA, providing two-dimensional dose maps that can be compared in near real-time with treatment planning system calculations [22]. In general, 2D arrays are limited by their

physical construction and geometry to specific measurement planes. However, they can be placed in cylindrical or rotating phantoms, allowing approximate verification in multiple planes. On the other hand, their spatial resolution is always limited by detector spacing (typically 5–10 mm), and interpolation is required between detectors, which can obscure fine dose gradients [23]. In addition, whilst the rotational measurement geometry used by some cylindrical phantoms (e.g. ArcCheck, Delta4) provides quasi-3D data, these are still not a true continuous planar measurement [24]. EPIDs used as dosimeters (and 2D arrays attached to the rotating linac gantry) are limited by having to condense a 3-D distribution into one 2D distribution, so losing any dose variation information that is linked to specific gantry angles.

By contrast, radiochromic film dosimetry remains the gold standard for high-resolution, two-dimensional dose verification. Radiochromic films, such as the Gafchromic™ EBT and EBT-XD series, exhibit near-tissue equivalence, high spatial resolution (better than 0.1 mm), and minimal energy dependence [25]. They can be positioned in any desired plane within a phantom (or even in multiple planes at the same time) to capture precise spatial dose distributions, a flexibility not achievable with discrete detector arrays. This makes film particularly valuable for small-field and stereotactic QA, as well as for benchmarking new intensity-modulated treatment delivery techniques [26]. Thus, while diode and ionisation chamber arrays provide speed and automation for QA, radiochromic film remains indispensable when high spatial fidelity is required**.**

There are different types of radiochromic films available, some of which are recommended for use in standard radiation therapy and some for high dose radiation therapy. Irrespective of the type of radiochromic film used, its readout is usually carried out using a commercial flatbed scanner to scan the film to produce a 2D light intensity pattern, which is related to radiation dose via suitable calibration. There are commercial software packages available for processing and comparing the delivered dose distribution with that predicted by the treatment planning system [27]. Radiochromic film dosimetry does, however, present a number of challenges related to the intrinsic behaviour of the film itself, combined with the scanner-based readout. These include longer time needed to process compared to electronic devices; various correction factors are required (see Section 1.6); and strict protocols must be followed; etc. If these are accounted for and followed closely, radiochromic film dosimetry is generally a good tool for patient QA especially when high resolution is needed.

Nevertheless, the use of radiochromic film is associated with significant uncertainties, which can limit its achievable accuracy. Some major ones arise from effects that require various corrections, which are specific to film-scanner combinations and often mitigated using empirical approaches. If these approaches can be improved and the uncertainties minimised, this could in turn lead to better-optimised and more accurate radiochromic film dosimetry for radiotherapy applications.

1.6 Outline of the problem addressed in this work: issues in Gafchromic film dosimetry, research question/s, aims and objectives

The most widely used radiochromic film is the series of Gafchromic (mainly External Beam Therapy, EBT) films (Ashland ISP, Wayne, NJ, USA). The active ingredient of these films is a monomer called lithium pentacosa-10,12-diynoate (LiPCDA) present in crystals in the film [28,29], which form hair or needle-like structures. Irradiation induces polymerization between parallel lying monomers. These crystals, 2 μm in width and 15 μm in length, are preferentially aligned with the coating direction parallel to the short side of the films as supplied [28]. This property of EBT films introduces polarization and anisotropic scattering of incident light. Ashland introduced EBT-XD (extended dose) and more recently MD-V3 (medical dosimetry version 3) with shorter crystal size of 2 μm in width and 4 μm in length to minimise these two effects. Like any other dosimeter, radiochromic film dosimetry system also comes with a few limitations, which are described below

Orientation effect: The orientation of radiochromic film compared to the orientation of the light source of the scanner produces a variation of optical density. This effect results from the needle like crystals of the active ingredients [28–30], and also from the scanner via polarization [30–33]. To avoid this limitation, a strict protocol of scanning the film always in the same orientation must be followed.

LRA (lateral response artefact): This effect is defined as the non-uniform response in the direction at right angles to the movement direction of the light source of the scanner. If a homogenously exposed radiochromic film is scanned and a profile, i.e. pixel value vs position of the film, is drawn across the direction at right angles to the direction of the light movement, an upward-bent parabola, with its highest point near the centre of the longitudinal light source, will be generated instead of a flat line.

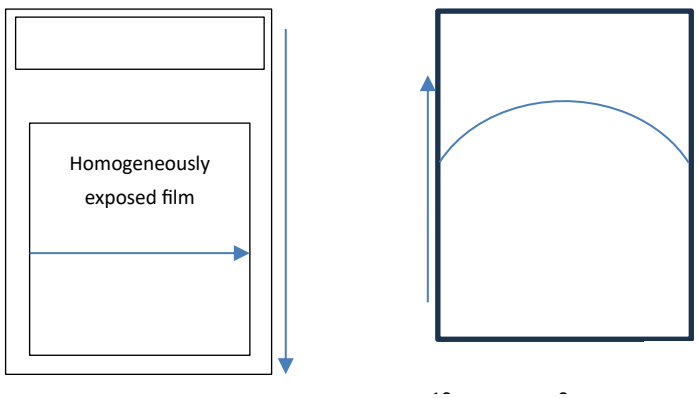

Figure 1-3: A schematic diagram of film position and profile drawn with respect to light source movement and the typical relative pixel values with respect to its position in the film

This effect results from the polarization and anisotropic scattering from the crystals of the active ingredient of the radiochromic film and also from components of the flatbed scanner. The lens of the scanner cannot gather all the light from the further points from the centre and the mirror system also causes light polarisation [28,34,35], This is the single most problematic issue with radiochromic film dosimetry, as unlike the orientation effect it cannot be eliminated by following a specific protocol. A correction must be applied to mitigate this problem, which introduces uncertainties; these corrections are often empirically based.

Temperature dependence: Optical density (OD) changes with change in temperature. The flatbed scanners use light sources, which create heat over time and affect the OD. Some studies reported this problem as change of OD with temperature in ^{0}C [29,36,37] and some reported as change of OD with increasing number of scans [38–40]. In practical use, radiotherapy centres are generally air conditioned and room temperature does not vary much and normal day to day patient QA takes only a few scans at time, which does not increase the temperature of the scanner bed up to the level where a noticeable effect could affect the dosimetry.

Post-irradiation colouration: Polymerization of active ingredients continues for some time after irradiation, i.e. the development of the radiochromic media continues even after the source of irradiation is turned off, which means films keep getting darker, typically for a certain period of time before plateauing, which varies with film type. Recommendations on how much time to wait before this slows down enough to reach an OD plateau vary from 2 hrs to 24 hrs.[41–43] (For more detail please see (iv) of section 2.5.1).

Newton's rings: If there is a gap between the film and the bed of the scanner an interference fringe effect artefact may create diffraction-like patterns, called "Newton's Rings" [44]. This may cause a large variation in the measured optical density. To avoid this unwanted effect, it is recommended to tape the film down to the scanner bed so that there is no air gap between film and glass. AAPM's recommendations on radiochromic film use (Task Group 235) [45] recommended using anti-Newton Ring glass on top of the film to keep it flat to the scanner bed.

Film Handling: Care needs to be taken during film handling. The material used as the top layer of the film tends to pick up dust because of static charge. It should be cleaned before using it. Though the radiochromic films are fairly insensitive to room light, they should not be kept in the open for hours [46,47]. For these two reasons, it is a good idea to store in an envelope or in a box [45]. The films should not be touched with bare hands as skin oil leaves marks on the film, which may introduce erroneous readings. Using gloves is recommended. If the film is cut into pieces, care needs to be taken to mark the orientation of all pieces to eliminate the orientation effect. A very sharp knife, scissors or guillotine should be used to cut the film to avoid putting extra pressure on the film, which may damage the integrity of the active layer, or the edges may open up.

1.7 Research problem

All limitations of film dosimetry except for LRA can be eliminated and/or minimised by following a well-documented protocol. There are many studies done to understand the origin of [42,43,48–50] LRA, the extent of the effect, and to propose ways to eliminate and/or minimise it. Two studies [36,51], reported at about the same time, showed pixel values depend not only on dose delivered, but also position, with the dose response non-uniform across the film in the direction at right angles to the light source movement. Fiandra et al [51] proposed a mathematical model to make the response uniform. The study calculated correction factors as the percent difference of every pixel from the centre 5 mm x 5 mm, to be multiplied with the pixel value. Some other studies [48–50,52] also made corrections in the same way. Paelink et al [38] created an 11 x 7 equally distributed matrix in the scan file and placed 2 cm x 2 cm film pieces across the scanner including a centre piece. All the pixel values were normalised with respect to the centre piece to find the correction factors needed at those points. These correction factors were generated for four different dose levels. Micke et al [41] proposed a triple channel dosimetry method, which reduces the LRA but does not eliminate it totally. Poppinga et al [53] took a different approach to correct for this effect by creating a parabola fitting curve of the profile and then created a correction formula to adjust for the LRA. Lewis et al [26] also proposed a similar method. Miura et al [54] have proposed an image stitching method to reduce the LRA effect. In this method, the film was marked in three equal sections and each section was scanned separately by moving from left to right (the direction where LRA occurs) keeping the intended section at the middle of the scanner and then the three sections were stitched together using software. By doing this, the whole film basically was scanned at the middle of the scanner where LRA is minimum, thus minimising the effect. A detailed methodology was provided in the paper.

Rink et al [29] explained the theory behind the chemical change of monomer to polymer and how those are aligned and packed in a crystal, because of which light polarisation and anisotropic scattering increases with increasing dose. Schoenfeld et al [28] performed experiments which support the theory. The study also supports the concept of increasing anisotropic scattering with increasing dose, which plays a part in increasing LRA as dose increases.

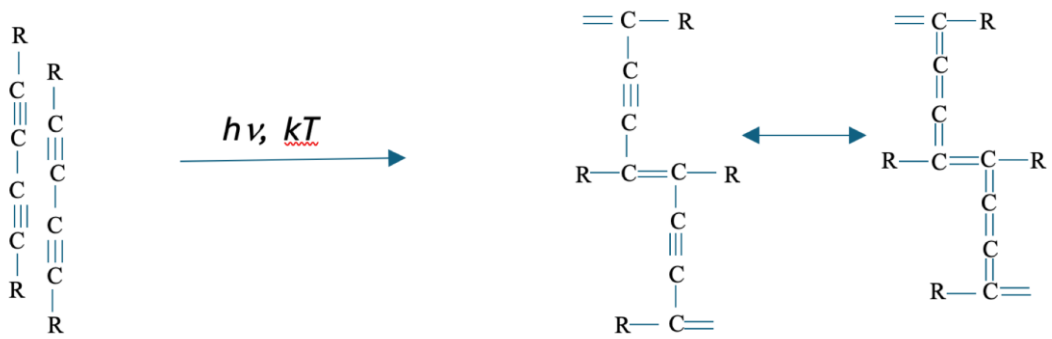

Figure 1-4: Parallel orientation of LiPCDA monomers, which polymerise upon irradiation and electronic oscillation between two alternative positions.

The lengthy polymer crystals of LiPCDA undergo molecular changes of conjugated double-bonds linking the polymers to form even longer rod-like structures [29,55] as shown in Figure 1-4. The conjugated double-bonds act as excitable oscillators with a preferential orientation, thereby causing a dependence of the light transmission on the polarization of the incident light and these oscillators act as linearly distributed sources of elementary light waves whose interference is the origin of the anisotropic angular distribution of scattered light and of the repolarization of the transmitted light [55].

Ashland introduced EBT-XD radiochromic film, a new generation of dosimetry films, with reduced aspect ratio, which is the quotient of length and width of LiPCDA monomer crystals in the active layer of the film. The aspect ratio of EBT3 films was about 10:1 and that of EBT-XD is about 2:1 [55,56]. The size of the crystals has been reduced, from typically 15 μm (even up to 20 μm) length in EBT3, to 2–4 μm [55] while the diameter remains the same at 1-2 μm. The aim of this shape change was to improve light polarization and scattering properties of the film, which in turn would reduce the known artifacts associated with film scanning in flatbed scanners, the orientation effect and the LRA. Several studies [55,57–61] found improvement of LRA, orientation and light polarization in EBT-XD compared to EBT3 for the same dose level.

Several studies [28,34,35] investigated if the different components of flatbed scanners have any effect on the LRA. The components investigated were the lens system, mirror system and scanner bed. A summary of the findings is that lens and mirror systems play a role in LRA, but the scanner bed has negligible effect as long as its refractive index does not differ from that of glass/plastic. These studies explained the effects qualitatively and provided theoretical explanations but did not clearly or systematically quantify the effects.

Gafchromic films for radiotherapy dosimetry use have continued to evolve and be improved. In addition, the explanations of the effects of scanner components and of film effects have continued to develop. However, there is still a need to quantify the effects for modern scanners and films and still a need to improve the accuracy of these measuring systems for practical

radiotherapy dosimetry use. These gaps and requirements (see Chapter 2) are the basis of the research work presented in this thesis. The overall aim is:

i) to evaluate uncertainties related to LRA effects arising from film and scanner components
ii) to assess what could be improved to reduce the LRA to a minimum and hence reduce or eliminate the need for LRA corrections, which in turn will reduce the uncertainties associated with that; and
iii) to make recommendations where possible on how to incorporate the findings into practical approaches to Gafchromic film dosimetry.

1.8 The overall research hypothesis of this project

Radiotherapy dosimetry using Gafchromic film can be improved, and ideally performed without applying any LRA correction factors, by systematic evaluation and quantification of effects arising from the components of the typical flatbed scanners being used as readout systems, leading to suggestions for improvement in those components causing LRA and in suggested readout systems and methods. This can be enhanced by the performance evaluation of modern radiochromic films and recommendations on film applications and practical use.

Complementary research questions are:

What changes could be made to scanner components, or more widely to imaging system design for film evaluation, so that LRA correction factors will be minimised, or ideally will not be necessary?

What recommendations can be made concerning selection of Gafchromic film type for specific applications in radiotherapy dosimetry?

1.9 Outline of thesis:

Chapter 2: This chapter includes a comprehensive literature review that, together with sections 1.5-1.7 above, provides the relevant background to the work presented.

Chapter 3 investigates and compares different characteristics of the most-widely-used currently available Gafchromic film types, produced by Ashland. As mentioned above, commercial products have evolved and continue to do so to reduce uncertainties that result from film itself. The widest-used film type has been EBT3 for standard radiotherapy patient QA for quite a long time, but it has recently been replaced by EBT4, which has been claimed to have better signal to noise ratio than EBT3. EBT-XD was provided as manufacturer-recommended for high dose radiotherapy, such as SRS and SBRT, and stated to have reduced LRA and orientation effects. Another product has been very recently made available called MD-V3, which is also recommended for high dose radiotherapy patient QA, but characteristics have not been previously investigated. This study investigates the comparative characteristics of these four

films and makes recommendations on their practical use. This study has been accepted for publication and published online.

Chapter 4 compares the performance of two popular models of A4-size EPSON flatbed scanners (V700 and V800) used in radiotherapy applications. Different models use different light sources and other components, and the aim of this study is to evaluate any practical differences between these different scanner models and any implications of changing from one to the other for use in radiotherapy film dosimetry. This study has been published.

Chapter 5 investigates the effect on LRA of the lens system in the scanner. At first, the lens of an EPSON V700 scanner was taken out and its focal length measured, which was 38 mm, and then a Canon 7D camera was used to capture images with varying focal length from 10 mm to 100 mm. Profiles drawn across film strips with different focal lengths were compared, to compare LRAs resulting from lenses with different focal lengths. Recommendations were made for potential improved measurement systems. This study has been published.

Chapter 6 investigates the effect of the mirror system and scanner bed material of flat-bed scanners on LRA. Different models of EPSON scanners use either 4 or 5 mirror systems. Commercially available mirrors, mostly used for common household purposes, were cut into pieces and laid out with the same orientation as in practical scanners. Images were captured placing film and a linear polarizer on top at one end and taking images using the Canon 7D camera from the other end. The procedure was repeated after rotating the polarizer by 10^0 at time from 0^0 to 180^0. The pixel values for each position were plotted with respect to polarizer position to find the amount of polarization caused by the mirror system. Then the whole process was repeated after removing one mirror at a time to evaluate polarization changes when reducing the number of mirrors in the mirror system. In this study, the scanner bed was also replaced by different materials and film strips given different dose levels were scanned to find out if the scanner bed introduces any LRA. Recommendations were made for potential improved measurement systems. This study has been published.

Together, these studies aim to form a systematic linked programme to meet the aims and research questions: (a) to provide an example quantifying the practical scanner differences clinics will face when they change hardware; (b) to determine which scanner components drive LRA so that corrections and/or new designs can be physically motivated rather than purely empirical; and (c) to re-evaluate how modern film chemistries modify scanner artefacts and together what the consequent uncertainty budget in clinical use might be and how they might be reduced. This combination of investigations aims to support clinical film dosimetry practice in radiotherapy, with a view to understanding and reducing uncertainties in practical use.

1.10 Refences:

[1] Australian Government, Radiotherapy in Australia 2018 – 19 Radiotherapy courses, Findings from this report, 2020. https://www.aihw.gov.au/reports/radiotherapy/radiotherapy-in-australia-2018-19/contents/introduction.

[2] Jacob Van Dyk, Radiation oncology overview, in: Jacob Van Dyk (Ed.), The Modern Technology of Radiation Oncology. A Compendium for Medical Physicist and Radiation Oncologists, Medical Physics Publishing, Madiosn, Wisconsin, 1999: pp. 2–17.

[3] E.B. Podgarsak, N. Suntharalingam, J.H. Hendry, Basic radiobiology, in: E.B. Podgarsak (Ed.), Radiation Oncology Physics: A Handbook for Teachers and Students, IAEA, Vienna, 2005: pp. 489–504.

[4] A. Dutreix, When and how can we improve precision in radiotherapy?, Radiotherapy and Oncology 2 (1984) 275–292. https://doi.org/10.1016/S0167-8140(84)80070-5.

[5] B.J. Mijnheer, J.J. Battermann, A. Wambersie, What degree of accuracy is required and can be achieved in photon and neutron therapy?, Radiotherapy and Oncology 8 (1987) 237–252. https://doi.org/10.1016/S0167-8140(87)80247-5.

[6] H. Svensson., Quality assurance in radiotherapy: Physical aspects, Int J Radiat Oncol Biol Phys 10 (1983) 59–65.

[7] D. Thwaites, Accuracy required and achievable in radiotherapy dosimetry: Have modern technology and techniques changed our views?, J Phys Conf Ser 444 (2013). https://doi.org/10.1088/1742-6596/444/1/012006.

[8] E. Aird, S. Bentzen, M. Coffey, I. Gomola, C. Hamilton, B. Healy, J. Hendry, G. Ibbott, J. Izewska, S. Korreman, T. Kron, A. Meghzifene, B. Mijnheer, S. Nag, A. Stewart-Lord, K. Tanderup, D. van der Merwe, G. Vandevelde, J. Van dyk, J. Venselaar, D. Verellen, A. Wambersie, E. Zubizarrwta, Accuracy requirements and uncertainties in radiiotherapy, Vienna, 2016. http://www.iaea.org/Publications/index.html.

[9] ICRU Report 24. Determination of absorbed dose in a patient irradiated by beams of x or gamma rays in radiotherapy procedures, Bethesda, Maryland, 1976.

[10] D. Thwaites, B. Mijnheer, John. Mills, Quality assumance of external beam radiotherapy, in: E.B.Podgarsak (Ed.), Radiation Oncology Physics: A Handbook for Teachers and Students, IAEA, Vienna, 2005: pp. 407–450. https://www-pub.iaea.org/MTCD/Publications/PDF/Pub1196_web.pdf.

[11] D. Thwaites, Quality assurance and its conceptual framework, Chapter 1 in: I. Patel, S. Weston, A.L. Palmer, W.P.M. Mayles, P. Whittard, R. Clements, A. Reilly, T.J. Jordan (Eds.), IPEM Report 81: Physics Aspect of Quality Control in Radiotherapy, 2nd Edition, IPEM, York, 2018: pp. 1–32.

[12] G.J. Kutcher, L. Coia, M. Gillin, W.F. Hanson, S. Leibel, R.J. Morton, J.R. Palta, J.A. Purdy, L.E. Reinstein, G.K. Svensson, M. Weller, L. Wingfield, Comprehensive Qa for Radiation Oncology: Report of AAPM Radiation Therapy Committee Task Group 40, Med Phys 21 (1994) 581–618. https://doi.org/10.1118/1.597316.

[13] I. Patel, S. Weston, A.L. Palmer, W.P.M. Mayles, P. Whittard, R. Clements, A. Reilly, T.J. Jordan, eds., Physics aspect of quality control in radiotherapy, 2nd Edition, IPEM, York, 2018.

[14] E.E. Klein, J. Hanley, J. Bayouth, F.F. Yin, W. Simon, S. Dresser, C. Serago, F. Aguirre, L. Ma, B. Arjomandy, C. Liu, C. Sandin, T. Holmes, Task group 142 report: Quality assurance of medical accelerators, Med Phys 36 (2009) 4197–4212. https://doi.org/10.1118/1.3190392.

[15] S.C. Lillicrap, Physics Aspects of Quality Control in Radiotherapy (Report No. 81), Phys Med Biol 45 (2000) 815–815. https://doi.org/10.1088/0031-9155/45/3/501.

[16] M. Teoh, C.H. Clark, K. Wood, S. Whitaker, A. Nisbet, Volumetric modulated arc therapy: A review of current literature and clinical use in practice, British Journal of Radiology 84 (2011) 967–996. https://doi.org/10.1259/bjr/22373346.

[17] B. Cho, Intensity-modulated radiation therapy: A review with a physics perspective, Radiat Oncol J 36 (2018) 1–10. https://doi.org/10.3857/roj.2018.00122.

[18] M. Miften, A. Olch, D. Mihailidis, J. Moran, T. Pawlicki, A. Molineu, H. Li, K. Wijesooriya, J. Shi, P. Xia, N. Papanikolaou, D.A. Low, Tolerance limits and methodologies for IMRT measurement-based verification QA: Recommendations of AAPM Task Group No. 218, Med Phys 45 (2018) e53–e83. https://doi.org/10.1002/mp.12810.

[19] T.J.LoSasso, IMRT Delivery System QA, in: J.R.Patla and T.R.Mackie (Ed.), Intensity-Modulated Radiation Therapy: The State of The Art, Medical Physics Publishing, Madison, Wisconsin, 2003: pp. 561–591.

[20] M.Alber, S.Broggi, C. De Wagter, I. Eichwurzel, P. Engstrom, C.Fiorino, D.Georg, G. Hartmann, T. Knoos, A. Leal, H. Marijnissen, B. Mijnheer, M. Paiusco, F. Sanchez-Doblado, R. Schmidt, M. Tomsej, H. Welleweerd, Guideline for verification of IMRT, 1st Edition, ESTRO, Brussels, 2008.

[21] N. Agazaryan, Patient specific quality assurance for the delivery of intensity modulated radiotherapy, J Appl Clin Med Phys 4 (2003) 40. https://doi.org/10.1120/1.1525243.

[22] L. Brodbek, J. Kretschmer, K. Willborn, A. Meijers, S. Both, J.A. Langendijk, A.C. Knopf, H.K. Looe, B. Poppe, Analysis of the applicability of two-dimensional detector arrays in terms of sampling rate and detector size to verify scanned intensity-modulated proton therapy plans, Med Phys 47 (2020) 4589–4601. https://doi.org/10.1002/mp.14346.

[23] S. Linsalata, J.H. Pensavalle, F. Perrone, P. Barca, F. Di Martino, F. Paiar, A.C. Traino, Classification performances of two diode arrays for patient-specific quality assurance of stereotactic body radiation therapy treatments based on absolute dose measurements in phantom, J Appl Clin Med Phys 26 (2025). https://doi.org/10.1002/acm2.70167.

[24] H. Miura, S. Ozawa, T. Okazue, T. Enosaki, Y. Nagata, Characterization of scanning orientation and lateral response artifact for EBT4 Gafchromic film, J Appl Clin Med Phys 24 (2023). https://doi.org/10.1002/acm2.13992.

[25] S. Devic, N. Tomic, D. Lewis, Reference radiochromic film dosimetry: Review of technical aspects, Physica Medica 32 (2016) 541–556. https://doi.org/10.1016/j.ejmp.2016.02.008.

[26] D. Lewis, M.F. Chan, Correcting lateral response artifacts from flatbed scanners for radiochromic film dosimetry, Med Phys 42 (2015) 416–429. https://doi.org/10.1118/1.4903758.

[27] A. Buddhavarapu, A comparison of three film analysis software for stereotactic radiotherapy patient-specific quality assurance, J Appl Clin Med Phys (2023). https://doi.org.10.1002/acm2.14203 (accessed November 14, 2025).

[28] A.A. Schoenfeld, D. Poppinga, D. Harder, K.J. Doerner, B. Poppe, The artefacts of radiochromic film dosimetry with flatbed scanners and their causation by light scattering from radiation-induced polymers, Phys Med Biol 59 (2014) 3575–3597. https://doi.org/10.1088/0031-9155/59/13/3575.

[29] A. Rink, Point-based ionizing radiation dosimetry using radiochromic materials and a fibreoptic readout system, Methods (2008). https://doi.org/10.1017/CBO9781107415324.004.

[30] M.J. Butson, P.K.N. Yu, T. Cheung, D. Inwood, Polarization effects on a high-sensitivity radiochromic film, Phys Med Biol 48 (2003). https://doi.org/10.1088/0031-9155/48/15/401.

[31] T. Cheung, M.J. Butson, P.K.N. Yu, Evaluation of a fluorescent light densitometer for radiochromic film analysis, Radiat Meas 35 (2002) 13–16. https://doi.org/10.1016/S1350-4487(01)00251-7.

[32] S.T. Chiu-Tsao, T. Duckworth, C. Zhang, N.S. Patel, C.Y. Hsiung, L. Wang, J.A. Shih, L.B. Harrison, Dose response characteristics of new models of GAFCHROMIC films: Dependence

on densitometer light source and radiation energy, Med Phys 31 (2004) 2501–2508. https://doi.org/10.1118/1.1767103.

[33] G.R. Gluckman, L.E. Reinstein, Comparison of three high-resolution digitizers for radiochromic film dosimetry, Med Phys 29 (2002) 1839–1846. https://doi.org/10.1118/1.1485056.

[34] L.J. Van Battum, H. Huizenga, R.M. Verdaasdonk, S. Heukelom, How flatbed scanners upset accurate film dosimetry, Phys Med Biol 61 (2015) 625–649. https://doi.org/10.1088/0031-9155/61/2/625.

[35] A.A. Schoenfeld, S. Wieker, D. Harder, B. Poppe, The origin of the flatbed scanner artifacts in radiochromic film dosimetry - Key experiments and theoretical descriptions, Phys Med Biol 61 (2016) 7704–7724. https://doi.org/10.1088/0031-9155/61/21/7704.

[36] B.D. Lynch, J. Kozelka, M.K. Ranade, J.G. Li, W.E. Simon, J.F. Dempsey, Important considerations for radiochromic film dosimetry with flatbed CCD scanners and EBT GAFCHROMIC® film, Med Phys 33 (2006) 4551–4556. https://doi.org/10.1118/1.2370505.

[37] L.E. Reinstein, G.R. Gluckman, Optical density dependence on postirradiation temperature and time for MD-55-2 type radiochromic film, Med Phys 26 (1999) 478–484. https://doi.org/10.1118/1.598538.

[38] L. Paelinck, W. De Neve, C. De Wagter, Precautions and strategies in using a commercial flatbed scanner for radiochromic film dosimetry, Phys Med Biol 52 (2007) 231–242. https://doi.org/10.1088/0031-9155/52/1/015.

[39] J.E. Matney, B.C. Parker, D.W. Neck, G. Henkelmann, I.I. Rosen, Evaluation of a commercial flatbed document scanner and radiographic film scanner for radiochromic EBT film dosimetry, J Appl Clin Med Phys 11 (2010) 198–208. https://doi.org/10.1120/jacmp.v11i2.3165.

[40] M. Martišíková, B. Ackermann, O. Jäkel, Analysis of uncertainties in Gafchromic® EBT film dosimetry of photon beams, Phys Med Biol 53 (2008) 7013–7027. https://doi.org/10.1088/0031-9155/53/24/001.

[41] A. Micke, D.F. Lewis, X. Yu, Multichannel film dosimetry with nonuniformity correction.pdf, Med Phys 38 (2011) 2523–2534.

[42] A. Rink, I. Alex Vitkin, D.A. Jaffray, Characterization and real-time optical measurements of the ionizing radiation dose response for a new radiochromic medium, Med Phys 32 (2005) 2510–2516. https://doi.org/10.1118/1.1951447.

[43] K. Roozen, T. Kron, A. Haworth, R. Franich, Evaluation of EBT radiochromic film using a multiple exposure technique, Australas Phys Eng Sci Med 34 (2011) 281–289. https://doi.org/10.1007/s13246-011-0067-3.

[44] M.J. Butson, P.K.N. Yu, T. Cheung, P. Metcalfe, Radiochromic film for medical radiation dosimetry, Materials Science and Engineering R: Reports 41 (2003) 61–120. https://doi.org/10.1016/S0927-796X(03)00034-2.

[45] A. Niroomand-Rad, S.T. Chiu-Tsao, M.P. Grams, D.F. Lewis, C.G. Soares, L.J. Van Battum, I.J. Das, S. Trichter, M.W. Kissick, G. Massillon-JL, P.E. Alvarez, M.F. Chan, Report of AAPM Task Group 235 Radiochromic Film Dosimetry: An Update to TG-55, Med Phys 47 (2020) 5986–6025. https://doi.org/10.1002/mp.14497.

[46] C.G. Soares, Radiochromic film dosimetry, Radiat Meas 41 (2006). https://doi.org/10.1016/j.radmeas.2007.01.007.

[47] C.G. Soares, S. Trichter, S. Davic, Radiochromic film, in: D.W.O. Rogers, Joanna E. Cygler (Eds.), Clinical Dosimetry Measurements in Radiotherapy, AAPM, 2009: pp. 759–813.

[48] L. Menegotti, A. Delana, A. Martignano, Radiochromic film dosimetry with flatbed scanners: A fast and accurate method for dose calibration and uniformity correction with single film exposure, Med Phys 35 (2008) 3078–3085. https://doi.org/10.1118/1.2936334.

[49] S. Saur, J. Frengen, GafChromic EBT film dosimetry with flatbed CCD scanner: A novel background correction method and full dose uncertainty analysis, Med Phys 35 (2008) 3094–3101. https://doi.org/10.1118/1.2938522.

[50] L.J. Van Battum, D. Hoffmans, H. Piersma, S. Heukelom, Accurate dosimetry with GafChromic™ EBT film of a 6 MV photon beam in water: What level is achievable?, Med Phys 35 (2008) 704–716. https://doi.org/10.1118/1.2828196.

[51] C. Fiandra, U. Ricardi, R. Ragona, S. Anglesio, F. Romana Giglioli, E. Calamia, F. Lucio, Clinical use of EBT model Gafchromic™ film in radiotherapy, Med Phys 33 (2006) 4314–4319. https://doi.org/10.1118/1.2362876.

[52] B.C. Ferreira, M.C. Lopes, M. Capela, Evaluation of an Epson flatbed scanner to read Gafchromic EBT films for radiation dosimetry, Phys Med Biol 54 (2009) 1073–1085. https://doi.org/10.1088/0031-9155/54/4/017.

[53] D. Poppinga, A.A. Schoenfeld, K.J. Doerner, O. Blanck, D. Harder, B. Poppe, A new correction method serving to eliminate the parabola effect of flatbed scanners used in radiochromic film dosimetry., Med Phys 41 (2014) 1–8. https://doi.org/10.1118/1.4861098.

[54] H. Miura, M. Miyazawa, S. Ozawa, T. Enosaki, M. Kagemoto, Lateral response artifact correction method using image stitching technique in radiochromic film dosimetry, J Appl Clin Med Phys 25 (2024). https://doi.org/10.1002/acm2.14373.

[55] A.A. Schoenfeld, S. Wieker, D. Harder, B. Poppe, Changes of the optical characteristics of radiochromic films in the transition from EBT3 to EBT-XD films, Phys Med Biol 61 (2016) 5426–5442. https://doi.org/10.1088/0031-9155/61/14/5426.

[56] Ashland Specialty Ingredients, Gafcrhomic Dosimetry media, Type EBT-XD, (n.d.). http://www.gafchromic.com/documents/EBTXD_Specifications_Final.pdf.

[57] D.F. Lewis, M.F. Chan, Technical Note: On GAFChromic EBT-XD film and the lateral response artifact, Med Phys 43 (2016) 643–649. https://doi.org/10.1118/1.4939226.

[58] H. Miura, S. Ozawa, F. Hosono, N. Sumida, T. Okazue, K. Yamada, Y. Nagata, Gafchromic EBT-XD film: Dosimetry characterization in high-dose, volumetric-modulated arc therapy, J Appl Clin Med Phys 17 (2016) 312–322. https://doi.org/10.1120/jacmp.v17i6.6281.

[59] M.P. Grams, J.M. Gustafson, K.M. Long, L.E.F. de los Santos, Initial characterization of the new EBT-XD Gafchromic film, Med Phys 42 (2015) 5782–5786.

[60] A.L. Palmer, A. Dimitriadis, A. Nisbet, C.H. Clark, Evaluation of Gafchromic EBT-XD film, with comparison to EBT3 film, and application in high dose radiotherapy verification, Phys Med Biol 60 (2015) 8741–8752. https://doi.org/10.1088/0031-9155/60/22/8741.

[61] S. Khachonkham, R. Dreindl, G. Heilemann, W. Lechner, H. Fuchs, H. Palmans, D. Georg, P. Kuess, Characteristic of EBT-XD and EBT3 radiochromic film dosimetry for photon and proton beams, Phys Med Biol 63 (2018). https://doi.org/10.1088/1361-6560/aab1ee.

2 Literature review of radiochromic film dosimetry

2.1 Introduction and scope of literature review

Modern radiotherapy techniques (IMRT, VMAT and stereotactic treatments) place very high demands on dosimetric verification because of steep dose gradients and small-field deliveries. For such applications, radiochromic film remains an indispensable tool owing to its near-tissue equivalence, very high spatial resolution and capability to be placed in any plane within a phantom for true planar dosimetry and detailed dose mapping. However, the film-to-image readout chain, typically a radiochromic film plus a commercial flatbed scanner and image processing software, introduces several systematic effects that limit absolute accuracy unless appropriately characterised and corrected. These scanner-related artefacts and film-specific sensitivities therefore represent a key barrier to meeting modern radiotherapy QA accuracy targets. The literature review is intended to outline and discuss the background to these issues and to identify gaps in knowledge and requirements, in order to provide information and analysis to improve the practice and accuracy of radiochromic film accuracy for radiotherapy applications.

The literature review presented in this chapter is focused on the above issues but firstly details why radiochromic film is necessary for radiotherapy dose verification, as compared to other systems (as simply stated in Chapter 1). It is intended to follow on from the description and discussion of introductory literature in Chapter 1 and to also link to the brief specific literature reviewed in each of chapters 3-6, noting that each of these is a published paper with its own focussed literature discussion related to each specific piece of work.

2.2 Need for radiochromic film dosimetry

Sections 1.4 and 1.5 outline the need for 2D and 3D dosimetry systems to measure and verify advanced dose distributions, such as IMRT, VMAT and SBRT and indicate that resolution is important where dose gradients are steep. Measurement systems used for IMRT plan QA (patient specific QA) and other relative dosimetry of complex dose distributions include 2D and 3D diode arrays, 2D ionisation chamber arrays, electronic portal imaging devices (EPIDs), and radiochromic film dosimetry[1,2]. The following discusses each of the alternative systems, in terms of specific commercial examples and in sufficient detail to demonstrate why film remains the gold standard for high-resolution, two-dimensional dose verification, as stated in section 1.5.

Diode arrays: Diode arrays are a fast and efficient way of performing IMRT plan QA. The result is available immediately after irradiation for comparison with the expected plan dose distribution. However, the spatial resolution of diode arrays is from 7 mm to 1 cm and the

software creates dose distributions between two diodes by interpolation. Diode arrays can be flat (2D) or cylindrical (semi-3D) in shape. An example of a commercially available flat diode array is the MapCheck3 (Sun Nuclear, Melbourne, FL, USA) [3]. The diode detectors of MapCheck3 are 0.23 mm^2 of size and spaced at 7.07 mm uniformly across the entire array of 32 cm x 26 cm. One limitation of this device is that either the dose delivery has to be forced to gantry 0^0 or the array has to be mounted on the gantry. In either case, the superimposed dose distributions at all gantry angles means that any gantry angle dependent dose variation is lost. To mitigate this limitation, Sun Nuclear introduced ArcCheck [4] which is a 21 cm long (44.29 cm including electronics), and 21 cm diameter cylinder containing a 3-D diode array with 0.64 mm^2 diode detectors spaced at 1 cm apart. The detectors are placed in a helical grid and software interpolates signals between these detectors, so the system is quasi-3D, or semi-3D in operation. Another semi-3D commercial product is the Delta4 (ScandiDos, Uppsala, Sweden) [5] which uses two orthogonal flat diode arrays inside a PMMA cylinder. The detectors are spaced at 5 mm in the central 6 cm x 6 cm area and at 1 cm in the outer region. Though Delta4 is 40 cm long (71 cm including electronics), the maximum field size it can measure is 20 cm x 20 cm. SRS MapCheck [6] is another product from Sun Nuclear , which is specially brought to market for patient QA of Stereotactic Radio Surgery (SRS) and Stereotactic Body Radio Therapy (SBRT), both of which deliver a very high dose in a small volume. The SRS MapCheck is a 2D array which has an active area of 7.7 cm x 7.7 cm with detectors, size 0.23 cm^2, spaced at 2.47 mm.

Ionization Chamber arrays: PTW (Freiburg GmBH, Germany) introduced an ionization chamber array, called Octavius [7] 1500, for IMRT patient QA. The size of the active area is 27 cm x 27 cm with parallel plate ionization chambers, size 4 mm x 4 mm, spaced at 7.1 mm from centre to centre. It can be placed in a rotating phantom, which moves with the gantry. PTW has a smaller version also, the Octavius 1600srs, with 2.5 mm spacing and active area of 15 cm x 15 cm for SRS and SBRT treatment plan QA.

Both 2D and semi-3D arrays are limited by the physical size and shape of the system, the arrangement of the detectors, the detector size and the detector spacing. Any doses at other places must be interpolated by software.

EPIDs: Linear accelerators (linacs) are standardly supplied with on-board imaging systems, based on flat-panel solid-state detectors and rotating with the linac gantry electronic portal imaging devices (EPIDs). These image-based patient QA systems were initially intended for qualitative imaging and geometric alignment (set up) of patients. However, they can be calibrated to be used quantitatively and hence also to provide dosimetric QA [8,9]. Sun Nuclear (https://www.sunnuclear.com/suncheck) and others have released commercial software to use with on board imaging systems to perform patient specific QA. This is a fast procedure and needs no pre-measurement preparation. This technology is still developing and has a limitation

in handling high dose rate from flattening filter free beams. The resolution is defined by the make and model of linac and their associated EPID. The latest versions of Elekta and Varian EPIDs have pixel pitch of 0.4 mm and 0.336 mm respectively [10]. However, all such systems suffer from the same limitation of super-imposed distributions as mentioned above re gantry-mounted 2D arrays.

Radiochromic film dosimetry is discussed separately in the next section. It is based on a colour change with irradiation and its response is near linear over a film-dependent dose range. It overcomes the various limitations of the above systems. Gafchromic film is near tissue-equivalent (unlike the solid-state systems) and exhibits minimal energy dependence [11]. Its spatial resolution (1200 lines/mm) [12] is such that it provides spatially continuous measurements of dose distributions. Films can be placed in any plane within a suitable phantom, even in multiple planes at the same time, with minimal perturbation of the irradiation conditions, and can therefore provide measurement of true 3D dose distributions to be compared and evaluated. It can be cut to shape to fit customised phantoms [11]. Thus, while the other systems mentioned can provide speed and automation for QA, radiochromic film remains indispensable when high spatial fidelity and flexibility or dosimeter customisation is required.

2.3 Film for radiation dosimetry

Since the introduction of IMRT and SBRT, film has been used by many radiotherapy centres for patient QA and verification dosimetry. Point dose measurement alone is not sufficient for demonstrating the accuracy of these complex treatments. Traditionally silver halide films were used, which is a very good dosimeter but comes with a few drawbacks, including the need for a dark room and processor, hazardous chemical handling for developing, variation in sensitivity, temperature dependence etc [13]. Radiochromic film overcame these problems and became popular to be used in radiotherapy dosimetry. The most-widely used radiochromic film is Gafchromic films, manufactured by International Speciality Products (ISP), Wayne NJ USA; part of Ashland Global, Wilmington, DE, USA. The properties of Gafchromic films, such as high spatial resolution; near tissue equivalence; temperature, pressure and humidity independence; and near energy independence [14], make it a popular choice for patient QA/plan verification [15]. It has also been investigated for its use for Linear Accelerator (Linac) QA [16]. The active ingredient of Gafchromic film is Pentacosa-10,12-diynoic acid (PCDA). There have been other approaches to the design of radiochromic films, based on other active ingredients, for example, using 4 Butoxy-carbonyl-methylurethane (4BCMU) as active ingredient [17,18]. These films create blue colouration when irradiated. Both radiochromic films work in the same way, monomers turn into polymer upon irradiation and change colour [18,19]. Watanabe et al [17] reported the advantages of this film over Gafchromic are that it is cheaper to make, very sensitive to low dose and the image can be archived upon exposing it to >110 ^{0}C. Some characteristics are the same for both films, such as not being sensitive to room

light, polymerisation makes the active ingredient size bigger, post irradiation OD keeps increasing fast up to a certain time and then slows down, near tissue equivalency, energy independence etc. Though, Watanabe et al [17] stated that the 4BCMU film could be used up to 10 Gy, they also reported, in the same study, that it saturates at 1.8 Gy. Mittal et al [18] reported the useful dose range of this film is up to 16 Gy, with no explanation of the difference to the other work. This different film is mentioned as an example here for completeness. However, the work presented in this thesis is based on the Ashland Gafchromic films as they have found the most widespread use in radiotherapy dosimetry.

Ashland produces different types of radiochromic films for different uses. Over the years, it has continued to improve the products, or develop films for specific applications, by changing the composition of the active layer, changing the thickness of the base layer, changing the size of the crystals, etc. The XR series of Gafchromic films are for use in diagnostic x-ray applications. In the active layer emulsion, Br and Cs are added in those films. The main Gafchromic films designed for use in radiotherapy applications are listed in the Table 2-1 below, with the older products typically discontinued as newer ones became commercially available.

Film	Approximate Release year	Thickness (μm)					Dose Range (Gy)
		Active layer	Glue	Gelatine /Middle Sheet	Top Sheet	Bottom Sheet	
HD-810	Pre 1990	6.5	None	0.75	None	97	10-1000
MD-55-1	1997	16	None	None	None	67	2-100
MD-55-2	2003	16 x 2	20	25	67	67	1-100
EBT	2004	17 x 2	None	6	97	97	0.05-100
EBT1	2004	25	None	3	None	97	0.1-200
HS	2005	38	None	None	97	100	1-5
RTQA	2006	17	12	3	97	97	0.01-5
EBT2	2009	30	25	5	50	175	Up to 50

HD-V2	2010	12	None	None	None	97	10-1000
EBT3	2011	28	None	None	125	125	0.2-10
EBT-XD	2015	25	None	None	125	125	0.4-40
RTQA2	2021	17	20	None	97	97	0.02-8
EBT4	2022	28	None	None	125	125	0.2-10
MD-V3	2010 and 2024	10	None	None	120	120	1-100

Table 2-1 : List of Gafchromic films with properties

EBT3 has until recently been the most widely used product of Ashland for radiotherapy dosimetry. It's matte polyester top and bottom sheets have microscopic silica particles embedded in the surface which keeps a gap of a few microns between film and scanner bed that helps in preventing Newton's ring formation [20,21] (where an interference pattern is created by the reflection of light between a curved surface and an adjacent touching flat surface). This film has been discontinued recently and replaced by EBT4. The active ingredient remains exactly the same as EBT3, but with improved active fluids designed to improve signal to noise ratio [21–25]. Gafchromic EBT-XD was designed to reduce the LRA effect. Its active ingredient crystal size was shortened from 15 μm to 6 μm to reduce this and some other problems, associated with radiochromic film dosimetry. The smaller crystals result in less sensitivity, with an increased dose range of up to 40 Gy.

Gafchromic MD-V3 was introduced in 2010 and was relaunched in 2024 with modified emulsion. There is little information available in the literature on this new product, as it has not been studied or reported on much to date. It is designed for high dose range applications, up to 100 Gy. The thickness of the active layer is 10 μm, which is quite a lot thinner than other Gafchromic films [26]. A verbal communication from Ashland (with M Butson) indicated that a special dye was introduced to inhibit the bonding between adjacent crystals so that the LRA does not increase with increased dose.

The most widely-used Gafchromic films for radiotherapy dosimetry until recently are EBT3 and EBT-XD which have nominal dose ranges of 0.1-10 Gy and 0.4-40 Gy respectively [27,28]. The construction of EBT3 film is shown in the Figure 2-1 below. The symmetrical layers on each side of the active layer allows scanning on either side.

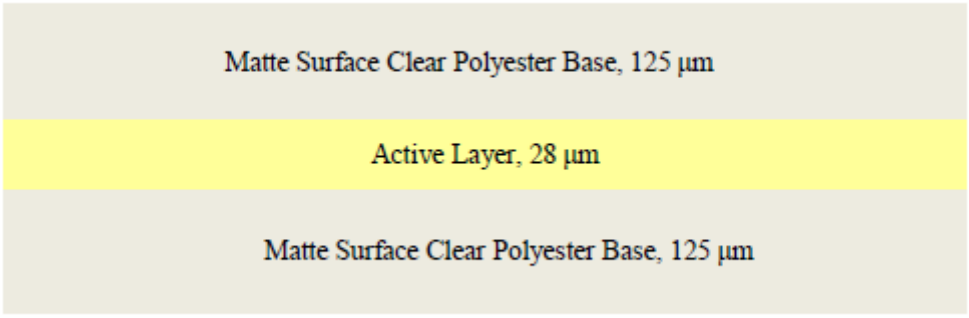

Figure 2-1: Construction of EBT3 Gafchromic film.

There are various choices in every step of radiochromic film dosimetry, which affect the overall accuracy in different ways. The choices are

- Using a background scan or not
- Time between film irradiation and scan
- Transmission or reflective scanning mode
- Orientation of film on the scanner
- Choosing image file format. Some image file formats save images in Red, Green and Blue colours and can be separated easily.
- Choosing a specific colour channel and, if used, the right image format for this. Different colour channels have different pros and cons
- Choosing a method of using the pixel values from the scanned image

Gafchromic film can be used as an accurate and reliable dosimeter if a consistent protocol is used in calibration and in measurement, with the same method used for every step and parameter mentioned above [14,29].

The common method of film dosimetry as described by different authors [14,30,31] is

- Scanning film before and after irradiation in transmission mode
- Save the scan as TIFF (Tagged Image File Format), which allows the user to access the pixel values in red, green and blue colour channels
- Convert red channel pixel values into netOD (net Optical Density), which is defined by the log of the ratio of pixel values of pre and post irradiated films.

$$netOD = log \frac{P_{pre}}{P_{post}}$$

where P_{pre} and P_{post} are the pixel values of pre and post irradiated films

- A non-linear calibration curve for different dose levels is obtained and applied

There are other authors, who used different methods, including saving the scan as JPEG [32], or using reflective modes [33,34], using the green channel, using raw pixel values [32], or normalised pixel values [34]. An investigation of the accuracy and efficiency of different radiochromic film dosimetry systems and methods [35,36] has summarised and compared different approaches by different authors.

Characteristics of Gafchromic films include:

i) Tissue equivalence: Gafchromic films generally consist of a layer of uniform and transparent radiosensitive material on or sandwiched between two polyester base sheets. The ingredients of active layer, thickness of polyester base and adhesives determines the effective atomic number (Z) of the films. These construction components have changed over time as film designs have evolved and therefore the effective Z has varied. The early generation of Gafchromic film, MD55-2, had effective Z within the range of 6.0-6.5 [14]. The active layer of MD55-2 is Pentacosa-10,12-diynoic acid (PCDA), which was initially designed to be used in the kV photon beam range. The EBT (External Beam Therapy) series was designed to be used in the MV beam range, with the active layer being a lithium salt of Pentacosa-10,12-diynoic acid (LiPCDA). Z_{eff} was increased to 6.98 [37] . The later versions of Gafchromic films (EBT2, EBT3, EBT-XD) used the same active layer but with different thicknesses of polyester base and added dye. The effective Z of EBT2 and later versions is 6.8, as compared to Z_{eff} of water of 7.34 [38].

ii) Energy independence: The older Gafchromic films had lower energy response to kV photons than in the MV photon range. The first generation of EBT films had moderate Z elements added, such as chlorine, which helped to boost photoelectric absorption of the kV photons which made the film less energy sensitive. The new Gafchromic EBT2 film had very low energy dependence with a 6.5% variation over the energy range of 50 kV to 10 MV as compared with 7.7% for the previous EBT film [39]. Another study [40] investigated the energy response of EBT2 films in kV and MV x-rays, Cs-137 and Co-60 γ- rays, 6 and 20 MeV electrons and also 100 and 250 MeV proton beams. The difference between maximum and minimum was 18% between Co-60 γ- rays and 100 MeV protons, with a data spread (one standard deviation) of ±4.5% from the mean. A similar study on EBT3 film reported that the difference between 100 MeV protons and 6 MV photons was 11.5% (maximum) and ±2.9% (average) [41] respectively. One investigation [38] found a maximum difference of 6% between photons and protons, whilst an investigation into relevant involved factors [42] showed that the energy dependence can be affected by absorbed dose, spatial resolution and the colour channel used to study the film.

iii) Temperature dependence: Lynch et al [43] found an increase of OD (Optical Density) up to 7% with increasing temperature from 18^0C to 34^0C for EBT film irradiated to 27 cGy. The effect reduced to 1.5% for an EBT film irradiated to 300 cGy. Rink et al [44] found that EBT2 film showed a 10% decrease in OD for an increase of temperature from 22 ^{0}C to 38 ^{0}C in the wavelength range of 630-640 nm. The difference between these two studies is that Lynch used air as background and scanned the film at a later time using a densitometer, whereas Rink used lasers to readout in real time and used an unirradiated film as background. The reason for having opposite trends in result is discussed by Rink [45]. The study of Lynch was closer to the clinical situation and it can be inferred that in a clinical situation the OD of Gafchromic film increases with increase in temperature. This change of temperature was induced during digitisation. Recently, Yamada et al [46] investigated temperature dependence of HD-V2 and MD-V3 during irradiation, which reported no significant change in variation of response with variation in temperature during irradiation. They repeated the investigation [47] with the same films but varied the temperature from that during calibration and found up to 0.4% change per ^{0}C difference from the temperature during dose calibration for HD-V2, whilst MD-V3 showed negligible effect on temperature change.

iv) Dose rate dependence: Dose rate independence is now a critical parameter for a dosimeter used in modern radiotherapy. New technologies in radiotherapy, e.g. VMAT, have varying dose rate as the gantry rotates during the treatment, or Flattening Filter Free (FFF) beams have very high dose rate compared to conventional beams. These innovations demand a dosimeter which is insensitive to dose rate variation.

Rink et al [48] found a small variation of response of Gafchromic EBT film when the dose rate was varied from 16 to 520 cGy/min. When dose rate variation effects were combined with varying dose from 5 cGy to 1000 cGy the standard deviation of the OD was reported less than 4.5%. This work was performed to find out the suitability of radiochromic film as a tool for measuring dose in real time. The polymerisation process is not instantaneous. It takes at least two hours to reach an acceptable stability. In real-time dose readout, slower dose rate allows more time for polymerization than that of higher dose rate. The following works investigated the dose rate dependency after allowing sufficient time to allow the polymerisation process to reach stability. Twork et al [49] used EBT3 film to study the effect of dose rate on Gafchromic film. They aimed to evaluate effects in the usual clinical ranges of dose and dose rate; dose rate was varied from 50 to 1000 cGy/min for doses of 50, 100 and 500 cGy. The study found a smaller dose rate dependence which is within experimental uncertainty of clinical film dosimetry. For this reason, the study reported that Gafchromic EBT3 film is dose rate independent. Work by Oyewale et al [50] used a FFF beam, producing more than 20

Gy/min, to study the dose rate effect on Gafchromic film. The study found dose rate dependency of EBT films to be negligible within the uncertainty of film dosimetry.

v) Resolution: Theoretically, the resolution of film dosimetry depends on the size of the active molecules, but practically the sampling rate/resolution of densitometer/scanner determines the resolution of the whole Gafchromic film dosimetry system [51]. The spatial resolution of a scanner is determined mainly by light source size and light scattering effects from the film. The correct bit level of data acquisition is another contributing factor in accuracy of measurement. An investigation was done with Gafchromic EBT film and an Epson 10000XL scanner to study the effect of scanner resolution on accuracy [52]. Scanner resolution of 50, 75, 150 and 300 dpi were investigated. No significant differences were found in the dose calibration curve. The best compromise between resolution and noise was found at 75 dpi for IMRT plan verification purposes.

2.4 Film readout systems:

A readout system is needed to convert film darkness into dose. The basic principle of a film readout system is to measure intensity of light passing through the film, which is inversely proportional to dose or in other words, proportional to darkness of the film. A spot densitometer can be used to measure light intensity at a point or of a small area. This type of device is useful for reading personal dosimeters. Radiochromic films are widely used for high-resolution two-dimensional dosimetry for which a 2D readout system is needed. In the early 1990s the 2D film readout systems were just motorized spot densitometers, in which either light source and detector combination or film itself were translated to produce a 2D matrix of measurement points. These devices usually had a laser light source and a PMT (photo multiplier tube) detector [53]. These systems were very expensive and used to show significant interference-pattern artefacts, producing Newton rings, and light-transmission artefacts, producing OD non-linearity [54]. Another choice was to use a radiographic (silver-halide) film digitiser, which was expensive and also had limitations, such as that the consistency could not be maintained for repeat scans and that such systems had lower sensitivity because of the broadband white light source used. Digitisers based on He-Ne laser light sources showed improved sensitivity, but at the expense of worsened Newton Ring artefact. A red LED-based digitiser overcame the Newton Ring artefact with improved sensitivity [55]. Devic et al [56] compared seven available film digitisers, including a document scanner, which included:

- Victoreen: A spot densitometer with LED light source
- LaserPro 16: Radiographic film digitiser with Laser Diode as light source
- Photoelectron Corp: A CCD array is used to image the film which is backlit with a LED array
- Agfa Arcus II: A desktop flatbed scanner with fluorescent lamp

- Molecular Dynamics: Point by point translation type densitometer with He-Ne Laser
- Vidar VXR-16: A photographic film digitiser with broadband white fluorescent lamp
- LKB Pharmacia: Point by point translation type densitometer with He-Ne Laser

The study compared sensitivity and dose uncertainty of these digitisers for two types of Gafchromic films, Gafchromic HS and Gafchromic XR-T. The Vidar VXR-16 was the least sensitive system and the Victoreen was the most sensitive. Dose uncertainty was below 5% above 5 Gy irradiation for all except LKB Pharmacia with Gafchromic XR-T film, which was 7%.

With development of technology of document/photo scanner over time, these became popular due to their versatility, wide availability and much cheaper price. Matney et al [57] compared Vidar VXR Dosimetry Pro and Epson V700 scanner for scanner consistency, film-to-film variation, orientation effect, scanner uniformity and noise. The study reported both digitisers had similar response for consistency, film-to-film variation and noise. The orientation effect was 17% for the Epson V700 for 4.5 Gy dose level, whilst Vidar VXR dosimetry Pro showed negligible effect. Scanner uniformity was higher in the Vidar VXR Dosimetry Pro. A huge number of studies have been done to investigate the efficacy, issues and potential solutions for film dosimetry with flatbed scanners, which are discussed in section 4 of this chapter.

A number of investigations have been carried out to develop a film digitiser, with different motivations. Aland et al [58] used a smart phone as a digitisation device for point dose measurement as a cheaper and convenient option. Piliero et al [59] used a commercial hand-held spectrometer for point dose measurement for high accuracy. Rosen et al [60] designed a glassless densitometer for a high accuracy reference dosimetry device traceable to national standards. Ranade et al [61] developed a red LED and dual detector spot densitometer device with motorised translating film plate. Jeminez-Alivez et al [62] used a dSLR camera as digitiser and built a reading system directly from the camera using an inhouse program for point dose measurement. The study compared the results on sensitivity and noise to that of an EPSON 11000XL scanner. Though sensitivity of this system was higher than that of the scanner, the noise was very high as well. A recent study by Bantan et al [63] used an overhead scanner with a light board for film dosimetry and compared its performance with an Epson V700 scanner. The study focused only on orientation effect, which is not present in the overhead scanner system. Rink et al [64] developed a real time dosimetry system for point dose measurement using a fibreoptic readout system. Casolaro et al [65] developed a real time point dose measurement device with film using a similar technology of that of Rink et al. Most recently, Mena et al [66] developed and patented a real time 2D dosimeter using an opto-electro-mechanical sensor.

2.5 Uncertainty of film dosimetry

2.5.1 Uncertainties contributing to radiochromic film dosimetry

In radiotherapy the aim is to achieve an overall dose delivery better than 5% [67–71] which includes the whole process from calibration of detector used for Linac calibration to the actual dose delivered to the patient. That means that the uncertainty of dose detection by film has to be less than this. The sources of uncertainties in film dosimetry are discussed in different studies [11,43,72–76] not all of the parameters investigated in these studies, have major impact on film dosimetry. A list of uncertainties, which introduces at least 1% uncertainty, associated with radiochromic film dosimetry is given below. This is not necessarily a complete list or listed in order of importance.

i) Intra batch variation: Van Battum et al [72] found 1% variation in background among the films of one batch of Gafchromic EBT films Another study [76] found an intra batch variation of <0.6%, which was also for the same type of film.

ii) Inter batch variation: Van Battum et al [72] found 13% variation in background reading between films from different batches. This variation could be eliminated by having calibration curves for each batch of films

iii) Fit accuracy: To convert pixel values of an irradiated film into dose, a dose-response calibration curve is needed. Change of pixel values with change of dose is not linear in radiochromic films. Different studies have recommended different mathematical formula for fit curves. Uncertainty can result from choosing the values of the different parameters of a suggested formula. According to AAPM TG-235 [11] a fit curve usually has 1.5% uncertainty. However, Van Battum et al found less than 0.3% uncertainty for a fit curve. Spelleken et al [35] compared some unconventional methods of calibration, which are widely used and verified, to two of the most common and verified methods, nonlinear fit and polynomial fit, proposed by Devic et al [30] and Aland et al [16] respectively in two different scanners V800 and 10000XL. At 25 Gy the maximum uncertainty was found to be 1.5% for conventional methods. The unconventional methods were comparable at 2 Gy but at 25 Gy uncertainty was up 30% or more.

iv) Post irradiation OD growth: Radiochromic film keeps darkening after irradiation, at a faster rate initially, typically up to 24 hrs, and then at a much slower rate after that which varies with different types of radiochromic film. According to AAPM TG-235 [11] in EBT3, polymerisation nearly stops after 24 hrs but it still changes the pixel values by 2.5% from 24 hrs to 14 days. Two investigations [64,77] recommended 2 hrs is sufficient for stabilization. Cheung et al [78] found EBT films stabilize sufficiently for analysis after 6 hrs. Several other studies also found similar trends in EBT film. Sharma et al

[79] found 6 hrs is enough for EBT3 film for stabilization. Muira el al [80] found 6 hrs stabilization time for EBT-XD. This uncertainty can be eliminated or reduced significantly if the time interval between irradiation and readout for the calibration film is kept exactly the same as that for the dosimetry or QA film irradiated with unknown dose.

v) Orientation effect: This is a well-known effect of radiochromic film, discussed above, and has been studied widely for different types of Gafchromic films [72,74,76,80,81]. The orientation effect is a difference of OD depending on the orientation of the film placement on the scanner bed. The magnitude of this effect can vary from 3 to 10% depending on the type of film. It can be minimised by following a strict protocol of keeping the film orientation the same with respect to the scanner bed all the time by marking the film

vi) Lateral Response Artefacts: This is another well-known and widely studied issue with radiochromic film dosimetry, also discussed above. It is the difference of OD at the lateral edges compared to that at the centre of the scan frame. This effect, which depends on film type, scanner type and dose level, is reported as high as 17% [43,72,76,82,83]. A correction factor has to be determined and be applied to all pixels to minimise its effect so that the overall uncertainty of the film dosimetry remains acceptable.

vii) Non-uniformity: The variation of thickness of active layer in radiochromic films causes a non-uniform response over a single film. While Fuss et al [76] reported less than 1%, Van Battum et al [72] and AAPM TG235 [11] reported 1.1% and 1.5% respectively. Multi-channel [84,85] dosimetry methods can minimise this effect. Martisikova et al [75] found the effect negligible when blank film response is subtracted from the exposed film values. Bennie et al [31] suggested that when subtracting blank film from exposed film, it was advisable to use the green channel.

2.5.2 Total uncertainty

Different studies have provided different values of total uncertainty associated with film dosimetry. The reason for the variation is that the various studies did not consider the same set of sources of uncertainty and different studies used different film types, different scanners, different software, different techniques and so on.

Saur et al [73] used EBT film with an EPSON 1680 scanner and considered sources of uncertainties from film-to-film variation, fit accuracy, film uniformity and noise. The study found a total uncertainty of 3.5% for portrait scans and 5% for landscape scans at the 2 Gy dose level. Devic et al [30] used EBT and HS films with an Agfa Arcus II (Agfa-Gevaert Corporation, Mortsel, Belgium) scanner and considered almost all the uncertainties mentioned above. This

study found total uncertainty of 3% for EBT film and 2% for HS films. Marroquin et al [12] used EBT3 film with an EPSON 750 scanner and the sources of uncertainties considered were fit accuracy, dose resolution film reproducibility and uniformity and also the reproducibility of the scanner. This study found a total uncertainty of 3.2% for red channel. Fiandra et al repeated the work of Devic et al [30] and applied correction factors for the LRA, which resulted in 1.35% total uncertainty at the 2 Gy dose level for red channel and 2.28% for green channel. Van Battum et al [72] used EBT films with an EPSON 1680 scanner and considered almost all the sources of uncertainties mentioned above, this study reported a total uncertainty of 1.8% at the 2.3 Gy dose level.

The number of steps involved in film dosimetry is high. If all the steps are not followed strictly the end result may show quite a different uncertainty value. Recently, Beveridge et al [86] conducted a study for assessing the accuracy of the film dosimetry process for audit purposes. The baseline film processes were set up under the auspices of the Australian national audit system centre, linked to the Australian national dosimetry standards lab and were aimed at minimising uncertainties and applying strict protocols. The study considered the uncertainty of film dosimetry is 2.3%. Six members of an international dosimetry audit network took part in the evaluation process, referencing to the Australian system. Different institutions use different film digitisers and different software, both inhouse or commercial, for film dosimetry. The SD of the dose was about 7% and results varied from -12.4% to 12.9% from the known dose. The large variation was attributed to failing to maintain strict protocol throughout all steps in the different systems. When an expert user of each participating institution followed their strict protocols, the SDs were 2.7% and 3.7% for inhouse and vendor-based software respectively. This study demonstrates the importance of following the film dosimetry procedure strictly to achieve an acceptable and consistent outcome.

The above review indicates that reported overall uncertainties on dose measurements using radiochromic film are highly variable. For specific uncertainty estimates within single research groups, these are reported to vary from around 2 - 5% (one SD), depending on which specific contributing uncertainties are taken into account and also for which specific films, scanners and evaluation software. Applying empirical corrections can reduce the estimated values, although it should be noted that those corrections also have associated uncertainties, that are situation specific.

Nevertheless, practical experiment-based measured doses between research groups, with different scanners and different digitising/evaluation software, but scanning the same films, showed much larger uncertainties (7% SD) [86] . Following strict consistent protocols was shown to reduce this to around 3% (SD). It should be noted that these were all national/international audit groups experienced in using radiochromic film and while their own internal processes would be more self-consistent, these variations were highlighted by

comparing across groups. It is likely that uncertainties between individual hospitals are at least as great as between these audit groups and realistically may be expected to be larger. This supports both the use of very consistent protocols, but also the potential advantage of finding ways to reduce uncertainties in the film and scanner technology where possible and in the measurement and evaluation processes.

2.6 Problems in film dosimetry

Radiochromic films provide attractive 2-D dosimetry because of their near-tissue equivalence and high spatial resolution, but the measurement chain, consisting of film and scanner, has well-documented sources of systematic error. Two issues that can commonly limit accuracy in routine use are (i) scanning-orientation dependence, a change in measured response when a film is rotated on a flatbed scanner, and (ii) the lateral response artefact (LRA), a position-dependent non-uniformity in scanner response across the scanner bed. Both effects arise from the interaction between the film's optical properties (including polarization and layered structure) and flatbed scanner optics/illumination, and both can be partially mitigated but not always eliminated by protocol and correction methods; therefore, they continue to be central concerns in radiochromic film dosimetry.

i) Orientation Effect: The orientation effect is the difference of OD depending on the orientation of the film placement on the scanner bed. It arises because the film's active diacetylene crystals and the scanner optics generate an angular dependence of measured optical density, which mandates strict scanning protocoling. The manufacturer of Gafchromic film, ISP, recommends scanning Gafchromic film always in the landscape direction, which means placing the film long axis (films typically supplied as rectangular) parallel to the scanning plane. Butson et al [51] found that the effect can vary from 4%-15% with a standard desktop scanner. Two other studies [43,73] also found a similar magnitude of orientation effect. In a further study by Butson et al [74], the orientation effect was found to be relatively independent of absorbed dose or film darkness within the limit of uncertainty. It was also independent of scanning resolution from 75 dpi to 1200 dpi. However, there was a variation for different scanner types.

ii) Lateral Response Artefact: The lateral response artefact (LRA)) results in a typical upward-bent profile across the scanner width for a uniformly exposed film and was first reported by Menegotti et al [83] and Saur et al [73]. It is defined as the difference of OD at the lateral edges compared to that at the centre of the scan frame. At a given lateral position, this difference increases with increasing dose delivered to the film piece. The magnitude of the LRA effect is reported up to 20% for 2 Gy of dose delivered and films scanned by a standard desktop scanner [20,30,43,81,82,87]. The LRA effect cannot be removed by simple user protocol and has to be corrected empirically for specific film-scanner combinations and can also vary with dose level to the film, requiring further

corrections. To deal with these issues, it requires a more systematic quantitative understanding and approach to the corrections, ideally reducing the size of the effect., or eliminating it. Finding a solution for this is a significant area of study in the radiochromic film research and clinical practice communities.

The source of both orientation and LRA effects is from the film itself, but then enhanced by the properties of flatbed scanners, as detailed below:

i) Contribution from film construction: The active component of Gafchromic films is lithium-10,12-pentacosa diynoate (LiPCDA) in crystal form, where the crystals are about 15μm in length and 2μm in width in EBT3 (Schoenfeld2014). Several studies [29,51,81] showed that Gafchromic film introduces polarisation of the light that is used for scanning the film. Light polarisation and anisotropic scattering from rod-like organic structures lying in an ordered assembly are described by several authors [82,83,88]. Gafchromic films are expected to have similar properties, as the needle-like crystals predominantly lie along the short side of the film [88,89]. The rod-like structures combine with each other to create even longer structures upon receiving radiation [44,88]. When the light from the scanner passes through, the rods act as excitable electronic oscillators, whose degree of excitation depends on polarisation of the incident light. The wavelets emitted from these oscillators align with the rod-like structures in the preferred direction which causes anisotropic scattering and re-polarisation of the light [88]. An investigation on Gafchromic film by Butson et al [90] stated that the orientation of the crystals behaves like a grating which only allows a certain orientation of electromagnetic waves. The light polarisation by the film and the scanner components is responsible for the two main problems mentioned for film dosimetry [30,74,81,88,90] i.e. orientation and LRA effects. Another issue for radiochromic film use may be anisotropic scattering from the active ingredients [88], which is supported by the Rayleigh-Debye-Gans theory of light scattering from rod-like structures, which is a part of the reason for the LRA effect. Van Battum et al [91] argued that anisotropic scattering cannot be a big contributor to the LRA effect.

ii) Contribution from Scanner construction

   a. Path length effect: the optical path length of a light ray towards the camera increases with increasing divergence and distance towards the edges in the x direction from the centre, resulting in increase in apparent OD. Van Battum et al [91] explained the theory and showed that OD increases by up to 3% for EBT2 and EBT3 Gafchromic films at the edges in the x-direction. The change in optical density is given by the equation

$$\frac{OD_d}{OD_{dx}} = \sqrt{1 - (sin\frac{\propto}{n})^2}$$

Where OD_d is the optical density for the light rays incident perpendicular to the film, OD_{dx} is the optical density for light rays incident at distance x from the centre at an angle ∝ and n the refractive index of the film. The definition of angle ∝ is given in the Figure 2-2 below, redrawn from Van Battum et al [91].

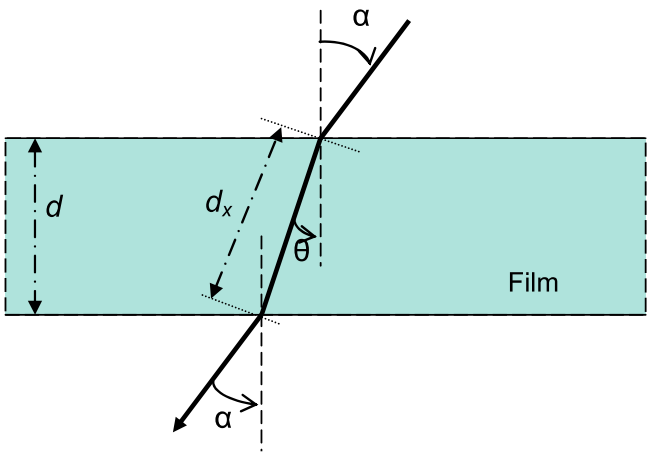

Figure 2-2: Origin of path length effect

Another study [81] verified and supported the path length effect. The path length effect is independent of dose delivered to the film.

b. Mirrors: Schoenfeld et al [88] stated that the light incident angles from source to mirror system are far from the Brewster angle and for this reason there will be no polarisation resulting from the mirrors in the flatbed scanner. In this study an Epson 1000XL was investigated. The scan area of this scanner is of A3 size. However, Van Battum [91] stated that an A4 size scanner has angles related to the mirror system close to Brewster angle and does cause some polarisation of the light, but the study didn't investigate the magnitude of it. Schoenfeld et al [81] later agreed that there is an influence of the mirror system in light polarisation and thus in LRA effect but none of the studies investigated its degree of effect separately.

c. Camera: Schoenfeld et al [88] stated that the CCD camera cannot record all the scattered light especially from the edges of the illuminated scanned regions at the ends of the short side of the scanner bed which causes an artificial enhancement of optical density towards the ends. This shortcoming is the combined result of focal

length of the camera lens and its close placement to the film compared to the size of the scanner bed.

2.7 Available solutions for these problems

i) Orientation effect: The most straightforward way to overcome this problem is to keep the calibration film pieces and the measurement film pieces in the same orientation on the scanner bed through all steps of the process, by marking the film pieces before cutting and using the markings as reference for the orientation. It is also necessary to make sure the pre-exposure scanning for background and post exposure scanning are in the same orientation.

ii) LRA effect: A lot of studies have been done to find an effective and efficient way to minimise this effect. Menegotti et al [83] used a single Gafchromic film for dose calibration and also for creating a dose matrix, which is to be used for correcting LRA in future measurements. Micke et al [84] proposed a multichannel system to correct nonuniformity. This approach separates a scanned film signal into two parts, one is dose dependent and the other is dose independent. The dose independent part of the signal contains information related to film thickness, film response differences in the coating, scanner noise and any other artefacts caused by the scanner including its contribution to the LRA. This study showed that multichannel film dosimetry approach reduced LRA more effectively than a single channel film dosimetry method. Butson et al [33] used the reflective mode of a flatbed scanner with matte backing instead of normal shiny backing to minimise the nonuniformity of Gafchromic film dosimetry without applying any correction factor. This method brought the overall nonuniformity within 1%. Zhu et al [92] and Klassen et al [29] used a "Double Exposure Technique (DET)" for radiochromic film dosimetry. In this method the film was first irradiated with a uniform known dose and a pixel-by-pixel sensitivity matrix was generated which was applied to correct the response of the same film pixel by pixel after irradiating with unknown dose. Roozen et al [77] proposed a "Multiple Exposure Technique (MET)", which involves two homogenous known dose exposures being given to the same film before and after the irradiation of dose to be measured. Two sensitivity matrices were created, and an average of these two matrices was applied to the response of unknown dose. According to this study MET not only corrects the variation in response in different parts of the film but also corrects the non-linearity of the response of the film with dose. For a 15 x 15 cm^2 field size, this technique showed a dose difference of 1.9% from that measured by an ionisation chamber. Poppinga et al [93] used a correction method for the LRA effect by calculating the effect for every pixel along the x-axis, where the LRA effect happens, and then introducing a correction factor to the OD calculation formula. The

study demonstrated that it gives a more accurate correction than a multichannel system. Lewis et al [20] introduced an updated multichannel dosimetry system to have more accurate results. This study reported that LRA is scanner specific. That means, for the same radiochromic film with the same dose, the LRA effect is different for different scanners. Bennie et al [31] proposed a method using free software ImageJ, instead of expensive commercial software, such as the "FilmQA Pro" which has been used by Micke et al [84] and Lewis et al [20]. Bennie et al [31] also proposed using the green channel, instead of the mostly used red channel in other single channel studies. This brought the uniformity problem within acceptable tolerance levels in clinical use. The method is applicable to both transmission mode and reflective mode, with normal white reflective backing. Recently Miura et al [94] proposed a method of image stitching to reduce the LRA effect (for a brief explanation of this process please see section 1.7). This method improved gamma analysis (3%/2mm) of an 18 cm x 18 cm open field of 2 Gy, 4 Gy and 6 Gy from 67.8%, 66.2 % and 35.9% to 95.7%, 95.5% and 91.8% respectively. All such methods require additional measurement steps and/or applying corrections, which makes practical processes more complex and introduces potential uncertainties into the film evaluation process and hence into the doses estimated.

2.8 Rationale for the current work, arising from the literature review and from clinical radiotherapy dosimetry needs:

The literature review demonstrates that foundational studies established correction approaches (e.g. centre-normalisation matrices, parabola fitting, and multichannel methods) to reduce LRA and orientation bias, and contemporary consensus/guidance documents summarise recommended scanning protocols and uncertainty budgets for film dosimetry. Nevertheless, recent work has shown that (i) the magnitude and character of LRA and orientation dependence vary substantially with scanner model and unit, (ii) scanner optical components (lens focal length, mirror systems and scanner bed) materially influence the effect, and (iii) successive generations of film (EBT3 vs EBT-XD vs EBT4 / MD-V3) modifies, but does not universally eliminate, these artifacts. This recent evidence indicates that a one-size correction is insufficient: scanner and film-specific characterisation remains necessary, since the effects have not been investigated systematically or in ways that sufficiently well identify/quantify the various contributions to effects separately and independently.

Thus, although the field has recognised and addressed LRA and orientation effects for many years, three important practical gaps remain which directly motivate the experiments and papers in this thesis:

1. Scanner component-level causes of LRA are not fully quantified. Flatbed scanners contribute to the LRA effect in three ways; causing pathlength effect, introducing more polarisation via the mirror system and the inability to capture all the light by its light

detection system. Several prior studies corrected LRA empirically, but few have systematically separated contributions from individual scanner optical components (lens focal length, mirror geometry, and scanner bed) to the overall LRA behaviour. Understanding component-level causes is essential to move towards hardware-focussed mitigation strategies rather than purely empirical, scanner-specific correction maps. Targeted experiments are required to isolate these contributions.

2. Scanner interchangeability and model-specific differences are under-documented for routine clinical hardware. Many centres use routine consumer/user flatbed scanners (most commonly, Epson models) for film readout (including prosumers, users or researchers who may modify scanners for customised use or participate in the scanner development process). It is practical and frequently assumed that newer models are interchangeable with older ones, but there has been limited formal comparison across widely used models (for example, the V700 vs V800). Without such comparison, sites risk unquantified shifts in LRA/orientation behaviour when upgrading hardware. Direct, systematic inter-model comparison is needed to inform clinical practice.

3. New generations of film require re-characterisation. As manufacturers introduce new film products (e.g. EBT4, MD-V3), the interplay between film microstructure and scanner optics can change, so earlier correction factors and uncertainty estimates may not remain valid. Comparative characterisation across film types is therefore necessary to update uncertainty budgets and best-practice guidance. Comparative studies of current film types are required to address this.

Based on these findings and identified gaps, the overall purpose of this work is to investigate the scanner and scanner component effects further for practical systems that are widely used in clinical radiotherapy dosimetry. This largely-experimental work is intended to provide useful quantitative data and greater understanding of the effects and to find ways to minimise their impact in radiotherapy applications, by considering how changing and/or modifying any component/s of a flatbed scanner might improve the situation.

In addition, manufacturers such as ISP are continuously modifying and evolving their radiochromic film products (e.g. Gafchromic films) to reduce or eliminate the film contributions to overall non-uniformity of radiochromic film dosimetry. EBT-XD is a relatively new product available on the market and Schoenfeld et al [81] showed that these films cause less light polarisation than that of EBT3 films, so less LRA is expected. Other (new generation) films have very recently been made available, as outlined above, i.e. EBT4 and MD-V3 and there is less information in the scientific literature about them, particularly the new MD-V3. The relevant characteristics of the currently widely used films and these new generation films are comprehensively compared, again to provide useful quantitative data, but also to form the basis of recommendations for use in different applications.

The overall aim is to make radiochromic film dosimetry more straightforward and easier to use in clinical practice, with no (or minimal) correction factors needed and hence reduced uncertainties in clinical dosimetry using films.

2.9 References

[1] M. Miften, A. Olch, D. Mihailidis, J. Moran, T. Pawlicki, A. Molineu, H. Li, K. Wijesooriya, J. Shi, P. Xia, N. Papanikolaou, D.A. Low, Tolerance limits and methodologies for IMRT measurement-based verification QA: Recommendations of AAPM Task Group No. 218, Med Phys 45 (2018) e53–e83. https://doi.org/10.1002/mp.12810.

[2] M.Alber, S.Broggi, C. De Wagter, I. Eichwurzel, P. Engstrom, C.Fiorino, D.Georg, G. Hartmann, T. Knoos, A. Leal, H. Marijnissen, B. Mijnheer, M. Paiusco, F. Sanchez-Doblado, R. Schmidt, M. Tomsej, H. Welleweerd, Guideline for verification of IMRT, 1st Edition, ESTRO, Brussels, 2008.

[3] MapCHECK3: The New Benchmark for 2D IMRT QA, Sun Nuclear, Melbourne, FL, n.d. https://www.sunnuclear.com/uploads/documents/datasheets/MapCHECK3_051118.pdf.

[4] ArcCheck The benchmark for 3D pre-treatment QA, (n.d.). https://www.sunnuclear.com/uploads/documents/datasheets/ArcCHECK_3DVH_090723.pdf.

[5] Delta4 Phantom+, (n.d.). delta4family.com.

[6] SRS Mapcheck, (n.d.). https://www.sunnuclear.com/uploads/documents/datasheets/SRS-MapCHECK-Product-Datasheet.pdf.

[7] OCTAVIUS 4D, (2019). https://www.ptwdosimetry.com/en/products/octavius-detector-1500.

[8] N. Dogan, B.J. Mijnheer, K. Padgett, A. Nalichowski, C. Wu, M.J. Nyflot, A.J. Olch, N. Papanikolaou, J. Shi, S.M. Holmes, J. Moran, P.B. Greer, AAPM Task Group Report 307: Use of EPIDs for Patient-Specific IMRT and VMAT QA, Med Phys 50 (2023) e865–e903. https://doi.org/10.1002/mp.16536.

[9] B.J. Zwan, M.P. Barnes, T. Fuangrod, C.J. Stanton, D.J. O'connor, P.J. Keall, P.B. Greer, An EPID-based system for gantry-resolved MLC quality assurance for VMAT, J Appl Clin Med Phys 17 (2016) 348–365.

[10] K. Hsier, C. Wu, M. Radevic, D. Asche, J. Bareng, A. Kroner, J. Lehmann, M. Logsdon, S. Dutton, S. Rosenthal, SU-E-T-164: Clinical Implementation of ASi EPID Panels for QA of IMRT/VMAT Plans, (2012) 3740–3741.

[11] A. Niroomand-Rad, S.T. Chiu-Tsao, M.P. Grams, D.F. Lewis, C.G. Soares, L.J. Van Battum, I.J. Das, S. Trichter, M.W. Kissick, G. Massillon-JL, P.E. Alvarez, M.F. Chan, Report of AAPM Task Group 235 Radiochromic Film Dosimetry: An Update to TG-55, Med Phys 47 (2020) 5986–6025. https://doi.org/10.1002/mp.14497.

[12] E.Y.L. Marroquin, J.A.H. Gonzalez, M.A.C. Lopez, J.E.V. Barajas, O.A. García-Garduño, Evaluation of the uncertainty in an EBT3 film dosimetry system utilizing net optical density, J Appl Clin Med Phys 17 (2016) 466–481.

[13] S. Devic, N. Tomic, D. Lewis, Reference radiochromic film dosimetry: Review of technical aspects, Physica Medica 32 (2016) 541–556. https://doi.org/10.1016/j.ejmp.2016.02.008.

[14] C.G. Soares, Radiochromic film dosimetry, Radiat Meas 41 (2006). https://doi.org/10.1016/j.radmeas.2007.01.007.

[15] T. Kairn, N. Hardcastle, J. Kenny, R. Meldrum, W.A. Tomé, T. Aland, EBT2 radiochromic film for quality assurance of complex IMRT treatments of the prostate: Micro-collimated IMRT, RapidArc, and TomoTherapy, Australas Phys Eng Sci Med 34 (2011) 333–343. https://doi.org/10.1007/s13246-011-0087-z.

[16] T. Aland, T. Kairn, J. Kenny, Evaluation of a Gafchromic EBT2 film dosimetry system for radiotherapy quality assurance, Australas Phys Eng Sci Med 34 (2011) 251–260. https://doi.org/10.1007/s13246-011-0072-6.

[17] Y. Watanabe, G.N. Patel, P. Patel, Evaluation of a new self-developing instant film for imaging and dosimetry, Radiat Prot Dosimetry 120 (2006) 121–124. https://doi.org/10.1093/rpd/nci551.

[18] A. Mittal, N. Gopishankar, J. Koleda, A.K. Verma, P. Kumar, Development and characterization of urethane substituted diacetylene based radiochromic films for medical radiation dosimetry, Radiation Physics and Chemistry 177 (2020) 109119. https://doi.org/10.1016/j.radphyschem.2020.109119.

[19] A. Rink, Point-based ionizing radiation dosimetry using radiochromic materials and a fibreoptic readout system, Methods (2008). https://doi.org/10.1017/CBO9781107415324.004.

[20] D. Lewis, M.F. Chan, Correcting lateral response artifacts from flatbed scanners for radiochromic film dosimetry, Med Phys 42 (2015) 416–429. https://doi.org/10.1118/1.4903758.

[21] A.L. Palmer, D. Nash, W. Polak, S. Wilby, Evaluation of a new radiochromic film dosimeter, Gafchomic EBT4, for VMAT, SABR and HDR treatment delivery verification, Phys Med Biol 68 (2023). https://doi.org/10.1088/1361-6560/aceb48.

[22] F. Guan, H. Chen, E. Draeger, Y. Li, R. Aydin, C. J.Tien, Z. Chen., Characterization of Gafchromic EBT4 film with clinical kV/MV photons and MeV electrons, Prec Radiat Oncol. 7 (2023) 84–91. https://doi.org/10.1002/pro6.1204.

[23] Y. Akdeniz, Comparative analysis of dosimetric uncertainty using Gafchromic™ EBT4 and EBT3 films in radiochromic film dosimetry, Radiation Physics and Chemistry 220 (2024). https://doi.org/10.1016/j.radphyschem.2024.111723.

[24] H. Miura, S. Ozawa, T. Okazue, T. Enosaki, Y. Nagata, Characterization of scanning orientation and lateral response artifact for EBT4 Gafchromic film, J Appl Clin Med Phys 24 (2023). https://doi.org/10.1002/acm2.13992.

[25] Ashland Specialty Ingredients, DGafcrhomic Dosimetry media, Type EBT-4, (2022). https://www.ashland.com/file_source/Ashland/Documents/Gafchromic EBT4 brochure.pdf.

[26] Ashland Specialty Ingredients, Gafcrhomic Dosimetry media, Type MD-V3, (2021). http://www.gafchromic.com/documents/gafchromic-mdv3.pdf.

[27] Ashland Specialty Ingredients, Gafcrhomic Dosimetry media, Type EBT-3, (n.d.). http://www.gafchromic.com/documents/EBT3_Specifications.pdf.

[28] Ashland Specialty Ingredients, Gafcrhomic Dosimetry media, Type EBT-XD, (n.d.). http://www.gafchromic.com/documents/EBTXD_Specifications_Final.pdf.

[29] N. V. Klassen, L. Van Der Zwan, J. Cygler, GafChromic MD-55: Investigated as a precision dosimeter, Med Phys 24 (1997) 1924–1934. https://doi.org/10.1118/1.598106.

[30] S. Devic, J. Seuntjens, E. Sham, E.B. Podgorsak, C.R. Schmidtlein, A.S. Kirov, C.G. Soares, Precise radiochromic film dosimetry using a flat-bed document scanner, Med Phys 32 (2005) 2245–2253. https://doi.org/10.1118/1.1929253.

[31] N. Bennie, P. Metcalfe, Practical IMRT QA dosimetry using Gafchromic film: a quick start guide, Australas Phys Eng Sci Med 39 (2016) 533–545. https://doi.org/10.1007/s13246-016-0443-0.

[32] Y. Hu, Y. Wang, G. Fogarty, G. Liu, Developing a novel method to analyse Gafchromic EBT2 films in intensity modulated radiation therapy quality assurance, Australas Phys Eng Sci Med 36 (2013) 487–494. https://doi.org/10.1007/s13246-013-0232-y.

[33] E. Butson, H. Alnawaf, P.K.N. Yu, M. Butson, Scanner uniformity improvements for radiochromic film analysis with matt reflectance backing, Australas Phys Eng Sci Med 34 (2011) 401–407. https://doi.org/10.1007/s13246-011-0086-0.

[34] T. Yao, L.H. Luthjens, A. Gasparini, J.M. Warman, A study of four radiochromic films currently used for (2D) radiation dosimetry, Radiation Physics and Chemistry 133 (2017) 37–44. https://doi.org/10.1016/j.radphyschem.2016.12.006.

[35] E. Spelleken, S.B. Crowe, B. Sutherland, C. Challens, T. Kairn, Accuracy and efficiency of published film dosimetry techniques using a flat-bed scanner and EBT3 film, Australas Phys Eng Sci Med 41 (2018) 117–128. https://doi.org/10.1007/s13246-018-0620-4.

[36] T. Santos, T. Ventura, M. do C. Lopes, A review on radiochromic film dosimetry for dose verification in high energy photon beams, Radiation Physics and Chemistry 179 (2021) 109217. https://doi.org/10.1016/j.radphyschem.2020.109217.

[37] M. Butson, A. Niroomand-Rad, Historical background, development and construction of radiochromic films, in: Radiochromic Film Role and Application in Radiation Dosimetry, 2018: pp. 7–32.

[38] S. Reinhardt, M. Hillbrand, J.J. Wilkens, W. Assmann, Comparison of Gafchromic EBT2 and EBT3 films for clinical photon and proton beams, Med Phys 39 (2012) 5257–5262. https://doi.org/10.1118/1.4737890.

[39] M.J. Butson, P.K.N. Yu, T. Cheung, H. Alnawaf, Energy response of the new EBT2 Radiochromic film to X-ray radiation, Radiat Meas 45 (2010) 836–839. https://doi.org/10.1016/j.radmeas.2010.02.016.

[40] B. Arjomandy, R. Tailor, A. Anand, N. Sahoo, M. Gillin, K. Prado, M. Vicic, Energy dependence and dose response of Gafchromic EBT2 film over a wide range of photon, electron, and proton beam energies, Med Phys 37 (2010) 1942–1947. https://doi.org/10.1118/1.3373523.

[41] J. Sorriaux, A. Kacperek, S. Rossomme, J.A. Lee, D. Bertrand, S. Vynckier, E. Sterpin, Evaluation of Gafchromic® EBT3 films characteristics in therapy photon, electron and proton beams, Physica Medica 29 (2013) 599–606. https://doi.org/10.1016/j.ejmp.2012.10.001.

[42] G. Massillon-JL, A. Cabrera-Santiago, N. Xicohténcatl-Hernández, Relative efficiency of Gafchromic EBT3 and MD-V3 films exposed to low-energy photons and its influence on the energy dependence, Physica Medica 61 (2019) 8–17. https://doi.org/10.1016/j.ejmp.2019.04.007.

[43] B.D. Lynch, J. Kozelka, M.K. Ranade, J.G. Li, W.E. Simon, J.F. Dempsey, Important considerations for radiochromic film dosimetry with flatbed CCD scanners and EBT GAFCHROMIC® film, Med Phys 33 (2006) 4551–4556. https://doi.org/10.1118/1.2370505.

[44] A. Rink, D.F. Lewis, S. Varma, I.A. Vitkin, D.A. Jaffray, Temperature and hydration effects on absorbance spectra and radiation sensitivity of a radiochromic medium, Med Phys 35 (2008) 4545–4555. https://doi.org/10.1118/1.2975483.

[45] A. Rink, D.F. Lewis, S. Varma, I.A. Vitkin, D.A. Jaffray, Temperature and hydration effects on absorbance spectra and radiation sensitivity of a radiochromic medium, Med Phys 35 (2008) 4545–4555. https://doi.org/10.1118/1.2975483.

[46] H. Yamada, A. Parker, Gafchromic™ MD-V3 and HD-V2 film response depends little on temperature at time of exposure, Radiation Physics and Chemistry 196 (2022) 1–7. https://doi.org/10.1016/j.radphyschem.2022.110101.

[47] H. Yamada, A. Parker, The influence of ambient temperature in Gafchromic™ MD-V3 and HD-V2 film response during 60Co gamma irradiation and optical density readings for doses from 10 to 1000 Gy, Radiation Physics and Chemistry (2025) 113356. https://doi.org/10.1016/j.radphyschem.2025.113356.

[48] A. Rink, I.A. Vitkin, D.A. Jaffray, Intra-irradiation changes in the signal of polymer-based dosimeter (GAFCHROMIC EBT) due to dose rate variations, Phys Med Biol 52 (2007). https://doi.org/10.1088/0031-9155/52/22/N03.

[49] G. Twork, A. Sarfehnia, SU-E-T-88: Evaluation of the Dose-Rate Dependency of GAFCHROMIC EBT3, Med Phys 40 (2013) 223–224. https://doi.org/10.1118/1.4814523.

[50] S. Oyewale, S. Ahmad, I. Ali, SU-E-T-85: Dose Rate and Energy Dependence of EBT, EBT2, EDR2 Films, and Mapcheck2 Diode Arrays in Beam Profiles from a Varian TrueBeam System, Med Phys 39 (2012) 3722. https://doi.org/10.1118/1.4735142.

[51] M.J. Butson, P.K.N. Yu, T. Cheung, P. Metcalfe, Radiochromic film for medical radiation dosimetry, Materials Science and Engineering R: Reports 41 (2003) 61–120. https://doi.org/10.1016/S0927-796X(03)00034-2.

[52] B.C. Ferreira, M.C. Lopes, M. Capela, Evaluation of an Epson flatbed scanner to read Gafchromic EBT films for radiation dosimetry, Phys Med Biol 54 (2009) 1073–1085. https://doi.org/10.1088/0031-9155/54/4/017.

[53] B.S. Rosen, Radiochromic film digitisers, in: Radiochromic Film: Role and Application in Rodiation Dosimetry, 2018: pp. 61–78.

[54] J.F. Dempsey, D.A. Low, A.S. Kirov, J.F. Williamson, Quantitative optical densitometry with scanning-laser film digitizers, Med Phys 26 (1999) 1721–1731. https://doi.org/10.1118/1.598664.

[55] G.R. Gluckman, L.E. Reinstein, Comparison of three high-resolution digitizers for radiochromic film dosimetry, Med Phys 29 (2002) 1839–1846. https://doi.org/10.1118/1.1485056.

[56] S. Devic, J. Seuntjens, G. Hegyi, E.B. Podgorsak, C.G. Soares, A.S. Kirov, I. Ali, J.F. Williamson, A. Elizondo, Dosimetric properties of improved GafChromic films for seven different digitizers, Med Phys 31 (2004) 2392–2401. https://doi.org/10.1118/1.1776691.

[57] J.E. Matney, B.C. Parker, D.W. Neck, G. Henkelmann, I.I. Rosen, Evaluation of a commercial flatbed document scanner and radiographic film scanner for radiochromic EBT film dosimetry, J Appl Clin Med Phys 11 (2010) 198–208. https://doi.org/10.1120/jacmp.v11i2.3165.

[58] T. Aland, E. Jhala, T. Kairn, J. Trapp, Film dosimetry using a smart device camera: A feasibility study for point dose measurements, Phys Med Biol 62 (2017) N506–N515. https://doi.org/10.1088/1361-6560/aa8b36.

[59] M.A. Piliero, F. Pupillo, S. Presilla, A diffuse reflectance spectrophotometer for radiation dosimetry of EBT3 GAFchromic films, Radiat Meas 154 (2022) 106777. https://doi.org/10.1016/j.radmeas.2022.106777.

[60] B.S. Rosen, C.G. Soares, C.G. Hammer, K.A. Kunugi, L.A. Dewerd, A prototype, glassless densitometer traceable to primary optical standards for quantitative radiochromic film dosimetry, Med Phys 42 (2015) 4055–4068. https://doi.org/10.1118/1.4922134.

[61] M.K. Ranade, J.G. Li, R.S. Dubose, J. Kozelka, W.E. Simon, J.F. Dempsey, A prototype quantitative film scanner for radiochromic film dosimetry, Med Phys 35 (2008) 473–479. https://doi.org/10.1118/1.2828203.

[62] G. Jiménez-Aviles, M.A. Camacho-López, O.A. García-Garduño, K. Isaac-Olivé, Vision-based radiochromic film densitometer: Setup and uncertainty analysis for its potential clinical usage, Journal of Instrumentation 16 (2021). https://doi.org/10.1088/1748-0221/16/05/P05006.

[63] H. Bantan, H. Yasuda, Reading of gafchromic EBT-3 film using an overhead scanner, Biomed Phys Eng Express 10 (2024). https://doi.org/10.1088/2057-1976/ad5cf8.

[64] A. Rink, I. Alex Vitkin, D.A. Jaffray, Characterization and real-time optical measurements of the ionizing radiation dose response for a new radiochromic medium, Med Phys 32 (2005) 2510–2516. https://doi.org/10.1118/1.1951447.

[65] P. Casolaro, L. Campajola, G. Breglio, S. Buontempo, M. Consales, A. Cusano, A. Cutolo, F. Di Capua, F. Fienga, P. Vaiano, Real-time dosimetry with radiochromic films, Sci Rep 9 (2019) 1–11. https://doi.org/10.1038/s41598-019-41705-0.

[66] S. Mena, N. Karkour, V. Alaphilippe, J.P. Botero, M. Jiménez, D. Linget, L. Gibelin, V. Le Ven, A. Marquet, S. Mellouh, E. Josson, W. Benassou, X. Muñoz-Berbel, G. Guirado, C. Guardiola, New opto-electro-mechanical sensor for two-dimensions dosimetry based on radiochromic films, Sci Rep 13 (2023) 1–11. https://doi.org/10.1038/s41598-023-43387-1.

[67] A. Dutreix, When and how can we improve precision in radiotherapy?, Radiotherapy and Oncology 2 (1984) 275–292. https://doi.org/10.1016/S0167-8140(84)80070-5.

[68] E. Aird, S. Bentzen, M. Coffey, I. Gomola, C. Hamilton, B. Healy, J. Hendry, G. Ibbott, J. Izewska, S. Korreman, T. Kron, A. Meghzifene, B. Mijnheer, S. Nag, A. Stewart-Lord, K. Tanderup, D. van der Merwe, G. Vandevelde, J. Van dyk, J. Venselaar, D. Verellen, A. Wambersie, E. Zubizarrwta, Accuracy requirements and uncertainties in radiiotherapy, Vienna, 2016. http://www.iaea.org/Publications/index.html.

[69] ICRU Report 24. Determination of absorbed dose in a patient irradiated by beams of x or gamma rays in radiotherapy procedures, Bethesda, Maryland, 1976.

[70] H. Svensson., Quality assurance in radiotherapy: Physical aspects, Int J Radiat Oncol Biol Phys 10 (1983) 59–65.

[71] D. Thwaites, Accuracy required and achievable in radiotherapy dosimetry: Have modern technology and techniques changed our views?, J Phys Conf Ser 444 (2013). https://doi.org/10.1088/1742-6596/444/1/012006.

[72] L.J. Van Battum, D. Hoffmans, H. Piersma, S. Heukelom, Accurate dosimetry with GafChromic™ EBT film of a 6 MV photon beam in water: What level is achievable?, Med Phys 35 (2008) 704–716. https://doi.org/10.1118/1.2828196.

[73] S. Saur, J. Frengen, GafChromic EBT film dosimetry with flatbed CCD scanner: A novel background correction method and full dose uncertainty analysis, Med Phys 35 (2008) 3094–3101. https://doi.org/10.1118/1.2938522.

[74] M.J. Butson, T. Cheung, P.K.N. Yu, Scanning orientation effects on Gafchromic EBT film dosimetry, Australas Phys Eng Sci Med 29 (2006) 281–284. https://doi.org/10.1007/BF03178579.

[75] M. Martišíková, B. Ackermann, O. Jäkel, Analysis of uncertainties in Gafchromic® EBT film dosimetry of photon beams, Phys Med Biol 53 (2008) 7013–7027. https://doi.org/10.1088/0031-9155/53/24/001.

[76] M. Fuss, E. Sturtewagen, C. De Wagter, D. Georg, Dosimetric characterization of GafChromic EBT film and its implication on film dosimetry quality assurance, Phys Med Biol 52 (2007) 4211–4225. https://doi.org/10.1088/0031-9155/52/14/013.

[77] K. Roozen, T. Kron, A. Haworth, R. Franich, Evaluation of EBT radiochromic film using a multiple exposure technique, Australas Phys Eng Sci Med 34 (2011) 281–289. https://doi.org/10.1007/s13246-011-0067-3.

[78] T. Cheung, M.J. Butson, P.K.N. Yu, Post-irradiation colouration of Gafchromic EBT radiochromic film, Phys Med Biol 50 (2005). https://doi.org/10.1088/0031-9155/50/20/N04.

[79] M. Sharma, R. Singh, S. Dutt, P. Tomar, G. Trivedi, N. Robert, Effect of absorbed dose on post-irradiation coloration and interpretation of polymerization reaction in the Gafchromic EBT3 film, Radiation Physics and Chemistry 187 (2021) 109569. https://doi.org/10.1016/j.radphyschem.2021.109569.

[80] H. Miura, S. Ozawa, F. Hosono, N. Sumida, T. Okazue, K. Yamada, Y. Nagata, Gafchromic EBT-XD film: Dosimetry characterization in high-dose, volumetric-modulated arc therapy, J Appl Clin Med Phys 17 (2016) 312–322. https://doi.org/10.1120/jacmp.v17i6.6281.

[81] A.A. Schoenfeld, S. Wieker, D. Harder, B. Poppe, The origin of the flatbed scanner artifacts in radiochromic film dosimetry - Key experiments and theoretical descriptions, Phys Med Biol 61 (2016) 7704–7724. https://doi.org/10.1088/0031-9155/61/21/7704.

[82] C. Fiandra, U. Ricardi, R. Ragona, S. Anglesio, F. Romana Giglioli, E. Calamia, F. Lucio, Clinical use of EBT model Gafchromic™ film in radiotherapy, Med Phys 33 (2006) 4314–4319. https://doi.org/10.1118/1.2362876.

[83] L. Menegotti, A. Delana, A. Martignano, Radiochromic film dosimetry with flatbed scanners: A fast and accurate method for dose calibration and uniformity correction with single film exposure, Med Phys 35 (2008) 3078–3085. https://doi.org/10.1118/1.2936334.

[84] A. Micke, D.F. Lewis, X. Yu, Multichannel film dosimetry with nonuniformity correction.pdf, Med Phys 38 (2011) 2523–2534.

[85] J.F. Pérez Azorín, L.I. Ramos García, J.M. Martí-Climent, A method for multichannel dosimetry with EBT3 radiochromic films, Med Phys 41 (2014) 1–10. https://doi.org/10.1118/1.4871622.

[86] S. Beveridge, C.H. Clark, P.E. Alvarez, A. Dimitriadis, A. Alves, N. Jornet, M. Hussein, C.C.B. Viegas, B. Reniers, G. Azangwe, An international film dosimetry intercomparison to establish a multi-center audit framework, Med Phys (2024) 9071–9087. https://doi.org/10.1002/mp.17428.

[87] L. Paelinck, W. De Neve, C. De Wagter, Precautions and strategies in using a commercial flatbed scanner for radiochromic film dosimetry, Phys Med Biol 52 (2007) 231–242. https://doi.org/10.1088/0031-9155/52/1/015.

[88] A.A. Schoenfeld, D. Poppinga, D. Harder, K.J. Doerner, B. Poppe, The artefacts of radiochromic film dosimetry with flatbed scanners and their causation by light scattering from radiation-induced polymers, Phys Med Biol 59 (2014) 3575–3597. https://doi.org/10.1088/0031-9155/59/13/3575.

[89] D.F. Lewis, M.F. Chan, Technical Note: On GAFChromic EBT-XD film and the lateral response artifact, Med Phys 43 (2016) 643–649. https://doi.org/10.1118/1.4939226.

[90] M.J. Butson, T. Cheung, P.K.N. Yu, Evaluation of the magnitude of EBT Gafchromic film polarisation effects.pdf, Australas Phys Eng Sci Med 31 (2009) 21–25.

[91] L.J. Van Battum, H. Huizenga, R.M. Verdaasdonk, S. Heukelom, How flatbed scanners upset accurate film dosimetry, Phys Med Biol 61 (2015) 625–649. https://doi.org/10.1088/0031-9155/61/2/625.

[92] Y. Zhu, A.S. Kirov, V. Mishra, A.S. Meigooni, J.F. Williamson, Quantitative evaluation of radiochromic film response for two- dimensional dosimetry, Med Phys 24 (1997) 223–231. https://doi.org/10.1118/1.598068.

[93] D. Poppinga, A.A. Schoenfeld, K.J. Doerner, O. Blanck, D. Harder, B. Poppe, A new correction method serving to eliminate the parabola effect of flatbed scanners used in radiochromic film dosimetry., Med Phys 41 (2014) 1–8. https://doi.org/10.1118/1.4861098.

[94] H. Miura, M. Miyazawa, S. Ozawa, T. Enosaki, M. Kagemoto, Lateral response artifact correction method using image stitching technique in radiochromic film dosimetry, J Appl Clin Med Phys 25 (2024). https://doi.org/10.1002/acm2.14373.

3 Comparative characterisation of different types of Gafchromic films for radiotherapy use.

This chapter consists of the manuscript

Shameem, T., Bennie, N., Butson, M. and D. Thwaites. Comparative characterisation of different types of Gafchromic films for radiotherapy use. *Phys Eng Sci Med* (2025), published online. https://doi.org/10.1007/s13246-025-01596-0

Preface: This chapter addresses the key dosimetric properties (signal-to-noise, orientation sensitivity and LRA susceptibility) of several modern film products (EBT3, EBT-XD, EBT4, MD-V3). This comparison clarifies how film formulation changes the magnitude and practical significance of LRA and orientation effects and therefore informs the need for film-specific calibration and scanner-film pairing. This is the first step of the wider investigation of film plus scanner characteristics to improve understanding and uncertainties ofradiochromic film dosimetry. It shows the evolution of radiochromic films by the vendors towards the improvement of film dosimetry and gives recommendations on applications of specific films.

Authors: Tarafder Shameem[1,2], Nick Bennie[1], Martin Butson[2,3], David Thwaites[2]

[1]North Coast Cancer Institute, Lismore, NSW, Australia; [2]Institute of Medical Physics, School of Physics, University of Sydney, Sydney, NSW, Australia; [3] EPA, NSW, Australia

Abstract

Different types of Gafchromic films, for radiotherapy use, are recommended for different dose ranges. Ashland Specialty Ingredients has aimed to continuously develop its products to improve their practical application. Thus, EBT3 was replaced by EBT4, intended to provide better signal to noise ratio (SNR); while MD-V3 was introduced for use at higher dose ranges, in addition to EBT-XD. At present there are limited studies on MD-V3. This study aimed to investigate some relevant characteristics of EBT4 and MD-V3, compared with those of EBT3 and EBT-XD. The parameters investigated were dose response, optical density change with post-irradiation time, orientation effect, signal to noise ratio, polarisation, and lateral response artefact (LRA). EBT4 is similar to EBT3 however it provides better SNR and larger response change with post-irradiation time. EBT-XD and MD-V3 are recommended by the suppliers for high dose range, although the sensitivity curves show that EBT3 and EBT4 could also be used for relatively high dose ranges. All films have orientation effects, with EBT3 the worst. An important characteristic of MD-V3 is that the LRA remains similar, irrespective of delivered dose. These comparative characteristics are intended to be informative for clinical practice involving Gafchromic film use in high dose therapy applications. Recommendations from this

study are to use EBT4 for dosimetry in lower-dose applications, provided that both calibration and clinical timings post-irradiation are kept similar, while MD-V3 is the preferred film for high-dose procedures.

Keywords: Radiotherapy dosimetry, Radiochromic Film, Gafchromic, EBT3, EBT4, EBT-XD, MD-V3, EPSON scanner, Film dosimetry

3.1 Introduction

Gafchromic EBT-series films, by Ashland Specialty Ingredients, G.P., Bridgewater, NJ, USA, are the most popular radiochromic films used in radiotherapy applications. EBT3 film has, been used widely for patient QA for standard dose ranges, until recently when it has been replaced by EBT4. Like any other dosimeter, EBT film dosimetry systems also come with some drawbacks, such as orientation effects and lateral response artefacts (LRA), which result from the film itself and from the scanner used to read the film. Previous studies explained how the rod-like active ingredients of radiochromic films contribute to these effects, which increase with increasing dose of radiation delivered to the film [1,2]. Dose dependent increase of these effects results from the bonding of the monomers into polymers. Ashland has continuously worked on improving the products to overcome the film-dependent drawbacks. Thus, they introduced EBT-XD in 2015 with shorter active components for use with higher doses and most recently introduced MD-V3, also for higher doses. These two film types, have useful application for dosimetry of high dose patient plans, e.g. for SBRT (Stereotactic Body Radiation Therapy) and SRS (Stereotactic Radiosurgery) radiotherapy. Ashland discontinued EBT3 recently and introduced EBT4, which has the same active ingredient as EBT3 but with different active fluid [3], which resulted in improved signal to noise ratio. Table 3-1 collates the information given in product brochures [4–7] produced by Ashland.

Film	Active layer Thickness	Total Thickness	Size	Dynamic Dose Range	Uniformity
EBT3	28µm	278 µm	8 x 10 inch	0.1 to 20Gy	±2%
EBT4	28 µm	278 µm	8 x 10 inch	0.2 to 10Gy* (optimal dose range)	±2%
EBT-XD	25 µm	275 µm	8 x 10 inch	0.1 to 60Gy	±2%

MD-V3	10 μm	260 μm	5 x 5 inch 8 x 10 inch	1 to 100Gy	±2%

Table 3-1: Physical properties of different Gafchromic films

*In Ashland's specifications only the optimal dose range is quoted for EBT4 which is up to half of EBT3's dynamic dose range. This may influence the quoted improved signal to noise ratio which in turn results in improved uncertainty [3,5].

For dosimetry above 10 Gy Ashland recommends EBT-XD, which has active ingredient lengths (2-4 μm) much smaller than that of EBT3 (15-20 μm) [8] and EBT4. The newest product is MD-V3, which has a significantly extended high dose range compared to the EBT films, however, there is little information available on this film. MD-V3 is supplied in two different standard sizes, 8 inch x 10 inch and 5 inch x 5 inch, and can also be ordered in other customised sizes. In this study, only the 5 inch x 5 inch size films were available. Orientation effects are a well-documented limitation of all radiochromic films. It was anticipated that advancements in film composition would mitigate this issue for MD-V3. The primary cause of the dose dependent variation of the orientation effect is the bonding of active ingredients upon irradiation. Communications with Ashland confirmed that specialised bond-retarding methodology was used to prevent adjacent active ingredients from forming intermolecular bonds upon irradiation (Butson – Private communication – June 2022).

The purpose of this work is to compare various characteristics of these four types of Gafchromic film to provide informative data for practical radiotherapy dosimetry applications. The following parameters were compared:

Dose response: Though all these four types of film use the same active ingredients, the size of the crystals of EBT-XD is different from that of EBT3 and EBT4, which have the same crystal size [3]. Little specific information is available for MD-V3. The active layer composition is different for all four film types which is apparent based on the colour of the films, which have different dyes in this layer. Because of these changes, the dose responses are different. Due to these differences in the active layer the dynamic range of each type of film is different. This study compares the dose response of 6 MV X-rays and 15 MV X-rays for all four types of film in all three colour channels. Film sensitivity as a function of dose is calculated using film dependent dose-pixel value curves as discussed in the Methods section.

Change of optical density with post-irradiation time: Following irradiation, radiochromic films continue to darken over time. After a certain period, the rate of colour change decreases significantly, reaching a state that may be considered relatively stable, less than 1% per day. Various studies [1,5,9–11] have provided recommendations regarding the optimal waiting

period before scanning, to minimize the time-dependent variability in dose response. These have been determined primarily for EBT3 and earlier generations of radiochromic film. This study aims to determine the stabilization time for the four film types, presenting a direct comparative analysis in a single graphical representation.

Orientation effect: This is a well-known effect in radiochromic films, with quantitative studies and theoretical explanations given in a number of publications [1,2,12], mostly for EBT3 and older films. As the active monomers create polymers upon irradiation, this effect increases with dose. There are few studies on EBT-XD [8,13–15] but no study known to the authors on MD-V3 or on EBT4. Given EBT4 has the same active ingredients as EBT3, it is expected that it may be similar in its behaviour. This study compares the percent change in pixel values for two orientations over six different dose levels.

Signal to noise ratio: The main supplier-stated improvement of Gafchromic EBT4 film over EBT3 is the improved signal to noise ratio (SNR) [3,16]. This study investigates this SNR improvement for EBT4, as well the SNR of MD-V3 against EBT-XD, as these two films are recommended for the same high dose range.

Polarisation: There are a number of studies [2,17–19] of sources of polarisation in radiochromic film dosimetry systems, which in turn contributes to both orientation and LRA effects. This study compares the change of pixel values due to film-induced light polarization with respect to dose for all four types of films in all three colour channels.

Lateral response artefacts: A significant challenge in radiochromic film dosimetry is the lateral response artefact (LRA), which refers to variations in pixel values across the film, depending on the position relative to the scanner's centre. In this study, the LRA effect was evaluated for all three colour channels across the four different film types.

3.2 Methods

An Elekta Synergy linear accelerator (Elekta AB (publ), Stockholm, Sweden) was used for all film irradiations, while hand gloves were worn for film handling and processing. Film scanning was performed on an EPSON V800 (Seiko Epson Corp, Nagano, Japan) scanner using the following settings

- Mode: Professional
- Document Type: Film (with Film Area Guide)
- Film Type: Positive Film
- Image Type: 48-bit colour
- Resolution: 75dpi
- No Colour Correction was applied

The scanned images were saved as *.tiff (tagged image file format) which were read and separated into three colour (RGB) channels, each of which were analysed using ImageJ V1.49 software [20]

Dose response: Samples of all four types of film were cut into small pieces of 4 cm x 4 cm and irradiated for doses of 0 Gy, 2 Gy, 5 Gy,10 Gy, 20 Gy, 40 Gy and 100 Gy for 6 MV and 15 MV photon beams. The film pieces were placed in plastic water in a 10 cm x 10 cm field at 10 cm depth, 100 cm SSD with 10 cm backscatter. The film pieces were left in the box for 24 hours before scanning. A ROI of 1 cm x 1 cm was drawn at the centre of the image and mean pixel values were calculated. The results were tabulated and plotted as pixel values vs dose. Sensitivity curves were calculated using the first derivative of each dose response curve, defined by the slope of dose (D) and pixel value (PV), using equation (1), and plotted against dose delivered.

$$\frac{\partial PV}{\partial D} = \frac{PV2 - PV1}{D2 - D1} \qquad \textbf{(1)}$$

Change of optical density with post irradiation time: Four film pieces of 4 cm x 4 cm, one each of the four types of film, were irradiated with 5 Gy using the same settings as described in the Dose Response section. The films were scanned just after irradiation (0 hrs) and then every hour for the next 12 hrs and then after 24 hrs, 48 hrs, 72 hrs and 100 hrs. The mean pixel values of a 1 cm x 1 cm ROI at the centre of the images were calculated in ImageJ. The values were tabulated and plotted as pixel values normalised to 0 hrs against time.

Orientation effect: Films were irradiated for 0 Gy, 2 Gy, 5 Gy, 10 Gy, 20 Gy and 30 Gy. The film pieces were marked to keep track of orientation. As the landscape orientation of Gafchromic films is known to result in higher pixel values [12,21] and MD-V3 is supplied square in shape, the orientation that gives the higher pixel value for MD-V3 was considered as landscape. Scanned images were read in ImageJ and mean pixel values of a 1 cm x 1 cm ROI were recorded for all film types for all dose levels for all three channels. The films were rotated 90^0 and the procedure was repeated. The difference of pixel values of the two orientations was calculated for each film in all three colour channels and normalised to the first orientation (portrait) and plotted against dose levels.

Signal to noise ratio: The same film pieces as used for dose response investigations were also used for this investigation. ROIs of 50 pixels x 50 pixels were drawn at the centre of each film pieces in ImageJ and mean pixel values and standard deviations were recorded. Signal to noise ratios (SNR) were calculated as

$$\textbf{\textit{Signal to noise ratio}}(\textbf{\textit{SNR}}) = \frac{PV}{\sigma} \qquad \textbf{(2)}$$

where PV is the mean pixel value of the ROI and σ is the standard deviation of those pixel values.

Polarisation: Figure 1 shows the setup for the investigation of film-induced polarisation caused by the four types of films used in this study. A Canon 6D (Canon Inc., Tokyo, Japan) camera was used with Canon 24-105 mm lens, having focal length fixed at 50 mm. The distances between different components are shown in the Figure **3-1** where aperture 1 and diffuser are touching each other, as are film, polariser and aperture 2. The size of aperture 1 and aperture 2 are a 6 cm radius circle and a 4 cm x 4 cm square respectively. Each type of film was irradiated for 0 Gy, 2 Gy, 5 Gy, 10 Gy, 20 Gy and 30 Gy. For each film, two photographs were acquired before and after a 90^0 rotation of the linear polarizer. Photos were captured in Canon raw format *.CR2 and converted to *.tiff using the Canon software, "Digital Photo Professional". These were then read and separated into the three colour channels and the mean pixel values found for the image of aperture 2 using ImageJ V1.49 software. The difference between mean pixel values of the two polariser positions for each film was recorded, normalised to the mean pixel values of the first orientation of linear polariser and plotted against the dose values. The LED light source was tested for any inherent polarization by taking two photos with no film, showing that the difference of mean pixel values was negligible, 0.01%, -0.06% and -0.23% in red, green and blue channels respectively.

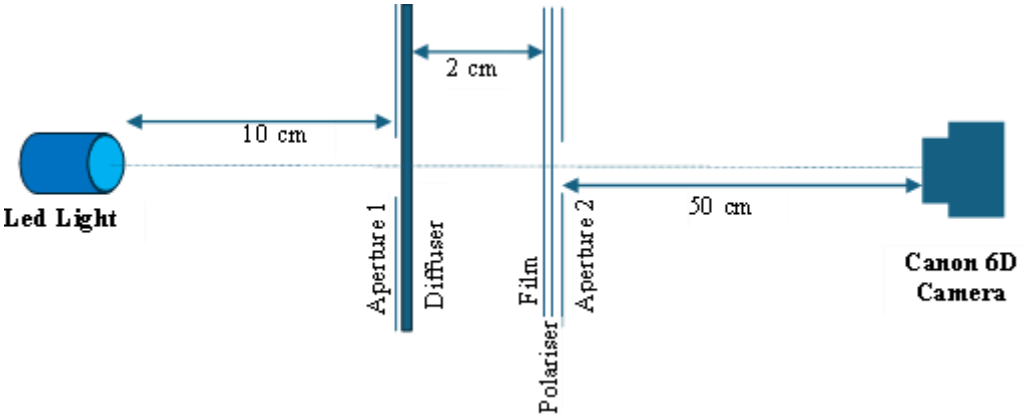

Figure 3-1: Experimental set up for polarisation measurement.

Lateral response artefacts: The EBT3, EBT4 and EBT-XD films, which are 20.3 cm x 25.4 cm in size, were cut along the short side to make 3 cm x 20.3 cm strips. For MD-V3 films, only 5 cm x 5 cm pieces were available for this study. These films came with a mark (cut) on one corner of each film piece to mark orientation. They were cut into 3 cm x 5 cm strips, and this orientation was marked on all strips. The film strips were placed in plastic water of 30 cm x 30 cm in size and irradiated at 90 cm SSD at 10 cm depth with 10 cm backscatter. A 6 MV photon beam was used to irradiate to 500 MU which corresponds to 5.65 Gy in a 40 cm x 40 cm field size. The film strips were kept in the box for 24 hrs before scanning. In ImageJ an average profile was generated across each film for each combination using a rectangular ROI of the

whole film strip but cropped 1 mm in from the film edge. The average profiles for each dose level and each colour channel were normalised to the mean of the central 20 data points for analysis. There is a small beam flatness variation over the films at irradiation in these conditions, however the profiles were not corrected for this, since they were only to be compared in a relative manner and this small variation would be common to all. The normalised pixel values were plotted against distance from the centre of the images.

3.3 Results:

Dose Response: Figure 3-2 presents pixel values normalized to an unirradiated (0 Gy) reference film as a function of delivered dose for 6 MV and 15 MV photon beams in the red channel. The response of EBT3 and EBT4 films is highly similar, while MD-V3 exhibits a similar dose response, though having a little flatter curve, to EBT-XD. No significant differences are observed between the 6 MV and 15 MV dose-response curves for each film type. Although the 6 MV and 15 MV curves for MD-V3 show slightly greater deviation compared to the other three films, the differences remain within the calculated uncertainty, expressed as the standard deviation as a percentage of the mean, which is approximately 0.7% for the selected region of interest (ROI). Other colour channels also showed very similar trends.

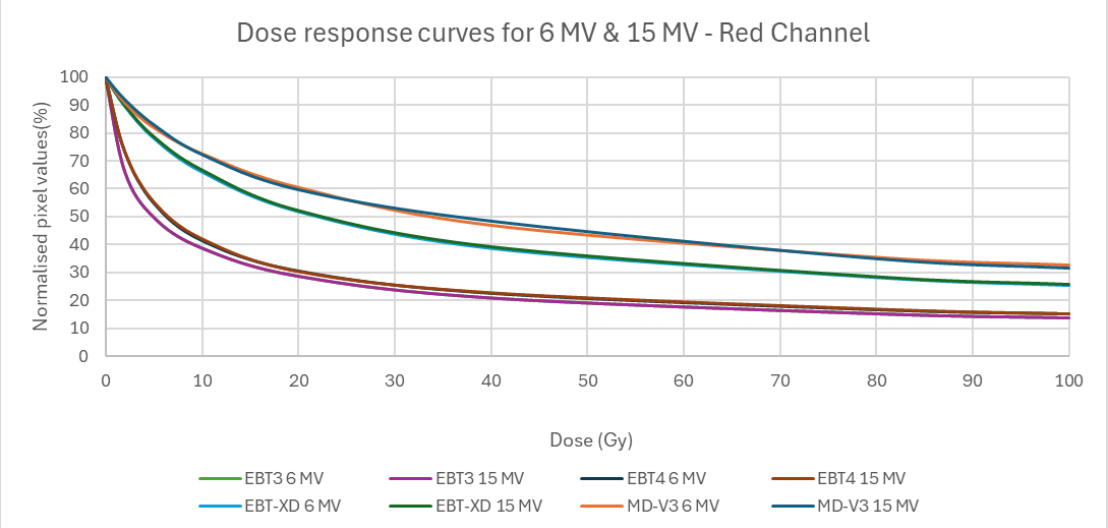

Figure 3-2: Dose response curves for 6 MV and 15 MV for red channel.

Figure **3-3** (a) shows film sensitivity as a function of dose derived from the corresponding dose response data presented in figure 2. It shows the change of slope of the dose response curves with respect to dose. The large scale of the y-axis can obscure the differences between the films. Therefore zoomed-in versions, which are presented as 3b and 3c varies the scale to better show the differences. Figure **3-3** (b) is from 2-10 Gy and Figure **3-3** (c) is from 10 to 100 Gy. As expected, in the lower dose region (up to 10 Gy), EBT3 and EBT4 are more sensitive in change of pixel values to change of dose than are EBT-XD and MD-V3, which are quite similar to each

other. Above 10 Gy, the sensitivity of EBT-XD and MD-V3 is better than that of EBT3 and EBT4, both of which can still be useful up to 40 Gy.

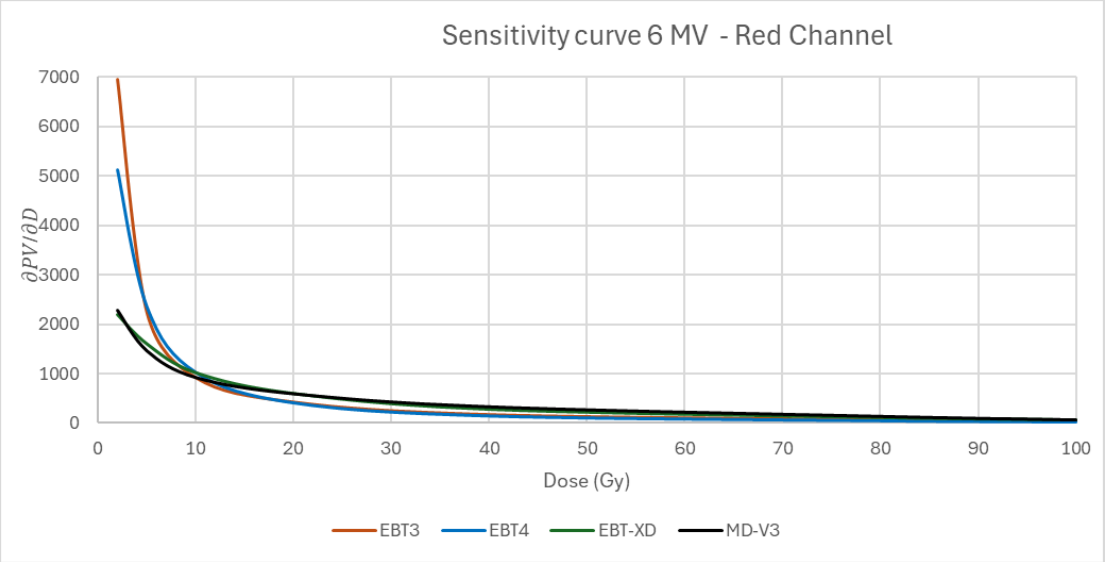

a

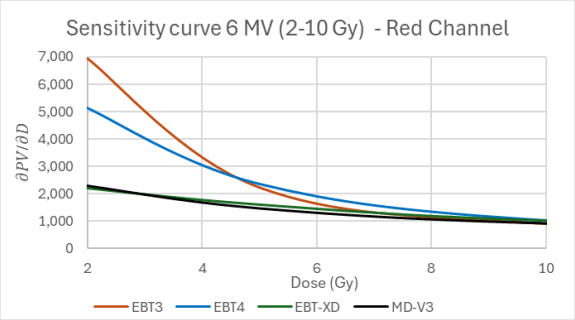

b

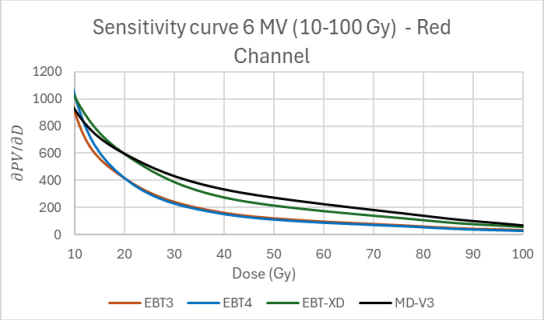

C

Figure 3-3: Sensitivity curves of 6 MV for red channel in (a) and the same graph divided into two for 0-10 Gy in (b) and for 10 – 100 Gy in (c).

Change of optical density with post irradiation time: Figure 3-4 shows the change of pixel values, normalised to 0 hrs (just after irradiation) with respect to time in hours in the red channel. EBT4 film has the steepest change of pixel values from the first scan. MD-V3 stabilised after about two hours and all three other films kept darkening to some extent. EBT3 and EBT4 show about 2% and 2.5% drop of pixel values after 2 hrs, about 0.2% and 0.3% drop per hour in the next 10 hrs and then 1% and 2% per day respectively. EBT-XD and MD-V3 darkening stabilises much faster, having a drop of pixel values by 1% and 0.6% after one hour, about ≤0.1% per hour up to 10 hours and about ≤0.5% per day after that. Other colour channels also showed very similar trends.

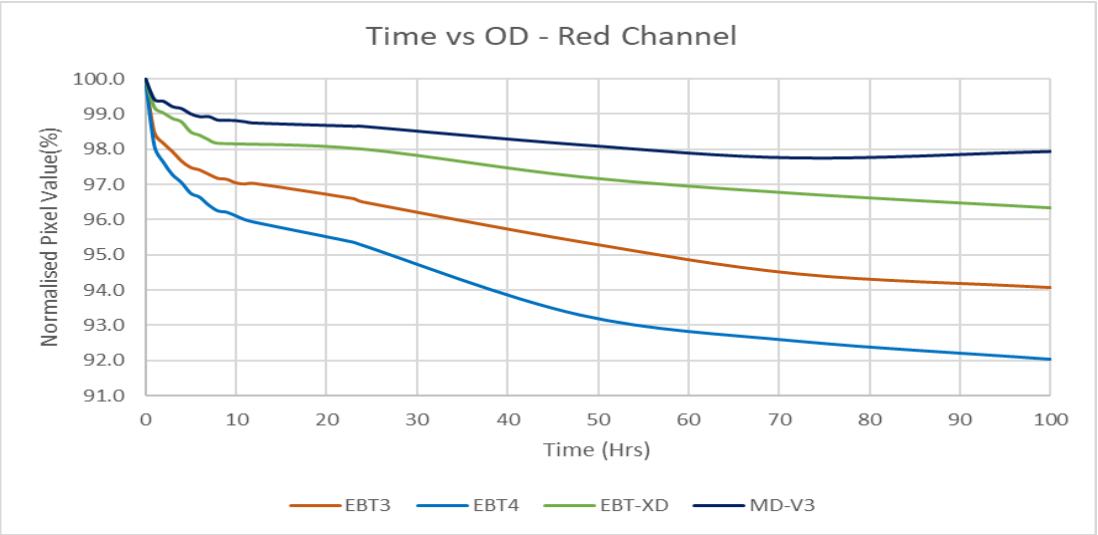

Figure 3-4: Normalised pixel values with respect to time after irradiation

Orientation effect: Figure 3-5 shows the change of pixel values due to change of orientation from portrait to landscape plotted against dose for the red channel. All films showed an orientation effect even at zero dose, with EBT4 having the biggest effect of about 5% at zero dose whereas the other three had about 2%. For EBT3 the effect increased steeply up to 5 Gy while the others showed less pronounced changes. MD-V3 and EBT-XD show, but smaller, effects, statistically significant between the two orientations, but in agreement within the statistical errors of the measurements for the two film types. Other colour channels also showed very similar trends.

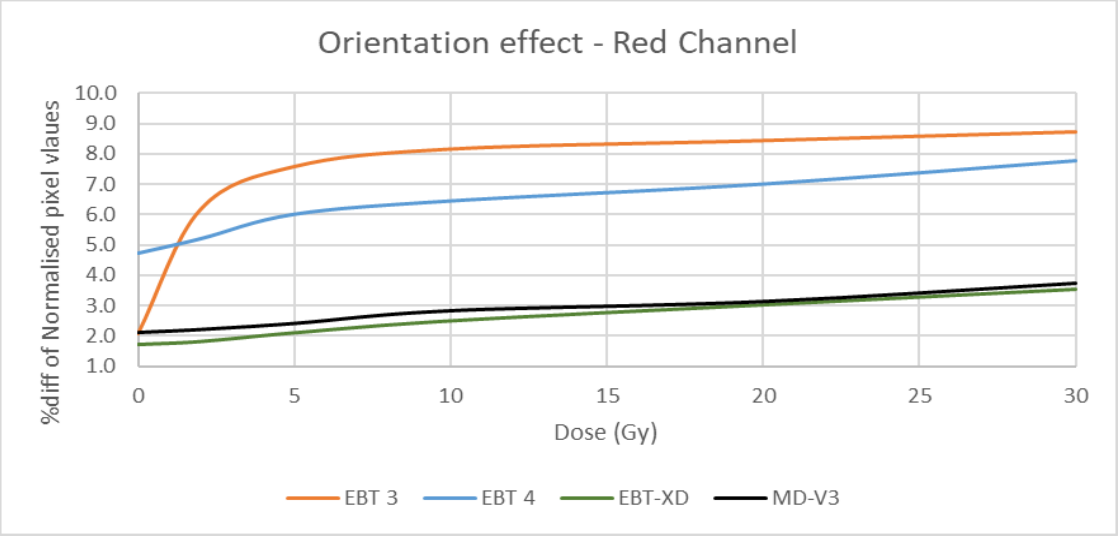

Figure 3-5: Change of pixel value due to orientation change with respect to dose.

Signal to noise ratio: Figure 3-6 (a), (b) and (c) show SNR with respect to dose from 0 Gy to 100 Gy for red, green and blue channels respectively. SNR of EBT4 is higher than that of EBT3 at all dose levels in the red channel. The other two channels do not show exactly the same

behavioural trends with dose, but still SNR is better at all dose levels. MD-V3 shows slightly better SNR than that of EBT-XD at all dose levels in all colour channels.

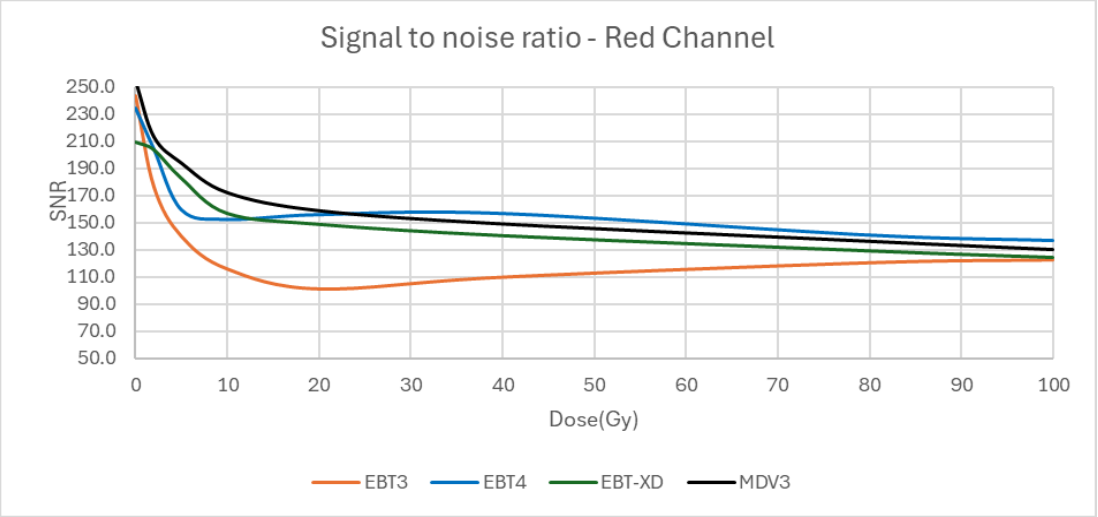

a. Red

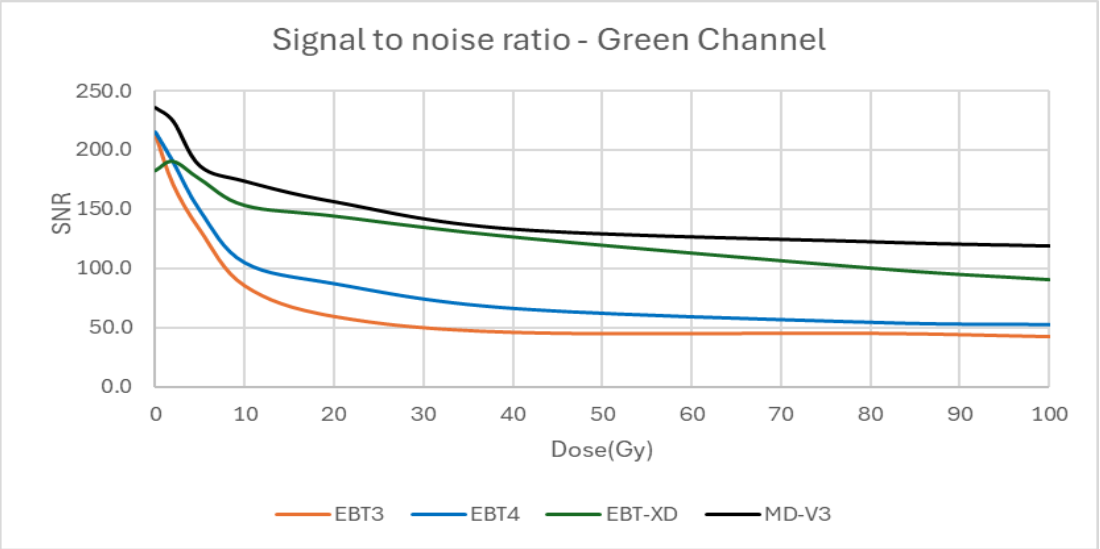

b. Green

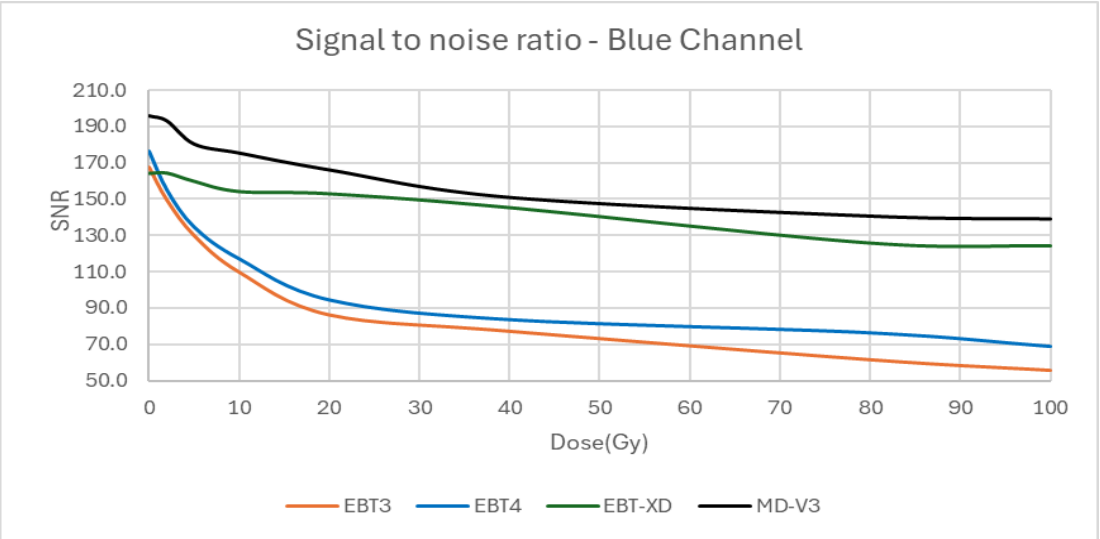

c. Blue

Figure 3-6: SNR of all four film types in (a) red, (b) green and (c) blue channel.

Polarization: Figure **3-7** (a), (b), and (c) illustrate the variation in pixel values between the two polariser positions, normalized to an unirradiated (0 Gy) reference film, as a function of dose for the red, green, and blue colour channels, respectively. While each colour channel exhibits slightly different behaviour, almost all follow a similar general trend: an initial increase up to a certain dose threshold varying across different films and colour channels, followed by either stabilization or a smaller further increase. Exceptions are observed in the red channel for EBT3, where the pixel value decreases after reaching a peak at 5 Gy and in the blue channel for EBT4. Additionally, in the red channel, responses continue to increase at a relatively higher rate in the region of 0 - 5 Gy compared to the other channels.

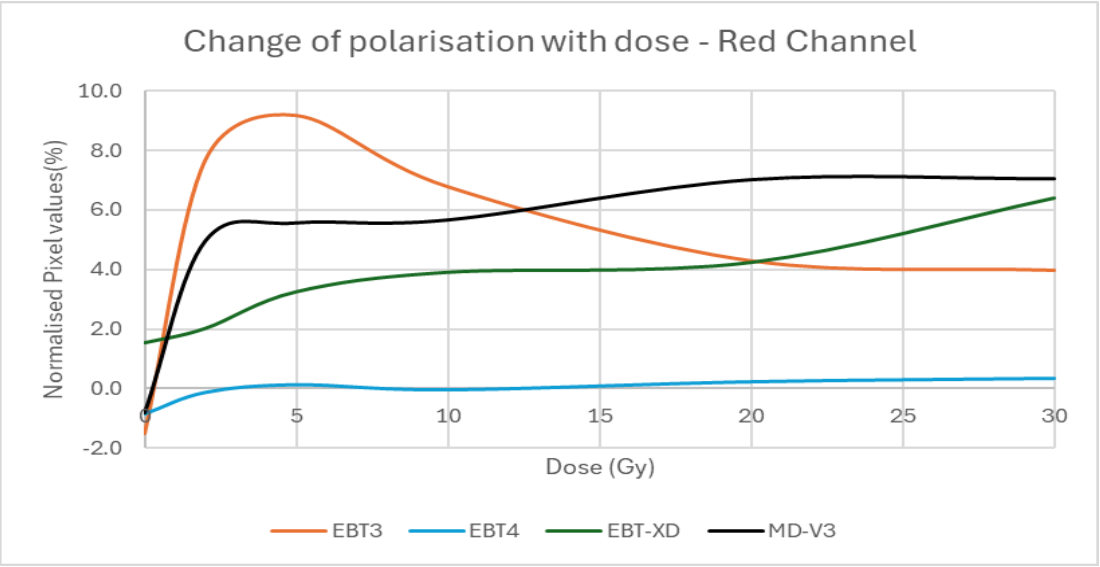

a: Red

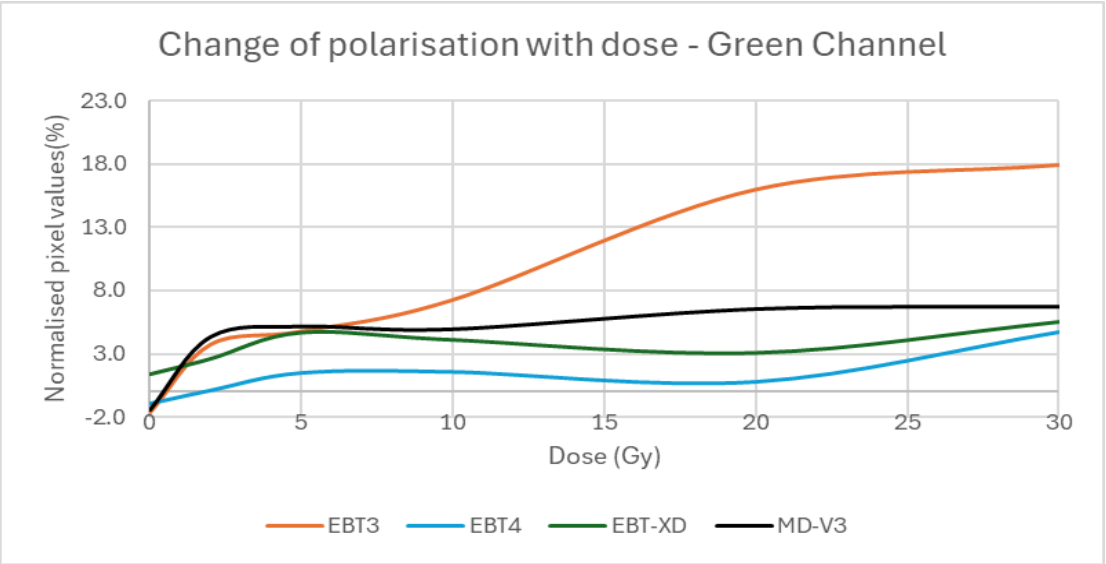

b: Green

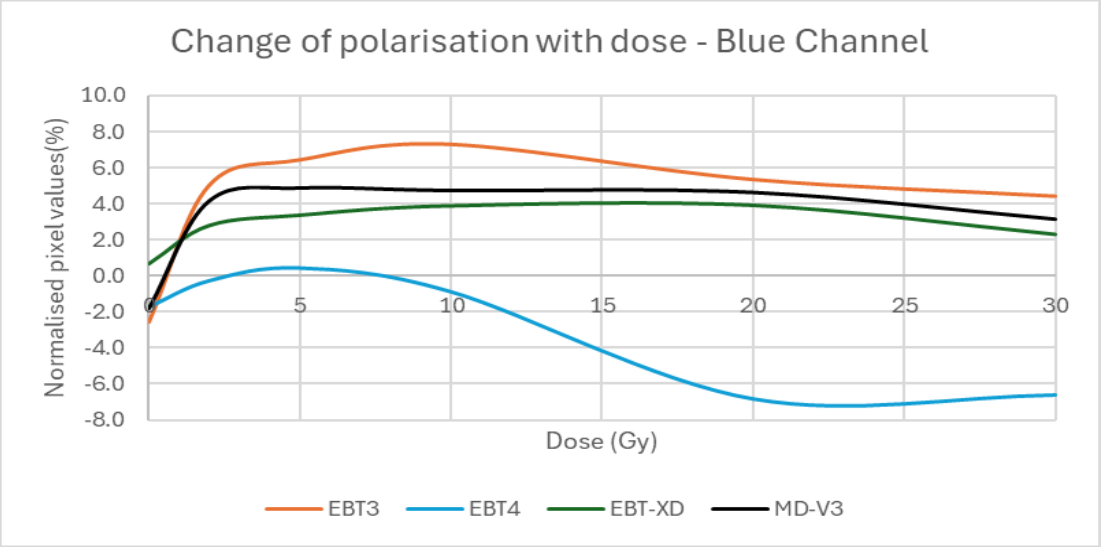

c: Blue

Figure 3-7: Change of pixel values because of polarisation with respect to dose in red channel (a) green, channel (b) and blue channel (c)

Lateral response artefact: Figure 3-8 presents the variation in pixel values in the red channel, normalized to the film centre, across the short side of the films in portrait orientation. For the MD-V3 films the strips were cut consistent with this, using the assigned orientations discussed in the orientation effects investigation. The dose profile curvature of EBT-XD and MD-V3 is similar, while EBT3 exhibits the most pronounced lateral response artefact (LRA), with EBT4 demonstrating an intermediate effect. Other colour channels also showed very similar trends.

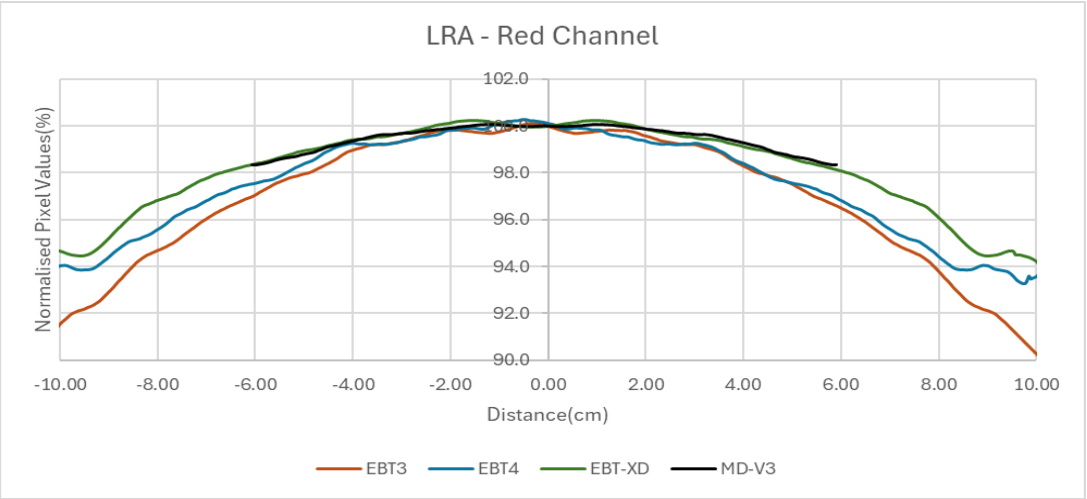

Figure 3-8: Change of pixel values from central axis for all four film types in red channel for 5Gy.

3.4 Discussion

Dose response: Consistent with findings from product brochures and previous studies [3,16,22–25], the difference in energy dependence between 6 MV and 15 MV photon beams is negligible for all four film types. While all three colour channels were analysed, only the red channel results are presented here, as the green and blue channels exhibit similar trends, showing no significant difference between 6 MV and 15 MV beams. The dose-response curves for EBT3 and EBT4 are very similar at the dose levels investigated in this study, differing by no more than 2%, which aligns with previous investigations [3]. The manufacturer recommends dose ranges of up to 60 Gy for EBT-XD and up to 100 Gy for MD-V3. However, an analysis of the first derivative (sensitivity curve) of the 6 MV dose-response curves reveals that there is not much difference between EBT3 and EBT4, or between EBT-XD and MD-V3 in terms of change of slope with dose beyond 10 Gy, indicating no significant calibration advantage in using MD-V3 over EBT-XD. In addition, this implies that although EBT3 and EBT4 are less sensitive in the higher dose ranges than the other two film types, they could still be used up to around 40 Gy. The manufacturer's brochures provide dose-response curve data only up to 22 Gy for EBT3, EBT4, and EBT-XD, and up to 100 Gy for MD -V3. Abe et al. [26] previously reported that EBT3 exhibits saturation beyond 100 Gy.

Change of OD with Time: The results of the red channel are presented here; as the green and blue channels follow similar trends. EBT-XD and MD-V3 exhibit substantially faster stabilization, with pixel value changes of approximately 1% between 2 hrs and 24 hrs post-irradiation. In contrast, EBT3 undergoes a ~2% change over the same period and continues to change by approximately 1% every subsequent 24 hrs. EBT4 demonstrates more prolonged darkening, stabilizing only after 48 hours. To minimize the impact of post-irradiation darkening the time interval between irradiation and readout for both calibration curve generation and

patient QA image acquisition must be kept similar when using EBT4 in clinical applications. This is a significant consideration for clinical use of the newer EBT4 film.

Orientation: The results of the red channel are presented here; the green and blue channels follow similar trends. Previous studies [12,21] showed EBT film has an orientation effect, which stays the same with increasing dose. However, both investigations were carried out only up to 3 Gy. The orientation effect was investigated for EBT-XD and EBT3 films by Khachonkham et al [22] but not given any numerical values with respect to dose. They presented two calibration curves of portrait mode and landscape mode. The curves showed increasing deviation until about 5 Gy for EBT3 and until 15 Gy for EBT-XD, after which the difference remained the same. The current study also found a similar trend for EBT3 but for EBT-XD the difference kept increasing, by about 1% from 15 Gy to 30 Gy. The uncertainty, on the values, calculated as the standard deviation as a percentage of mean pixel value of the selected ROI, is 0.7%. The measured orientation effects are statistically significant for all films.

Signal to noise ratio: Guan et al [16] reported SNR for red channel and Palmer et al [3] reported SNR for red and green channels for EBT3 and EBT4 for up to 10 Gy. The results for red channel of this current investigation are in line with these two previous red channel results, showing that SNR for EBT4 is better than for EBT3 at all dose levels. The green channel results are also similar to those reported by Palmer et al [3], but the raw pixel values are not exactly the same. Shameem et al [27] reported that pixel values produced by different scanners are different for the same film. Palmer et al [3] used an EPSON 12000XL scanner, whilst an EPSON V800 scanner was used in this study. The difference in raw pixel values for similar dose levels may result from the use of different scanners in these two investigations.

MD-V3 exhibits a higher signal-to-noise ratio (SNR) than EBT-XD across all dose levels and in all three colour channels. This slight improvement may be attributed to the different dye formulation used in MD-V3, although this was neither reported nor mentioned in the product brochures [7]. In contrast, the EBT4 product brochure [5] explicitly highlights its SNR enhancement as a key advantage, as compared to EBT3.

Polarization: Previous studies have investigated light polarization effects in various Gafchromic films, including EBT, MD-55 [17], EBT-HS [28], EBT [18], EBT3 and EBT-XD [8]. With the exception of EBT-HS, all Gafchromic films have been shown to induce light polarization, with the effect increasing as a function of dose.

The current study employed a methodology similar to that of Schoenfeld et al. [8], utilizing a camera instead of a scanner to analyse light polarization in Gafchromic films. This approach was adopted based on our recent findings [29] indicating that the mirror systems in scanners can themselves introduce polarization artefacts, which contribute to LRA and orientation effects and which are likely to vary with scanner [29,30]. We previously suggested [29] that imaging

systems with modified designs using only one mirror (or ideally none) would reduce the scanner-induced polarisation effect.

Results demonstrated that light polarization patterns vary across different colour channels, particularly in EBT3, where each channel exhibits a distinct response. Further investigation is currently underway to better understand these variations. Additionally, EBT4 shows a notably different response in the blue channel. In contrast, EBT-XD and MD-V3 exhibit more consistent behaviour across all three colour channels, characterized by an initial increase in polarization followed by stabilization.

These findings generally align with previous studies, confirming that, except for EBT-HS, light polarization induced by Gafchromic films increases with dose when compared to an unirradiated film.

Lateral response artefact: Initially, for the investigation of lateral response artefacts (LRA) in this study, the films used were exposed to 5 Gy. Previous studies [8,14,15,19] have examined the LRA effect on EBT3 and EBT-XD, revealing that the lateral profile for EBT-XD is flatter than that of EBT3 at the same dose, with the improvement attributed to the smaller size of the active ingredients [13]. Lewis et al. [14]demonstrated that when the transmitted light intensity through the films is the same, the curvature of the profile remains consistent. Since EBT-XD darkens less than EBT3 for the same dose, due to its smaller size active ingredients, the resulting curvature is flatter.

Given that MD-V3 darkens even less than EBT-XD, it was expected to exhibit a flatter curve. However, the results showed that the profile of MD-V3 was very similar to that of EBT-XD, contradicting previous findings. Therefore, further investigation was conducted to explore this discrepancy, considering the LRA at different doses to the films.

Figure 3-9 presents the relative dose profiles for films irradiated with 5 Gy and 20 Gy for EBT-XD, and 0 Gy, 5 Gy, 20 Gy, and 30 Gy for MD-V3. As expected, the LRA effect for EBT-XD increased with dose, with the 20 Gy profile exhibiting more pronounced LRA than that for 5 Gy. However, all profiles for MD-V3 were very similar, showing no significant dependency on dose. This lack of LRA dose dependence in MD-V3, suggests that the dose profile remained constant due to a factor beyond darkening alone. This phenomenon is tentatively attributed to the addition of the bond-retarding ingredients in the active layer formulation, which may inhibit bonding between the monomers of the active ingredients, as discussed in the introduction. This lack of increasing LRA with dose gives MD-V3 an advantage over EBT-XD for clinical applications.

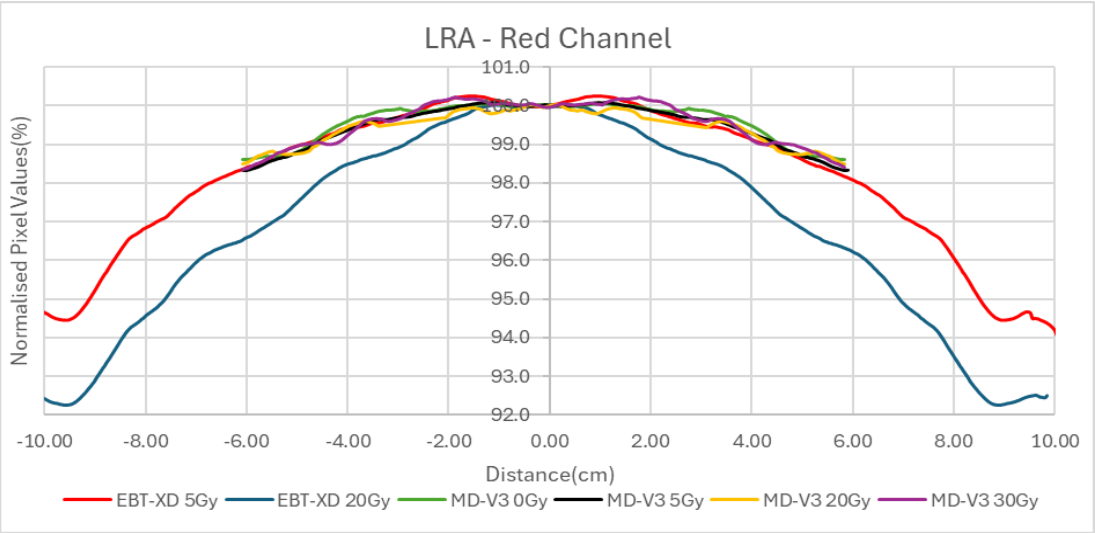

Figure 3-9: LRA for different dose values of EBT-XD and MD-V3.

3.5 Conclusions

This study provides a comprehensive characterization and comparison of four types of Gafchromic films, EBT3, EBT4, EBT-XD and MD-V3, investigated mainly on an Epson V800 scanner, selected as one widely used in clinical dosimetry. For measurements on the different films for each part of the study, the scanner and other experimental parameters were kept as consistent as possible between film types to draw out differences due to the films themselves. It may be noted that exact results may differ on other scanners, but that the relative findings between the film types are expected to be similar.

Among these four film types, MD-V3, the newest addition to the Gafchromic family, has not been extensively studied previously, making it a key focus of this investigation. EBT3, which has recently been replaced by EBT4, and EBT-XD are widely used in radiotherapy applications for standard and high-dose ranges, respectively. While EBT3 and EBT4 are recommended for standard dose ranges (up to 10 Gy), and EBT-XD (up to 60 Gy) and MD-V3(up to 100 Gy) for high-dose applications, this study found that EBT-XD and MD-V3 exhibit similar sensitivity curves, indicating that each could be utilized across a broad range of doses. EBT3 and EBT4 have a significant advantage over the other two in low dose ranges (<10 Gy) in terms of dose response sensitivity but could still be used up to 40 Gy.

Despite initial assumptions that the supplied square shape of the available MD-V3 films might indicate reduced orientation effects, it was observed that its orientation effect is similar to EBT-XD, though much smaller than those seen in EBT3 and EBT4. As expected, EBT4 demonstrated a significantly improved signal-to-noise ratio (SNR) over EBT3. The SNR was also improved for MD-V3 in comparison to EBT-XD, however, this was to a lesser extent than that between EBT3 and EBT4. The major limitation of EBT4 film is the increased post-irradiation darkening

which extends beyond 100 hours. This can have a significant impact when using EBT4 film clinically. To mitigate this, it is important to maintain a consistent time gap between irradiation and scanning, for both calibration and QA measurement films. Provided this recommendation is adhered to, EBT4 provides more reliable results than EBT3. For MD-V3 film, the most noticeable advantage is the consistent lateral response artifact with increasing dose which was not observed for EBT-XD.

Based on our investigation of EBT3, EBT4, EBT-XD and MD-V3 film, it has been determined that EBT4 is a suitable replacement for EBT3 film, provided consistent post-irradiation analysis times are followed. It is recommended to use EBT4 film for all low dose measurements, while MD-V3 should be utilized for high-dose measurements exceeding 10 Gy. These recommendations are made from consideration of the various effects studied here, ensuring optimal performance of the films with the least need for scanner or software corrections.

3.6 References:

[1] A. Rink, I. Alex Vitkin, and D. A. Jaffray, "Characterization and real-time optical measurements of the ionizing radiation dose response for a new radiochromic medium," *Med Phys*, vol. 32, no. 8, pp. 2510–2516, 2005, doi: 10.1118/1.1951447.

[2] A. A. Schoenfeld, D. Poppinga, D. Harder, K. J. Doerner, and B. Poppe, "The artefacts of radiochromic film dosimetry with flatbed scanners and their causation by light scattering from radiation-induced polymers," *Phys Med Biol*, vol. 59, no. 13, pp. 3575–3597, 2014, doi: 10.1088/0031-9155/59/13/3575.

[3] A. L. Palmer, D. Nash, W. Polak, and S. Wilby, "Evaluation of a new radiochromic film dosimeter, Gafchomic EBT4, for VMAT, SABR and HDR treatment delivery verification," *Phys Med Biol*, vol. 68, no. 17, pp. 0–11, 2023, doi: 10.1088/1361-6560/aceb48.

[4] D. Media, "Dosimetry media, type ebt-3."

[5] A. S. Ingredients, "Dosimetry media, gafchromic EBT4 dosimetry films," 2022.

[6] Ashland Specialty Ingredients, "gafchromic ebt-xd films,"

[7] Ashland Specialty Ingredients, "gafchromic md-v3 films absorbed dose of high-energy photons," 2021.

[8] A. A. Schoenfeld, S. Wieker, D. Harder, and B. Poppe, "Changes of the optical characteristics of radiochromic films in the transition from EBT3 to EBT-XD films," *Phys Med Biol*, vol. 61, no. 14, pp. 5426–5442, 2016, doi: 10.1088/0031-9155/61/14/5426.

[9] M. J. Butson, P. K. N. Yu, T. Cheung, and P. Metcalfe, “Radiochromic film for medical radiation dosimetry,” *Materials Science and Engineering R: Reports*, vol. 41, no. 3–5, pp. 61–120, 2003, doi: 10.1016/S0927-796X(03)00034-2.

[10] T. Cheung, M. J. Butson, and P. K. N. Yu, “Post-irradiation colouration of Gafchromic EBT radiochromic film,” *Phys Med Biol*, vol. 50, no. 20, 2005, doi: 10.1088/0031-9155/50/20/N04.

[11] S. Devic *et al.*, “Precise radiochromic film dosimetry using a flat-bed document scanner,” *Med Phys*, vol. 32, no. 7, pp. 2245–2253, 2005, doi: 10.1118/1.1929253.

[12] M. J. Butson, T. Cheung, and P. K. N. Yu, “Scanning orientation effects on Gafchromic EBT film dosimetry,” *Australas Phys Eng Sci Med*, vol. 29, no. 3, pp. 281–284, 2006, doi: 10.1007/BF03178579.

[13] A. L. Palmer, A. Dimitriadis, A. Nisbet, and C. H. Clark, “Evaluation of Gafchromic EBT-XD film, with comparison to EBT3 film, and application in high dose radiotherapy verification,” *Phys Med Biol*, vol. 60, no. 22, pp. 8741–8752, 2015, doi: 10.1088/0031-9155/60/22/8741.

[14] D. F. Lewis and M. F. Chan, “On Gafchromic EBT-XD film and the lateral response artefact,” *Med Phys*, vol. 43, no. 2, pp. 643–649, 2016.

[15] M. P. Grams, J. M. Gustafson, K. M. Long, and L. E. F. de los Santos, “Initial characterization of the new EBT-XD Gafchromic film,” *Med Phys*, vol. 42, no. 10, pp. 5782–5786, 2015.

[16] Z. C. Fada Guan, Huixiao Chen, Emily Draeger,Yuting Li,Resal Aydin,Christopher J.Tien, “Characterization of Gafchromic EBT4 film with clinical kV/MV photons and MeV electrons,” *Prec Radiat Oncol.*, vol. 7, pp. 84–91, 2023.

[17] N. V. Klassen, L. Van Der Zwan, and J. Cygler, “GafChromic MD-55: Investigated as a precision dosimeter,” *Med Phys*, vol. 24, no. 12, pp. 1924–1934, 1997, doi: 10.1118/1.598106.

[18] C. G. Soares, “Radiochromic film dosimetry,” *Radiat Meas*, vol. 41, no. SUPPL. 1, 2006, doi: 10.1016/j.radmeas.2007.01.007.

[19] A. A. Schoenfeld, S. Wieker, D. Harder, and B. Poppe, “The origin of the flatbed scanner artifacts in radiochromic film dosimetry - Key experiments and theoretical descriptions,” *Phys Med Biol*, vol. 61, no. 21, pp. 7704–7724, 2016, doi: 10.1088/0031-9155/61/21/7704.

[20] “ImageJ_Citation_paper”.

[21] S. Saur and J. Frengen, “GafChromic EBT film dosimetry with flatbed CCD scanner: A novel background correction method and full dose uncertainty analysis,” *Med Phys*, vol. 35, no. 7, pp. 3094–3101, 2008, doi: 10.1118/1.2938522.

[22] S. Khachonkham *et al.*, “Characteristic of EBT-XD and EBT3 radiochromic film dosimetry for photon and proton beams,” *Phys Med Biol*, vol. 63, no. 6, 2018, doi: 10.1088/1361-6560/aab1ee.

[23] G. Massillon-JL, A. Cabrera-Santiago, and N. Xicohténcatl-Hernández, “Relative efficiency of Gafchromic EBT3 and MD-V3 films exposed to low-energy photons and its influence on the energy dependence,” *Physica Medica*, vol. 61, no. October 2018, pp. 8–17, 2019, doi: 10.1016/j.ejmp.2019.04.007.

[24] G. Massillon-JL, S.-T. Chiu-Tsao, I. Domingo-Munoz, and M. F. Chan, “Energy Dependence of the New Gafchromic EBT3 Film:Dose Response Curves for 50 KV, 6 and 15 MV X-Ray Beams,” *Int J Med Phys Clin Eng Radiat Oncol*, vol. 01, no. 02, pp. 60–65, 2012, doi: 10.4236/ijmpcero.2012.12008.

[25] and Y. N. Y.N.H. Miura, S. Ozawa, N. Sumida, T. Okazue, K. Yamada, “Gafchromic EBT-XD film: Dosimetry characterization in high-dose, vlumetric-modulated arc therapy,” *J Appl Clin Med Phys*, vol. 17, no. 6, pp. 312–322, 2016.

[26] Y. Abe *et al.*, “Dosimetric calibration of GafChromic HD-V2, MD-V3, and EBT3 films for dose ranges up to 100 kGy,” *Review of Scientific Instruments*, vol. 92, no. 6, pp. 3–8, 2021, doi: 10.1063/5.0043628.

[27] T. Shameem, N. Bennie, M. Butson, and D. Thwaites, “A comparison between EPSON V700 and EPSON V800 scanners for film dosimetry,” *Phys Eng Sci Med*, vol. 43, no. 1, pp. 205–212, 2020, doi: 10.1007/s13246-019-00837-3.

[28] M. J. Butson, P. K. N. Yu, T. Cheung, and D. Inwood, “Polarization effects on a high-sensitivity radiochromic film,” *Physics in Medicine and Biology*, vol. 48, no. 15, 2003, doi: 10.1088/0031-9155/48/15/401.

[29] T. Shameem, N. Bennie, M. Butson, and D. Thwaites, “Effect of mirror system and scanner bed of a flatbed scanner on lateral response artefact in radiochromic film dosimetry,” *Physical and Engineering Sciences in Medicine*, pp. 1651–1663, 2024, doi: 10.1007/s13246-024-01478-x.

[30] J. E. Matney, B. C. Parker, D. W. Neck, G. Henkelmann, and I. I. Rosen, “Evaluation of a commercial flatbed document scanner and radiographic film scanner for radiochromic EBT film dosimetry,” *J Appl Clin Med Phys*, vol. 11, no. 2, pp. 198–208, 2010, doi: 10.1120/jacmp.v11i2.3165.

4 A comparison between EPSON V700 and EPSON V800 scanners for film dosimetry

This chapter consists of the manuscript

1. T. Shameem, N. Bennie, M. Butson, and D. Thwaites, "A comparison between EPSON V700 and EPSON V800 scanners for film dosimetry," *Phys Eng Sci Med*, vol. 43, no. 1, pp. 205–212, 2020.

   https://doi.org/10.1007/s13246-022-01136-0

Preface: This chapter documents practical, clinically relevant differences between two commonly used Epson A4-size flatbed models and evaluates whether they can be used interchangeably. This work investigates the inter-model differences in LRA, orientation dependence, and scanner response, and thereby provides pragmatic guidance for actions required in a clinical service when scanners are changed or upgraded. It shows that scanners cannot necessarily be interchanged without significant re-commissioning and complements the work in Chapter 3 on changing film type.

Authors: Tarafder Shameem[1,2], Nick Bennie[1], Martin Butson[2,3], David Thwaites[2]

[1]North Coast Cancer Institute, Lismore, NSW, Australia; [2]Institute of Medical Physics, School of Physics, University of Sydney, Sydney, NSW, Australia; [3] Dept of Radiation Oncology Chris O'Brien Lifehouse, Sydney, NSW, Australia

Abstract

Radiochromic film is a good dosimeter choice for patient QA for complex treatment techniques (IMRT, VMAT, SABR, SBRT) because of its near tissue equivalency, very high spatial resolution and established method of use. Commercial scanners are usually used for film dosimetry, among which EPSON scanners are the most common. NCCI have used an EPSON V700 scanner, but recently acquired a new model EPSON V800 scanner. The purpose of this work was to evaluate any differences between these two scanners to consider whether they can be used interchangeably or not. Different aspects of film dosimetry, e.g. LRA effect, orientation effect, scanner response etc., were compared. EBT3 films were irradiated with 40x40 cm^2 field size 6 MV beams and scanned in both the scanners. The scanned images were read in ImageJ V1.49 software. The data obtained was then copied in MS Excel to compare the scanners. The V800 scanner causes more polarisation, which results in more LRA effect than for the V700 scanner. The responses of the scanners in all three colour channels are not the same for the same film and irradiation. The V800 scanner shows an increase of response of up to 1.6% compared to 3.7% increase in the V700 scanner after scanning a piece of irradiated film 20 times. The

scanners cannot be used interchangeably. The correction factors for LRA effect and the calibration curves are different. Further characterisation, evaluation and commissioning is required before clinical use.

Keywords: Radiotherapy, Radiochromic Film, EPSON scanner, Film dosimetry

4.1 Introduction

Radiochromic film is a good dosimeter of choice for patient QA for complex treatment techniques (IMRT, VMAT, SABR, SBRT) because of its near tissue equivalency, very high spatial resolution and established method of use [1–5]. There are two main problems associated with radiochromic film dosimetry, which are the orientation effect and the lateral response artefact (LRA) effect [5–13]. The orientation effect is the difference in response depending on the orientation of the film on the scanner bed and the LRA effect is the difference of response from middle to side of the film, orthogonal to the scanner's light source travel direction [9,12].

The scanner construction elements play a major role in contributing to the LRA effect [9,11] Those that are responsible for light source polarisation and thus for the LRA effect include

- lens size of the camera with respect to the width of the scanner
- the mirror system of the scanner and
- optical path length variation due to difference in refractive index of scanner glass and the film.

Another contributor to the orientation effect and LRA effect is the needle like crystals in the active layer of the radiochromic films. Schoenfield et. el.[9,12] showed that the crystals have a rod-like shape of about 2 μm width and 15 μm length, and the rods are preferentially aligned in the coating direction parallel to the short side of the film. These crystals introduce more polarisation to light that is already polarized by the scanner element. Upon being irradiated these crystals form dipole polymers, which enhances the light polarization capabilities [12,13].

The magnitude of light polarization, introduced by the scanner and film, increases with increasing lateral distance from the centre of the scanner[9]. The size of the LRA effect depends on irradiated dose and position of the film on the scanner bed [9,11,13]. To manage the LRA effect, a correction factor is needed. The orientation effect can be minimised by placing the film on the scanner bed always in landscape orientation.

There are other sources of potential error. For example, the light source of a scanner causes some darkening of the radiochromic films, which is usually negligible but if the film is required to be scanned several times it might have a measurable effect and may need a correction factor [14,15]. In addition, all of the glass scanner bed is not covered by the CCD camera. Larraga-Guiterrez et al [15] showed that the light spectrum produced by the V800 scanner is different

from that of the 11000XL scanner which results in inconsistent responses of the three colour channels. 11000XL scanners have higher sensitivity in the blue and red channels whereas V800 scanners have higher sensitivity in the green channel. V700 scanners use a cold cathode fluorescent light source, which is different from the light sources of 11000Xl and V800 scanners. Matney et. El [16] found reproducibility of ±0.3% standard deviation for 10 repeated scans for Epson V700 scanners but Plaelinck et el [14] reported a darkening effect caused by repeated scans on an EPSON Pro1680 scanner and Maria et el [17] reported a darkening effect for EPSON 10000XL scanners.

EPSON scanners are commonly used for film dosimetry. Our centre has access to both the Epson V700 and V800 scanners. The V800 was an updated A4 size model of the V700. No particular instructions were provided by the manufacturer as to the differences between these two models and the V800 is sold as the model replacement for the V700. The main difference, from the dosimetry perspective, is the change of light source in the V800 scanner, which uses a white LED as compared to the cold cathode fluorescent light in V700 scanners. The purpose of this work is to evaluate any differences between the two scanners to consider whether they can be used interchangeably or not for film dosimetry with radiochromic film.

4.2 Method

Irradiated EBT3 films were left in the box for two hours and then scanned using both the EPSON V700 and EPSON V800 scanners, where the film pieces were taped down to the scanner bed to flatten the curvature. Gloves were used all the time during handling the film to avoid any contamination from finger print marks. The following settings were used for both scanners,

- Mode: Professional
- Document Type: Film (with Film Area Guide)
- Film Type: Positive Film
- Image Type: 48-bit color
- Resolution: 508 dpi
- No Color Correction was applied

The characteristics of the scanners to be compared include differences in the LRA effect, light polarization, scanner response, repeated scan effect, calibration curve, noise and warm up time. The edges of the films were excluded in all the tests where films were used. The scans in both scanners were performed consecutively, within two minutes, to avoid any time dependent darkness difference. All irradiations were carried out on an Elekta Synergy linear accelerator (linac) using a 6MV beam and a 40cm x 40 cm field size, The film was placed at 10cm depth of plastic water with 10cm backscatter in a phantom that was 30 cm x 30 cm area presented to the beam.

LRA effect: EBT3 films were cut into 3cm x 11cm strips along the short side (Figure 4-1) for comparing the LRA effects and these were exposed on the linac as above. One strip was also exposed in sunlight for 10min, with no backscatter or build up, to have film responses excluding any possible linac dependent contribution in the LRA effect. The film pieces were placed at the centre of the scanner and the scanned images were saved as *.tiff format which were read and separated into three colour channels in ImageJ V1.49 software. Profiles were drawn across the film (Figure 1) in all three channels, which were copied in MS Excel. All the profiles drawn in ImageJ software show a high degree of noise in the first 30-50 of about 8000 data points from the end of the film strips, which were avoided by excluding 50 data points from either end of all the profiles. Different authors have presented the LRA effect data in different ways. All of these are based on the difference in pixel values between the centre to a lateral position [9–11,13,17]. In this study, the LRA effect is presented as the percent difference of pixel values from the centre to the edge of the film strip. The LRA effect was therefore calculated as the percentage difference between the highest point at the middle and the lowest point at the edge of the curve.

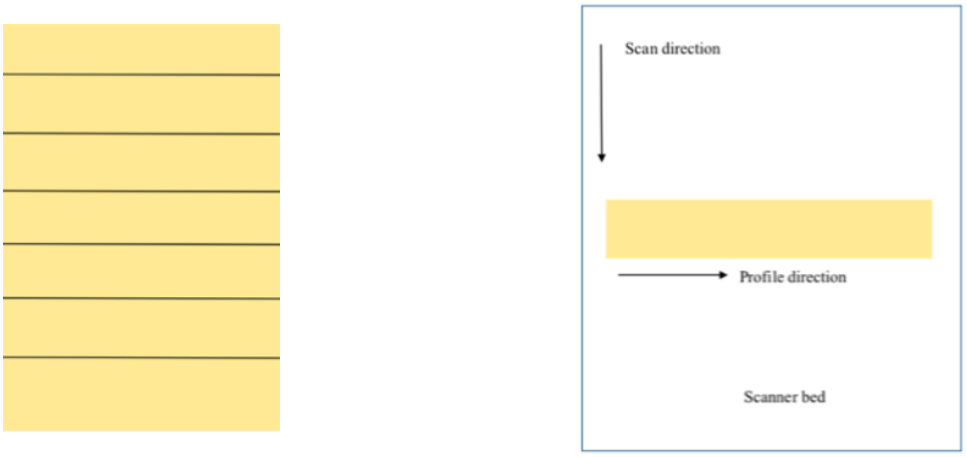

Figure 4-1 : Film orientation, scan direction and profile direction

Light Polarization: To compare light polarization caused by the scanners, a piece of linear-polarizer film sheet; which selectively allows the passage of only certain orientations of plane polarized light, was placed in three different locations on the scanner bed from left to right (Fig 2) and scanned with varying angle from 0^0 to 180^0 at10^0 intervals in each position on each scanner bed. ImageJ was used to find the mean pixel values of a region of interest, placed at the centre of the polarizer, and these were plotted in MS Excel for all three positions in all three channels. The pixel values were normalised to the highest transmission position, which was at 90^0.

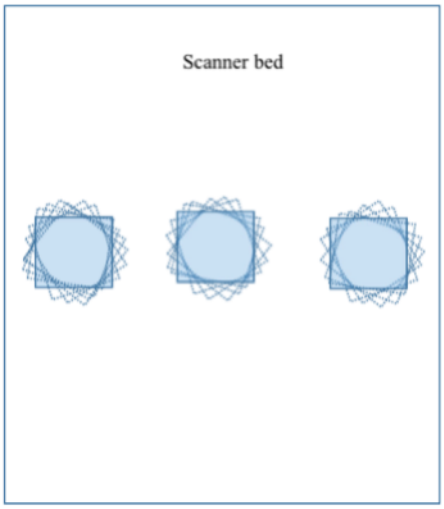

Figure 4-2: Linear polarizer orientation on the scanner bed.

Scanner Response: The same EBT3 film pieces used in the LRA effect test were used for the scanner response test, which shows the differences in pixel values resulting from the different scanners. Profiles were drawn in the same way as for the LRA effect test for both scanners and normalised pixel values were calculated, using:

$$N_p = \frac{P(I)}{P(0)}$$

Where N_p is the normalised pixel value, *P(I)* is the pixel value of irradiated film and *P(0)* is the pixel value of the un-irradiated film. These normalised pixel values are then plotted using MS Excel to compare the scanner response. The process was repeated five times and the result was tabulated as the average of the five repeats.

Repeated scan effect: Twenty 3x3cm^2 film pieces, irradiated on the linac as above, were used for the repeated scan effect test. The images were read and mean pixel values of a region of interest selected at the centre of the images were obtained in ImageJ in all three colour channels. The percentage difference between the 1st scan and the 20th scan is calculated. The process was repeated for 20 pieces of film and the result was presented as plot of scan no vs the average of the twenty film pieces with standard deviation as error bars.

Noise: Four pieces of 5x5cm^2 film pieces were used, three of which were irradiated in the 6MV beam and given doses of 2Gy, 10Gy and 15Gy and one was kept as un-irradiated. The film pieces were scanned in both the scanners. For all the scanned images of the film pieces, a very similar region of interest was selected in ImageJ and histograms were produced, which gives information on the number of Pixels, Mean Pixel Value and Standard Deviation in the region of interest. Standard deviation is the noise present in the pixel values, which incorporates noise resulting from the film itself and from the scanners. As the same film pieces were used for both

scanners the film noise contributions were the same and the difference in standard deviations represents differences in the scanner noise. Noise is calculated as standard deviation as the percent of mean pixel values of the region of interest.

Calibration curve: Two sets of eleven 3x3cm^2 film pieces were used to create calibration curves for both V700 and V800 scanners. The film pieces were placed in a 6MV photon beam at the centre of a 10x10cm^2 field, at 10cm depth with 10cm of plastic water backscatter to simulate normal linac calibration setup and were irradiated from 100MU to 3000MU to give varying doses of 1Gy to 30Gy to each set of films. The pixel values were obtained as described in the "repeated scan effect" section. The optical density (OD) was calculated as suggested by Bennie et. el (13) given as $OD = \frac{P(0)}{P(I)} - 1$

Where P(0) and P(I) are the pixel values of un-irradiated and irradiated films respectively.

Start up time: A stopwatch was used to measure the time needed from turning on the scanner to get it ready to scan. The results reported here are the median values of 10 observations. Uncertainty was calculated by as

$$\sigma_{median} = \frac{2\pi\sigma}{4\sqrt{n}}$$

4.3 Results:

LRA effect: Table 4-1: LRA effect (%) for two scanners from linac and sunlight exposure shows the LRA effect as a percentage difference of highest and lowest pixel values of profiles drawn across the film piece (Figure 4-1) in both scanners in all three channels. The EPSON V800 scanner is observed to have greater LRA effects than the EPSON V700 scanner.

Irradiation	Blue		Green		Red	
	V700	V800	V700	V800	V700	V800
LINAC	6.4±0.15	8.5±0.20	5.1±0.05	6.8±0.17	6.1±0.18	8.4±0.14
Sunlight	7.5±0.10	9.7±0.05	6.5±0.15	7.0±0.10	6.7±0.17	8.1±0.10

Table 4-1: LRA effect (%) for two scanners from linac and sunlight exposure

Sunlight exposure shows higher LRA than that of linac. This is because the linac does not produce perfectly flat profiles for a 40x40cm^2 field which counteracts the LRA effect of the radiochromic film dosimetry system.

Light polarization:

Figure 4-3 shows that the curves at the middle part of the scanner are flatter than at the left and right sides of the scanner which means at the edges light is being polarised more than in the centre, which is in agreement with the scanner introducing light polarization.

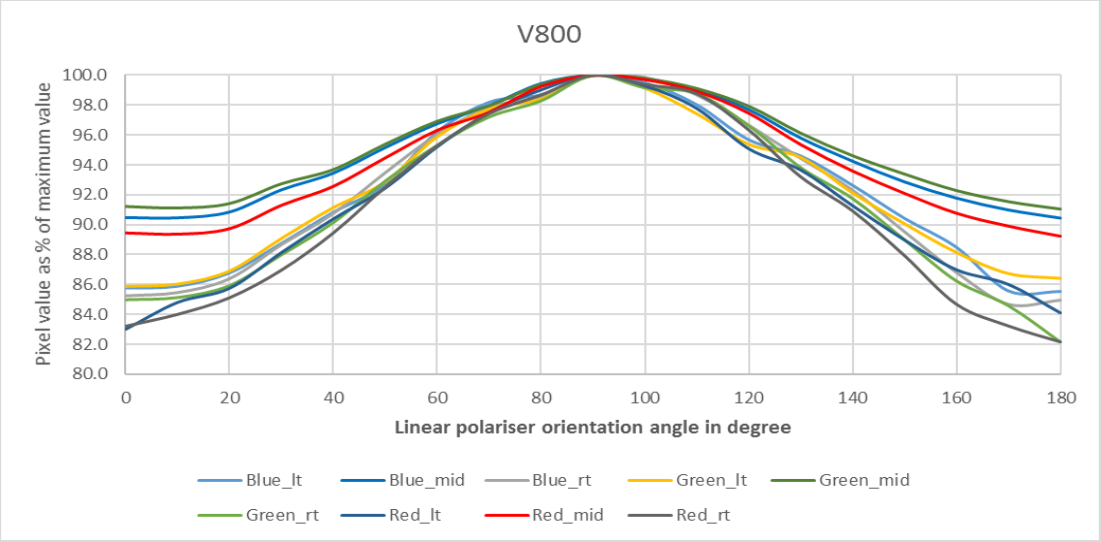

Figure 4-3: Polarization of light on the EPSON V800 scanner for all three colour channels and at three positions

If there was no light polarization in the film dosimetry system, all three lines in all three colour channels would be horizontal straight lines.

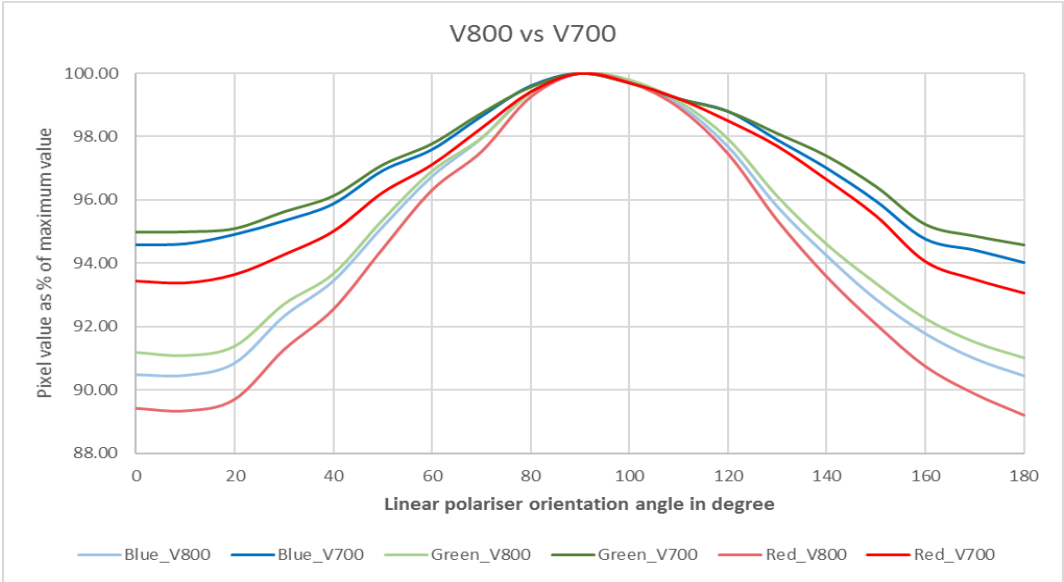

Figure 4-4: Comparison of light polarization caused by the EPSON V800 and the EPSON V700 scanner in the central (middle) positions

Figure 4-4 shows that the equivalent curves for the EPSON V700 scanner are flatter than those for the EPSON V800 scanner, indicating that the EPSON V800 scanner introduces more polarisation and would have a greater LRA effect, in agreement with the findings from the LRA effect test.

Scanner response: Pixel values produced by the EPSON V800 scanner are not exactly the same as from the EPSON V700 scanner. In the blue and green channels, the V800 scanner has lower values and in the red channel it has higher pixel values.

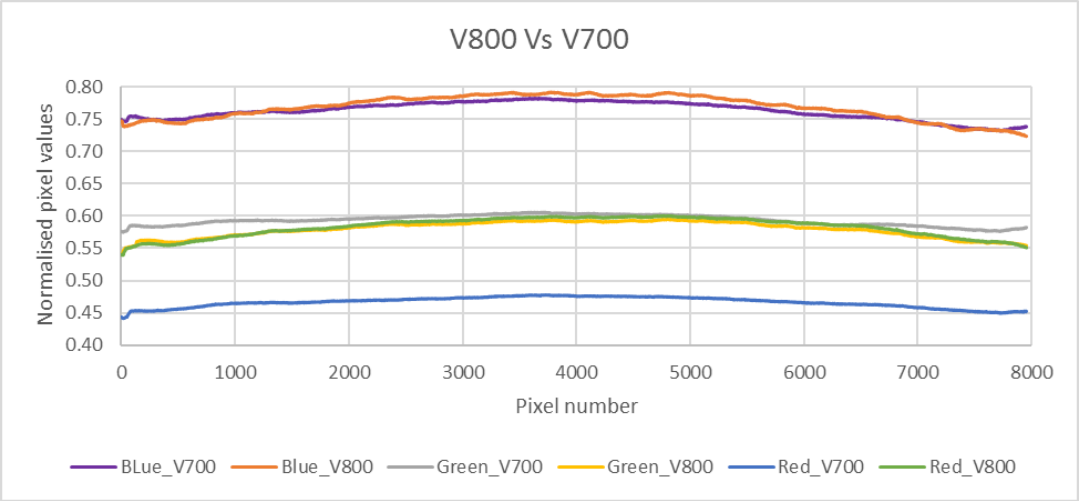

Figure 4-5: Scanner responses for blue, green and red channels

The Figure 4-5 shows that blue and green channel response is almost identical for these two scanners, within 2.0% and 6.2% for blue and green channel respectively, but in the red channel the V800 scanner response is higher than that of the V700 scanner, where the differences of normalised pixel values vary from 21.6% to 26.9%. The maximum uncertainties for five repeats of all 8000 pixels, calculated as the standard deviation as a percentage of mean, are 0.08%, 0.03% and 0.04% for blue, green and red channels respectively. A previous study showed that the different light sources have different light spectra, which results in different scanner response [15]. The V800 scanner uses LED light and the V700 uses cold cathode fluorescent light which is the likely reason for the red channel difference.

Repeated scan effect: The same piece of film was scanned twenty times. Figure 4-6 shows the average of twenty films, with standard deviation as the error bar of 20 consecutive scans in all three channels of both V700 and V800 scanners.

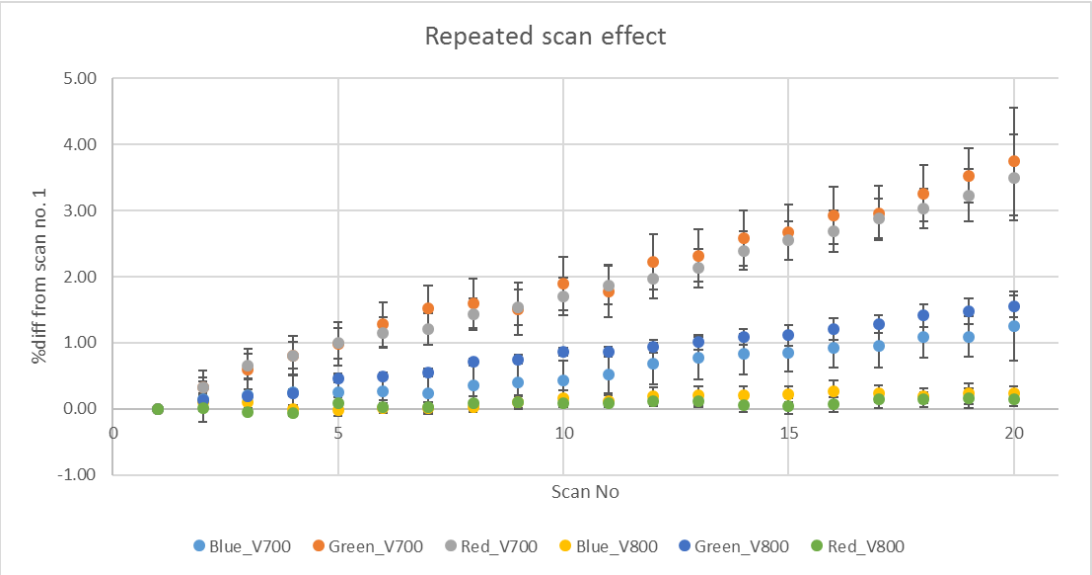

Figure 4-6: Average percent difference of twenty films from scan no.1 in all three channels of V700 and V800 scanner. The standard deviations of twenty film readings are presented as error bars.

Noise: Table 4-2 shows the standard deviations as percentages of mean pixel value of the region of interest in all three channel in both the V700 and V800 scanners. In blue and green channels the V800 produces more noise but in the red channel the V700 is noisier.

Dose	Blue		Green		Red	
	V700	V800	V700	V800	V700	V800
0Gy	1.02	1.25	1.00	1.19	1.07	1.06
2Gy	1.13	1.14	1.15	1.16	1.24	1.05
10gy	1.30	1.45	2.23	2.39	2.03	1.67
15Gy	1.45	1.63	2.93	3.12	2.10	1.78

Table 4-2: Standard deviation as the % of mean pixel values at different dose levels in both scanners

Calibration curve: Figure 4-7 shows the calibration curves, from 1Gy to 30Gy, of V700 and V800 scanners in all three channels. Up to 3Gy there are only small differences for all three channels and this continues for higher doses for blue and green channels, but the red channel shows significant difference in higher dose regions.

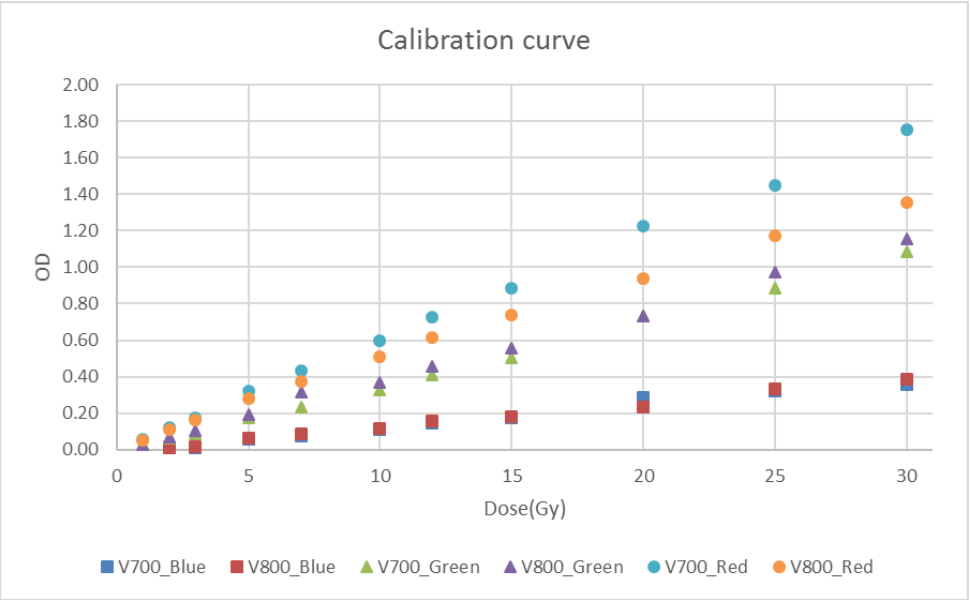

Figure 4-7 : Calibration curve for V700 and V800 scanners in all three channels.

Start up time: The median values of time required from turning the scanner on to it being ready to scan were measured as 1min 40.12±0.44s and 22.05±41s for V700 and V800 scanners respectively.

4.4 Discussion:

LRA effect: The LRA effect measured on V700 and V800 scanners is different. The results show that the V800 scanner has a greater LRA effect, by about 2%, in all three channels than that of the V700 scanner. Matney et.el. [16] compared an Epson V700 scanner with a Vidar VXR Dosimetry Pro Advantage scanner and found no difference in this aspect for a blank EBT film. Larraga-Guiterrez et.el [15] compared EPSON V800 and EPSON 11000XL scanners and found that the V800 introduces more LRA effect than the 11000XL. Schoenfeld et.el [9] and Larraga-Guiterrez et.el [15] concluded that the LRA effect mainly results from the optical system. Both the scanners use the same lenses, but other optical properties which impact on the LRA effect e.g. mirrors and the material of the scanning bed, can be different.

Light polarization: The light polarization test shows that the V800 scanner introduces more polarization of the light source, contributing to the greater LRA effect, than does the V700 scanner. This is in agreement with the findings in the LRA effect test. Previous studies [1,6–8,12] found that light polarization caused by the irradiated film and the scanner is responsible for the orientation effect and the LRA effect. Van Buttum et. al [11] and Schoenfeld et. al [13] described how the flatbed scanner components introduce the light polarization.

Scanner response: The V800 scanner uses a white LED light source and the V700 scanner uses a white cold cathode fluorescent lamp. The change of light source might affect the differences

in pixel value created by these scanners, as observed in the scanner response test. The V700 scanner has greater pixel values in the blue and green channels and less in the red channel. A previous study [15] also showed differences in pixel values resulting from two different EPSON scanners, which used different light sources.

Repeated scan effect: Our study found that V700 scanners introduce a darkening effect after repeated scans but the magnitude of darkening is much less in the V800 scanner than that for the V700 scanner in all three channels. This is also linked to the new light source used in the V800 scanner. There are varying results found in previous studies. Two studies [14,17]found a darkening after repeated scans in an EPSON 1680 Pro scanner and an EPSON 1000XL scanner and one study [16] found no noticeable darkening after repeated scans on a V700 scanner. This latter study didn't describe the method used for the test.

Noise: Our study shows that the V800 is noisier in blue and green channels, but in the red channel the V700 produces more noise. The difference in noise in the scanners does not exceed 0.4% at any dose level in all three channels. Matney et el [16] reported that V700 scanner produces noise of no more than 0.3%, in 16 bit image and 150dpi resolution, up to the dose level of 5.119Gy. To compare with this result, the experiment was repeated for a 0Gy, unexposed, dose level with the same set up that Matney [16] used. The noise produced was 0.73% whilst Matney [16] reported 0.1%

Calibration curve: Up to 3Gy the calibration curves are almost identical but in the higher dose regions the red channel shows significant differences. Larraga-Guiterrez et al [15] investigated the sensitivity, presented as dose vs netOD, of Epson 11000XL and EPSON V800 scanners and similarly found significant difference in the red channel, but in the green and blue channels differences are small.

4.5 Conclusion:

The LRA, scanner response, noise, calibration curve and repeated scan effect has been evaluated using EBT3 gafchromic film in EPSON V700 and V800 scanners. For the purpose of film dosimetry with radiochromic film the V700 scanner cannot be directly interchanged with the V800 scanner. A proper characterization and commissioning is needed before using the alternative scanner and appropriate correction factors need to be obtained.

Conflict of Interest: All authors declare that there is no conflict of interest.

Ethical Approval: this article does not contain any studies with human participants or animal experiments performed by any of the authors.

4.6 References

[1] N. V. Klassen, L. Van Der Zwan, and J. Cygler, “GafChromic MD-55: Investigated as a precision dosimeter,” *Med Phys*, vol. 24, no. 12, pp. 1924–1934, 1997, doi: 10.1118/1.598106.

[2] B. M. Coursey *et al.*, “Radiochromic Film Dosimetry Radiochromic film dosimetry: Recommendations of AAPM Radiation Therapy Committee Task Group 55,” 1998.

[3] T. Aland, T. Kairn, and J. Kenny, “Evaluation of a Gafchromic EBT2 film dosimetry system for radiotherapy quality assurance,” *Australas Phys Eng Sci Med*, vol. 34, no. 2, pp. 251–260, 2011, doi: 10.1007/s13246-011-0072-6.

[4] T. Kairn, N. Hardcastle, J. Kenny, R. Meldrum, W. A. Tomé, and T. Aland, “EBT2 radiochromic film for quality assurance of complex IMRT treatments of the prostate: Micro-collimated IMRT, RapidArc, and TomoTherapy,” *Australas Phys Eng Sci Med*, vol. 34, no. 3, pp. 333–343, 2011, doi: 10.1007/s13246-011-0087-z.

[5] N. Bennie and P. Metcalfe, “Practical IMRT QA dosimetry using Gafchromic film: a quick start guide,” *Australas Phys Eng Sci Med*, vol. 39, no. 2, pp. 533–545, 2016, doi: 10.1007/s13246-016-0443-0.

[6] M. J. Butson, T. Cheung, and P. K. N. Yu, “Scanning orientation effects on Gafchromic EBT film dosimetry,” *Australas Phys Eng Sci Med*, vol. 29, no. 3, pp. 281–284, 2006, doi: 10.1007/BF03178579.

[7] M. J. Butson, T. Cheung, and P. K. N. Yu, “Evaluation of the magnitude of EBT Gafchromic film polarisation effects.pdf,” *Australas Phys Eng Sci Med*, vol. 31, no. 1, pp. 21–25, 2009.

[8] H. Alnawaf, M. J. Butson, T. Cheung, and P. K. N. Yu, “Scanning orientation and polarization effects for XRQA radiochromic film,” *Physica Medica*, vol. 26, no. 4, pp. 216–219, 2010, doi: 10.1016/j.ejmp.2010.01.003.

[9] A. A. Schoenfeld, D. Poppinga, D. Harder, K. J. Doerner, and B. Poppe, “The artefacts of radiochromic film dosimetry with flatbed scanners and their causation by light scattering from radiation-induced polymers,” *Phys Med Biol*, vol. 59, no. 13, pp. 3575–3597, 2014, doi: 10.1088/0031-9155/59/13/3575.

[10] D. Lewis and M. F. Chan, “Correcting lateral response artifacts from flatbed scanners for radiochromic film dosimetry,” *Med Phys*, vol. 42, no. 1, pp. 416–429, 2015, doi: 10.1118/1.4903758.

[11] L. J. Van Battum, H. Huizenga, R. M. Verdaasdonk, and S. Heukelom, “How flatbed scanners upset accurate film dosimetry,” *Phys Med Biol*, vol. 61, no. 2, pp. 625–649, 2015, doi: 10.1088/0031-9155/61/2/625.

[12] A. A. Schoenfeld, S. Wieker, D. Harder, and B. Poppe, “Changes of the optical characteristics of radiochromic films in the transition from EBT3 to EBT-XD films,” *Phys Med Biol*, vol. 61, no. 14, pp. 5426–5442, 2016, doi: 10.1088/0031-9155/61/14/5426.

[13] A. A. Schoenfeld, S. Wieker, D. Harder, and B. Poppe, “The origin of the flatbed scanner artifacts in radiochromic film dosimetry - Key experiments and theoretical descriptions,” *Phys Med Biol*, vol. 61, no. 21, pp. 7704–7724, 2016, doi: 10.1088/0031-9155/61/21/7704.

[14] L. Paelinck, W. De Neve, and C. De Wagter, “Precautions and strategies in using a commercial flatbed scanner for radiochromic film dosimetry,” *Phys Med Biol*, vol. 52, no. 1, pp. 231–242, 2007, doi: 10.1088/0031-9155/52/1/015.

[15] J. M. Lárraga-Gutiérrez, O. A. García-Garduño, C. Treviño-Palacios, and J. A. Herrera-González, “Evaluation of a LED-based flatbed document scanner for radiochromic film dosimetry in transmission mode,” *Physica Medica*, vol. 47, no. December 2017, pp. 86–91, 2018, doi: 10.1016/j.ejmp.2018.02.010.

[16] J. E. Matney, B. C. Parker, D. W. Neck, G. Henkelmann, and I. I. Rosen, “Evaluation of a commercial flatbed document scanner and radiographic film scanner for radiochromic EBT film dosimetry,” *J Appl Clin Med Phys*, vol. 11, no. 2, pp. 198–208, 2010, doi: 10.1120/jacmp.v11i2.3165.

[17] M. Martišíková, B. Ackermann, and O. Jäkel, “Analysis of uncertainties in Gafchromic® EBT film dosimetry of photon beams,” *Phys Med Biol*, vol. 53, no. 24, pp. 7013–7027, 2008, doi: 10.1088/0031-9155/53/24/001.

5 Effect of scanner lens on Lateral Response Artefact in Radiochromic film dosimetry.

This chapter consists of the manuscript

T. Shameem, N. Bennie, M. Butson, and D. Thwaites, "Effect of scanner lens on lateral response artefact in radiochromic film dosimetry," *Physical and Engineering Sciences in Medicine*, vol. 45, pp. 721–727, 2022.

https://doi.org/10.1007/s13246-022-01136-0

Preface: This chapter experimentally assesses how focal length of the readout imager lens and the imaging geometry influence the LRA. It begins to consider scanner components separately and independently, as opposed to whole system evaluation (as in Chapter 4). By demonstrating that lens optics materially affect lateral non-uniformity, this paper shows that component-level optical design can be a controlling factor in LRA magnitude and shape and thus motivates exploring hardware-based mitigation strategies.

Authors: Tarafder Shameem[1,2], Nick Bennie[1], Martin Butson[2,3], David Thwaites[2]

[1]North Coast Cancer Institute, Lismore, NSW, Australia; [2]Institute of Medical Physics, School of Physics, University of Sydney, Sydney, NSW, Australia; [3] EPA, NSW, Australia

Abstract

Radiochromic film is a good dosimeter choice for patient QA for complex treatment techniques because of its near tissue equivalency, very high spatial resolution and established method of use. Commercial scanners are typically used for film dosimetry, among which EPSON scanners are the most common. Radiochromic film dosimetry is not straightforward as there are some well-defined problems which must be considered, one of the main ones being the Lateral Response Artefact (LRA) effect. Previous studies showed that the contributing factors to LRA are due to the structure of the active ingredients of the film and to the components and construction of the flatbed scanner. The purpose of this study is to investigate the effect of the scanner lens on the LRA effect. EBT3 films were irradiated with 40x40 cm^2 field size 6 MV beams. Films were analysed using images captured by a Canon 7D camera utilising 18 mm, 50 mm and 100 mm focal length lenses compared to images scanned with a conventional EPSON V700 scanner. The magnitude of the LRA was observed to be directly related to the focal length of the lens used to image the film. A substantial reduction in LRA was seen with the use of the 50 mm and 100 mm lenses, by factors of 3-5 for the 50 mm lens and 4-20 for the 100 mm lens compared to conventional desktop scanner techniques. This is expected to be from the longer focal length camera lens system being able to collect more light from distant areas compared to

the scanner-based system and provides an opportunity to design film dosimetry systems that minimise this artefact.

Keywords: Radiotherapy dosimetry, Radiochromic Film, GafChromic, EPSON scanner, Film dosimetry, lens effect

5.1 Introduction

Complex radiotherapy treatment techniques (IMRT, VMAT, SABR, SBRT) need patient-specific QA to check dose delivery and target volume localisation in three dimensions. Radiochromic film is a very good dosimeter of choice for this purpose because of its properties of near tissue equivalency, very high spatial resolution and established method of use [1–5]. Like other dosimeters available it also has some drawbacks. Two main issues associated with radiochromic film dosimetry are the orientation effect and the lateral response artefact (LRA) effect [5–13]. The orientation effect is defined as the change of response of radiochromic film depending on the orientation of the film on the scanner bed and the LRA effect is the change of response from middle to side of the film, orthogonal to the scanner's light source travel direction [1,6,9,13–15]. The orientation effect can be minimised with a strict protocol of marking and placing the film in the same orientation throughout the process. Hence the LRA effect remains as a main issue which has been investigated widely [10,16–20]. The magnitude of light polarization, introduced by the scanner and the film, increases with increasing lateral distance from the centre of the scanner [11]. The size of the LRA effect depends on irradiated dose and position of the film on the scanner bed [11,14,16]. One contributor to the LRA effect is the needle-like crystal structure [9,21,22] in the active layer of radiochromic films. The rod- or hair-like crystals contribute to polarisation and anisotropic light scattering [23]. Upon irradiation, the neighbouring polymers create bonds and turn into even longer rods which enhances both of these phenomena. The other contributor is the scanner itself, e.g. from lens, mirror system and scanner bed [12]. Schoenfeld [9] showed a schematic diagram of the mirror system which shows the light travel path from light source to the lens system. The different scanner components contribute to the LRA effect [11,14,16] in different ways. Wide angle lenses and a mirror system [9] are used in the EPSON scanners to make them compact. However, wide angle lenses fail to collect all the light. In addition, these components and the scanner bed [12]add extra light polarisation. To manage the LRA effect, a correction factor is needed.

The purpose of this work is to investigate a novel technique using cameras and different lenses for radiochromic film imaging and analysis to evaluate the effect of focal length of the scanner lens on the LRA effect in radiochromic film dosimetry and to consider whether LRA effects, and correction factors, could be reduced by using a different lens system. This is part of wider investigations considering each component of the scanning system, aiming to explore the potential for a more optimised design for film dosimetry.

5.2 Method

The film preparation, handling and irradiation methods were similar to those described in previous work [24], but essential detail is repeated here for completeness. EBT3 films were cut into 3cm x 20.3cm strips along the short side of the film. Figure 5-1 shows schematically how the films were cut and the orientation of the film pieces on the scanner bed. The light source of the scanner is across the short side of the scanner bed, which means the longer side of a film strip on the scanner bed is parallel to the light source. This orientation of film pieces with respect to the light source was kept the same when images were taken with the camera. Films were irradiated at 10cm depth of plastic water with 10cm backscatter in a phantom that was 30 cm x 30 cm area presented to large area beams to achieve uniform dose across the film. Films pieces were irradiated individually for 100MU, 200MU, 500MU and 1000MU on an Elekta Synergy linear accelerator (linac) using a 6MV beam and a 40cm x 40 cm field size, giving doses to the film of 1.13Gy, 2.25Gy, 5.64Gy and 11.28 Gy respectively.

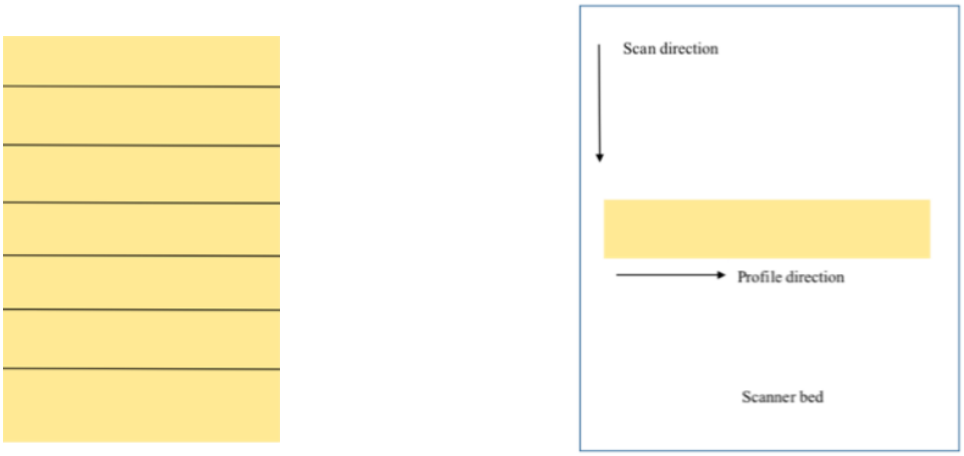

Figure 5-1 : A representative schematic diagram showing the manner in which the films werecut, the orientation of the film pieces with respect to scan direction and the profile direction

Different studies used different time, ranging from hours to days, for leaving the film in the box before scanning. Roozen et al [24] stated that 2-3 hours is sufficient to stabilise the response of EBT film, referring to information from the manufacturer. Rink [25] presented a graph of time versus change of OD, showing insignificant change after 2hours. In this study, irradiated EBT3 films were left in the box for two hours and then scanned using an EPSON V700 [26]. The film pieces were taped down to the scanner bed to flatten the curvature. In addition, photos were taken with a Canon 7D DSLR camera. Gloves were used all the time during handling the film to avoid any contamination from fingerprint marks. The following settings were used for the scanner

- Mode: Professional
- Document Type: Film (with Film Area Guide); this setting allows transmission scanning
- Film Type: Positive Film
- Image Type: 48-bit colour
- Resolution: 508dpi
- No Colour Correction was applied

The following settings were used for the Canon 7D camera

- ISO: 100
- Shutter speed; 1/500
- Aperture: f4.5
- The room light was on
- No colour correction was applied when converting the RAW image to .tiff image

The lens system of an EPSON V700 scanner has two lenses; one has a larger diameter than the other. The smaller one is for high resolution scanning. The larger lens is used for the scanning mode and so is the one used in this work. The lens assembly (both the lenses) was taken out and the focal length measured, by putting it against a vertical steel ruler on the floor on a piece of paper and moving it vertically to get a sharp image of a ceiling light. The distance from the image to the bottom lens is the effective focal length of the lens system. The focal lengths of both the lenses were found to be the same. The focal lengths of the Canon camera lenses were also verified in the same manner.

Previous studies have used a variety of methods to quantify the LRA effect, all of which are based on the difference in pixel values between the centre and a lateral position [9–12]. In this study, the LRA effect is represented as the maximum percent difference of average pixel values of 25 data points at both ends from the average of the central 25 data points.

A flatbed scanner and a DSLR camera work quite differently. Schoenfled et al [9] described, with a schematic diagram, how light travels from the light source to the scanner's CCD imager through five mirrors and a lens system. In a DSLR camera, light travels through the lens directly onto the sensor. There is a mirror in the Canon 7D camera, which moves away from the light path when a picture is taken. As such, both systems are using a transmission style readout with the light source and detector on opposing sides of the film.

The light sources used in the scanner and for the camera studies are different. The EPSON V700 camera uses a white cold cathode fluorescent light (CCFL) source, whilst a white LED light source was used in the camera work. Larraga-Guiteraz [27]compared the light sources of an EPSON V800 and an EPSON 11000XL and presented spectra for both, as wavelength versus relative intensity. The EPSON V800 uses a white light source and the EPSON 11000XL uses a

CCFL source and the two are generally representative of the two sources used in this work. Both light sources have the main peak at 550nm. However, their difference is that the CCFL peak is sharp and has other distinct peaks around the main peak, whilst the spectrum of the LED source is broad, ranging from 470nm to 650nm. The LED source also has another smaller peak at 450nm. If all the peaks are considered both the light sources have wave lengths from 450nm to 650nm.

Scanning with an Epson V700 scanner: The scanning area, which is smaller than the scanner bed of the EPSON V700 scanner is the same as an A4 document size. The short side of EBT3 film is also the same as A4 document size. The edges of the film strip therefore match the edge of the scanning area in the measured profile direction. The film pieces were placed at the central position on the scanner bed to ensure the whole film piece is in the scanning area. Each film piece was scanned 20 times. The scanned images were saved as *.tiff (tagged image file format) which were read and separated into three colour channels in ImageJ V1.49 software.

Photos with a DSLR camera: A LED light source, wrapped with a diffuser, was placed on a wall. A V700 scanner bed was placed in front of the LED light source to keep the path-length effect [28] the same as in the scanner. The orientation of the film strips with respect to the light source are kept the same as in the scanner by putting the long side of the film strip along the light source, but the glass bed was rotated by 90^0 to make it stable on the table as the vertical side of it is curved. This change of orientation of the scanner bed (glass) does not have any effect as the orientation of the film with respect to the linear light source remains the same. The film pieces were taped on the scanner bed. A Canon 7D camera was used to take photos with three different lenses of 18mm, 50mm and 100mm focal length. Figure 5-2 shows the set up for taking photos with the camera. 20 images were taken for each film with each lens, which produced 240 photos (4 films pieces for 4 dose levels x 3 lenses x 20 photos for each film-lens combination). The distances from lens to film strip were 150mm, 500mm and 950mm for 18mm, 50mm and 100mm lenses respectively. These distances were determined by moving the camera back and forth so that the camera captures just the entire film strip, which is 203mm in the horizontal direction. The images were captured as RAW, which were converted to *.tiff format by using Canon software and then were read and separated into three colour channels in ImageJ V1.49 software.

It is acknowledged that the two systems being evaluated utilize two different detectors. These being a CCD (Epson scanner) or a CMOS (Camera) detector with the respective systems. The RGB components and quantum efficiency of both systems may vary with respect to wavelength in the Red Green and Blue bandwidths. Although this paper does not analyse or quantify these potential variations, the effect of lens focal length shows similar trends in each bandpass components and as such does not diminish the validity of the trends observed in this work

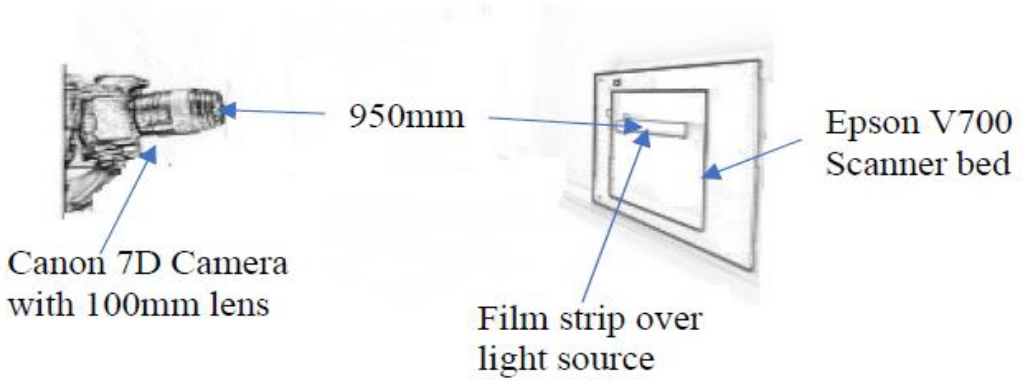

Figure 5-2: Camera set up for taking photos of film strips. This schematic example shows the set up for the 100 mm lens, with a distance between lens and film of 950mm. The distances for the other lenses were 150mm and 500mm for the 10mm and 50mm lenses respectively.

In ImageJ an average profile was generated across each film for each combination using a rectangular ROI cropped 1mm in from the film edge. The average profiles for each colour channel, 20 in total, were analysed in MS Excel where they were normalised to the mean of the central 100 data points. The edges of images from the scanner were noisier than those from the camera images. There were a few hours of time gap between photos taken by the camera and the scanned images being acquired because of the time needed for the large number of photos taken. This extra time caused deterioration of the edges, which made the noise spread more in the scanned images. Avoiding this increased spread of noise made the profiles of the scanner images a few mm shorter at both ends.

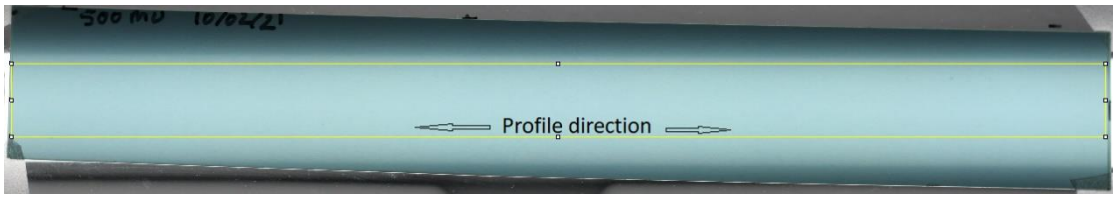

Figure 5-3 : Selection of a rectangle in ImageJ to create a profile along the short side of scanner.

Mean and standard deviation of these 20 images for each combination were calculated. The LRA effects were calculated from these profiles as the difference between the maximum (centre) and minimum (edges) values as a percentage, where the values used were the average over 25 data points at the centre and each end respectively. The propagation of uncertainty, which is the standard deviation of normalised pixel values of 20 images, was calculated as root mean square of uncertainty values of maximum and minimum mean percentage value.

$$LRA\ Uncertainty\ = \sqrt{Stdv(center)^2 + \max\left(Stdv(left), Stdv(right)\right)^2}$$

5.3 Results:

The Epson V700 has two lenses. The smaller one is for high resolution scanning and the bigger lens is used for the scanning mode we used (film with film area guide). The effective focal length of each of the lenses of the Epson V700 scanner was measured to be 38 mm. Figures 4a to 4d show the profiles in the red channel from films irradiated with 100MU, 200MU, 500MU and 1000MU respectively, each showing four profiles, three from images taken with the Canon DSLR camera using 18mm, 50mm and 100mm lenses and the fourth from scanning the films using the Epson V700 scanner, with a lens system of 38mm focal length. . Each profile is for average pixel values from 20 photos and scans. Green channel results were also obtained and showed very similar trends to those of the red channel results. The highest uncertainty as standard deviation of these 20 photos and scans is 1.7% and 1.3% for green channel and red channel respectively.

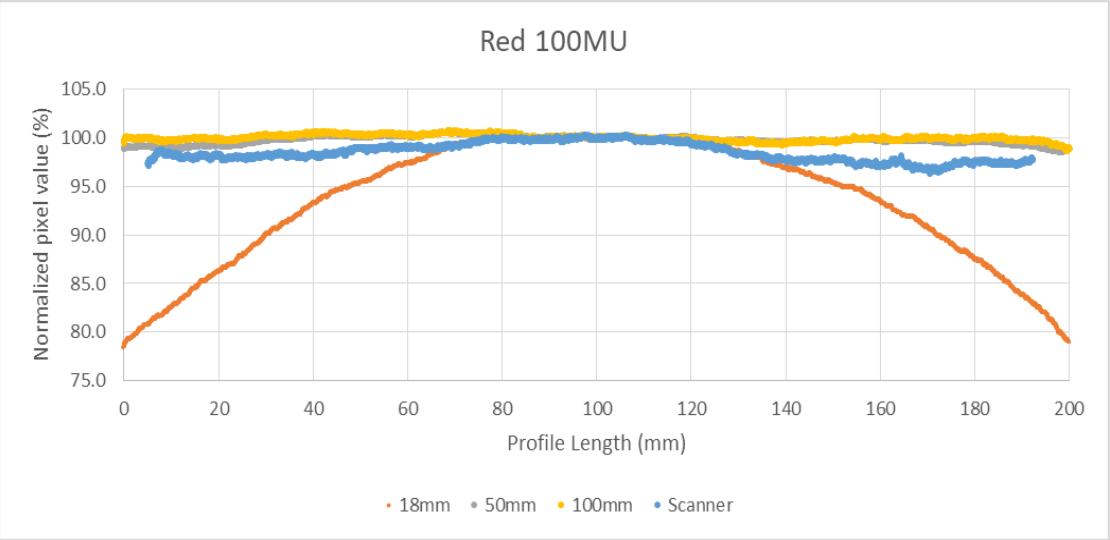

a: 100MU

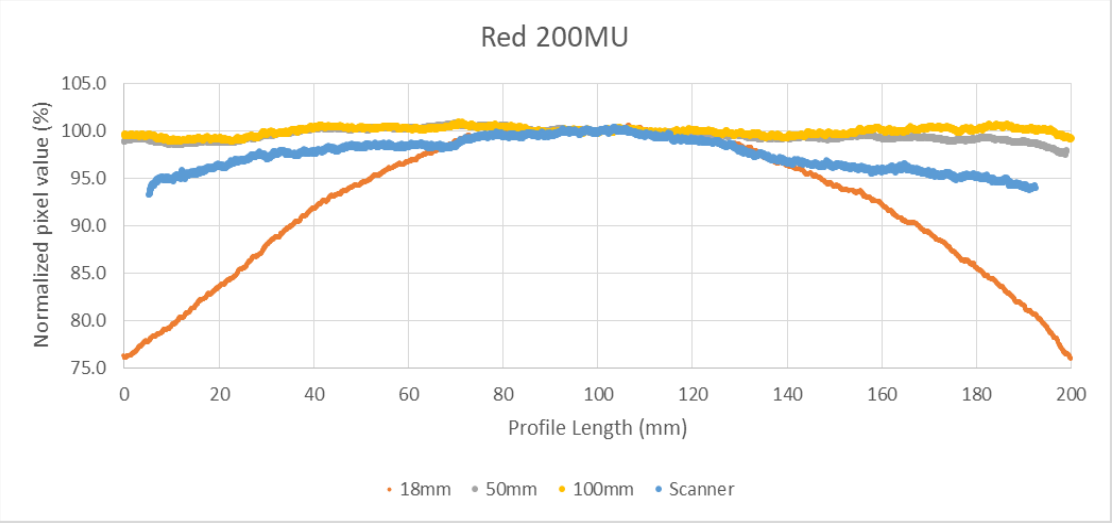

b: 200MU

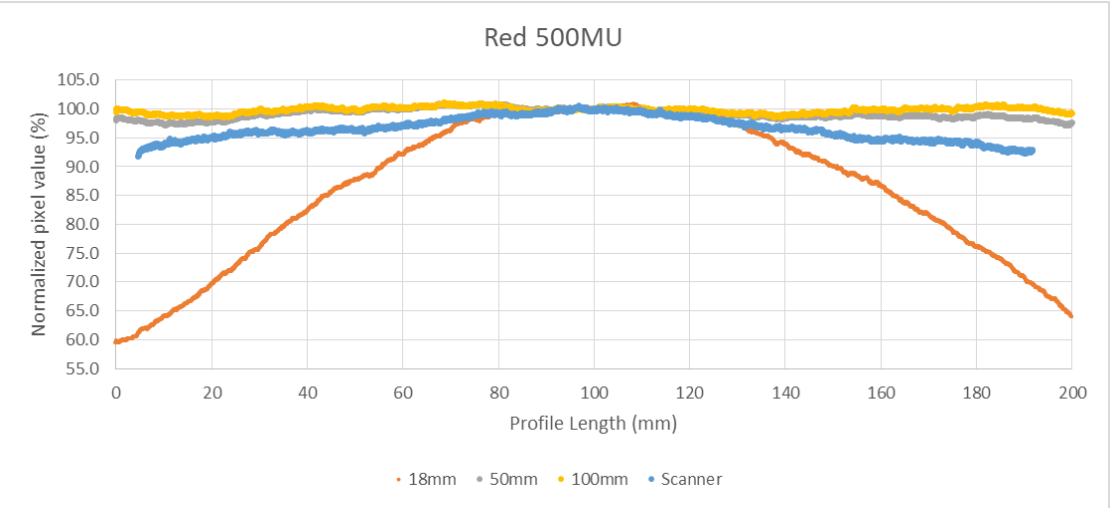

c: 500MU

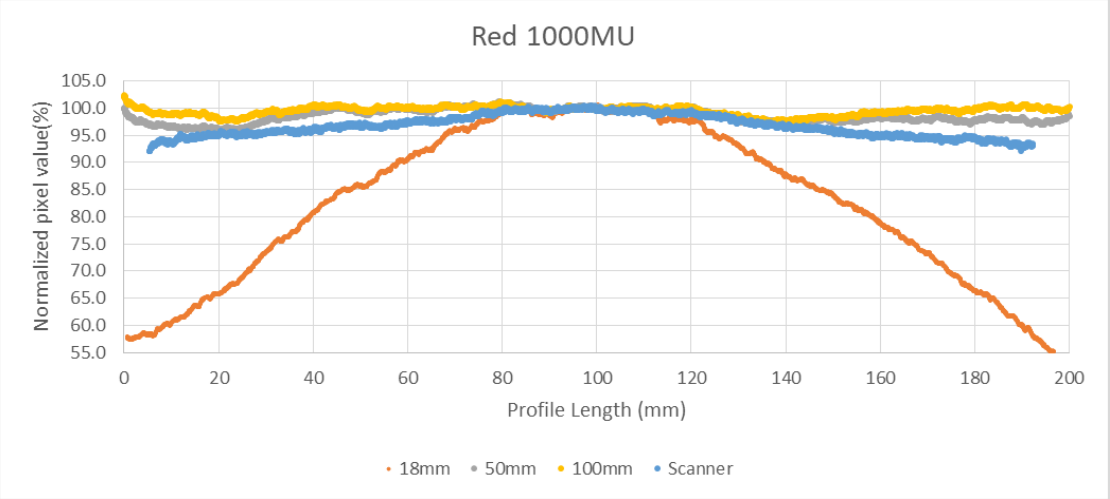

d: 1000MU

Figure 5-4: Profiles measured across a strip of EBT3 film that has been exposed at depth in solid water. 4a: for 100 MU, 4b for 200MU, 4c, for 500MU and 4d for 1000MU.

The four profiles in each figure are based on the red channel analysis of images of the film acquired with the EPSON V700 flatbed scanner and with a Canon DSLR 7D camera equipped with an 18mm, 50mm and 100mm focal length lens

LRA effect: Table 5-1 shows the maximum LRA effect as a maximum percentage difference of edges from the centre of profiles drawn across the film pieces (Figure 1 and Figure 5-3) for all the dose levels for all the lenses. Only the results of green and red channels are presented here as no previous studies recommended the use of the blue channel for film dosimetry. A

substantial reduction in LRA was seen with the use of the 50mm and 100mm lenses, by factors of 3-5 for the 50 mm lens and 4-20 for the 100 mm lens compared to conventional desktop scanner techniques. Using the 100 mm lens, the LRA effect is observed to be 0.3-1.2% at 10 cm out from the centre of the film. Given the expected +0.7% in beam flatness in the experimental irradiation conditions at that position, this indicates that the lower normalised pixel values at the edges are reflecting the higher dose values at that position.

Dose level	18mm		38mm(scanner)		50mm		100mm	
	Green	Red	Green	Red	Green	Red	Green	Red
100MU	19.1±0.6	21.1±0.5	4.9±1.1	4.5±0.9	1.5±0.2	1.0±0.2	1.0±0.1	1.2±0.2
200MU	20.6±0.3	23.9±0.3	5.9±0.9	7.1±1.7	2.1±0.2	1.4±0.2	0.7±0.1	0.8±0.1
500MU	37.0±0.9	40.5±1.0	10.3±1.4	10.6±1.6	1.8±0.3	2.6±0.5	0.9±0.2	0.8±0.3
1000 MU	43.2±0.3	46.6±1.0	10.7±1.4	11.6±1.0	2.4±0.2	2.1±0.4	0.3±0.2	0.4±0.5

Table 5-1: LRA effect (%) for four lens systems of different focal lengths

5.4 Discussion:

The images acquired with different lens systems highlight a systematic variation in the LRA effect with the focal length of the image capturing system. Results show that with a smaller focal length lens system, higher LRA effects are observed. The LRA effect is also observed to increase with dose[9,10,16], which is a well-known phenomenon of radiation induced polymerization of active ingredient LiPCDA, which enhances polarization and anisotropic light scattering [9,21]. Schoenfeld et.al [9] investigated the effect of scanner components on LRA effect and stated that the lens system of a flatbed scanner cannot collect all the light scattered from the edges of films. The loss of light collection enhances the optical density towards the edge. The polarization and anisotropic scattering of light caused by the crystals in the active ingredient of the film increases the optical density further at the edge. Wide-angle lenses, i.e. smaller focal length, are used in flatbed scanners to make them compact in size, which creates this loss of light collection from the edges. A bigger focal length lens system needs to be moved further away which results in more scattered light being collected by the lens and a smaller LRA effect.

Figure 5-5 plots the average LRA of the four dose levels investigated, with respect to the focal lengths of the lens systems used in the study. It shows decreasing LRA for both red and green channels with increasing focal length of the lens systems. It is likely that the current results would be qualitatively similar for other scanners of similar design, but this would need to be confirmed by further studies. Likewise, the changes in LRA effect for other types of film would require specific investigation.

The decreased LRA effect using larger focal length imaging systems to analyze films provides an opportunity to create a film scanner system which has the potential to minimize the lateral response artifact. The increase in focal length necessary to capture more light from the edges of the film requires an increased distance between the film and the detection camera. Thus these results highlight the fact that the LRA can be reduced by design choices of specific characteristics of the equipment and imaging system. But the practicalities of using longer focal length imaging systems are not simple and imply larger systems. Nevertheless, this provides an avenue for further work to continue to optimize the design of a new imaging system which may be able to remove or at least minimize the LRA effect for EBT GafChromic film. This could potentially reduce or negate the need for scan processing or corrections to scanned raw data for radiochromic film analysis.

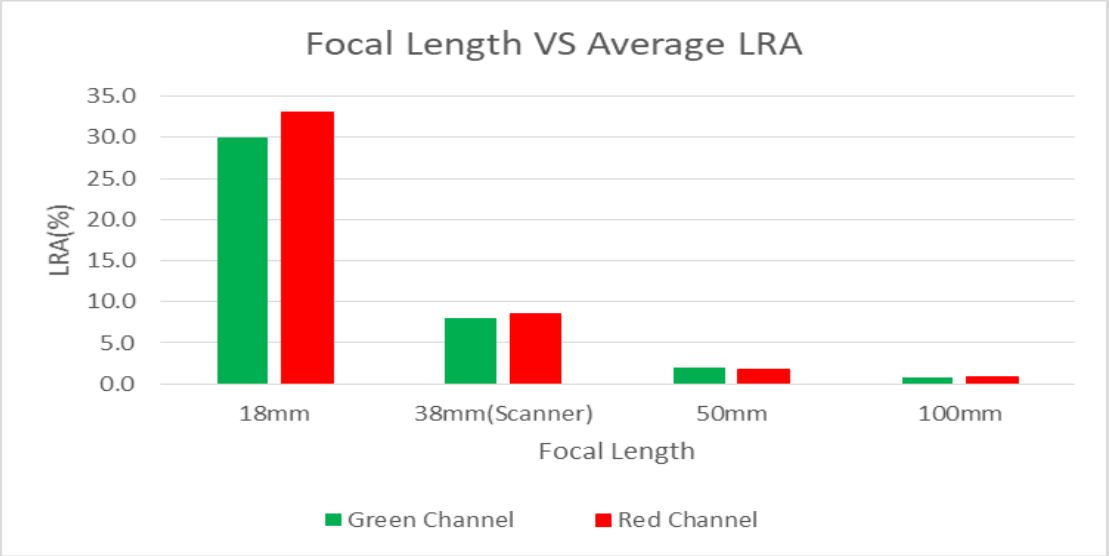

Figure 5-5: Average LRA of four dose levels of 100MU, 200MU, 500MU and 1000MU measured from images acquired with an Epson V700 scanner and a Canon 7D camera with three lenses of focal lengths of 18mm, 50mm and 100mm

5.5 Conclusion:

One significant contributing factor to the LRA effect from a flatbed scanner is the lens system [9]. By utilizing a 100mm lens the LRA was reduced from roughly 5-10% to 1.2% or less for doses delivered to Gafchromic film in the range of 1-11 Gy compared to the standard Epson

V700 film scanner lens system. As such, an imaging system based on a larger focal length lens could potentially improve the film dosimetry system by reducing the LRA effect and the need for making corrections for it, although this would increase system size.

5.6 References

[1] N. V. Klassen, L. Van Der Zwan, and J. Cygler, "GafChromic MD-55: Investigated as a precision dosimeter," *Med Phys*, vol. 24, no. 12, pp. 1924–1934, 1997, doi: 10.1118/1.598106.

[2] C. G. Soares, "Radiochromic film dosimetry," *Radiat Meas*, vol. 41, no. SUPPL. 1, 2006, doi: 10.1016/j.radmeas.2007.01.007.

[3] T. Kairn, N. Hardcastle, J. Kenny, R. Meldrum, W. A. Tomé, and T. Aland, "EBT2 radiochromic film for quality assurance of complex IMRT treatments of the prostate: Micro-collimated IMRT, RapidArc, and TomoTherapy," *Australas Phys Eng Sci Med*, vol. 34, no. 3, pp. 333–343, 2011, doi: 10.1007/s13246-011-0087-z.

[4] T. Aland, T. Kairn, and J. Kenny, "Evaluation of a Gafchromic EBT2 film dosimetry system for radiotherapy quality assurance," *Australas Phys Eng Sci Med*, vol. 34, no. 2, pp. 251–260, 2011, doi: 10.1007/s13246-011-0072-6.

[5] N. Bennie and P. Metcalfe, "Practical IMRT QA dosimetry using Gafchromic film: a quick start guide," *Australas Phys Eng Sci Med*, vol. 39, no. 2, pp. 533–545, 2016, doi: 10.1007/s13246-016-0443-0.

[6] M. J. Butson, T. Cheung, and P. K. N. Yu, "Scanning orientation effects on Gafchromic EBT film dosimetry," *Australas Phys Eng Sci Med*, vol. 29, no. 3, pp. 281–284, 2006, doi: 10.1007/BF03178579.

[7] M. J. Butson, T. Cheung, and P. K. N. Yu, "Evaluation of the magnitude of EBT Gafchromic film polarisation effects.pdf," *Australas Phys Eng Sci Med*, vol. 31, no. 1, pp. 21–25, 2009.

[8] H. Alnawaf, M. J. Butson, T. Cheung, and P. K. N. Yu, "Scanning orientation and polarization effects for XRQA radiochromic film," *Physica Medica*, vol. 26, no. 4, pp. 216–219, 2010, doi: 10.1016/j.ejmp.2010.01.003.

[9] A. A. Schoenfeld, D. Poppinga, D. Harder, K. J. Doerner, and B. Poppe, "The artefacts of radiochromic film dosimetry with flatbed scanners and their causation by light scattering from radiation-induced polymers," *Phys Med Biol*, vol. 59, no. 13, pp. 3575–3597, 2014, doi: 10.1088/0031-9155/59/13/3575.

[10] D. Lewis and M. F. Chan, “Correcting lateral response artifacts from flatbed scanners for radiochromic film dosimetry,” *Med Phys*, vol. 42, no. 1, pp. 416–429, 2015, doi: 10.1118/1.4903758.

[11] L. J. Van Battum, H. Huizenga, R. M. Verdaasdonk, and S. Heukelom, “How flatbed scanners upset accurate film dosimetry,” *Phys Med Biol*, vol. 61, no. 2, pp. 625–649, 2015, doi: 10.1088/0031-9155/61/2/625.

[12] A. A. Schoenfeld, S. Wieker, D. Harder, and B. Poppe, “The origin of the flatbed scanner artifacts in radiochromic film dosimetry - Key experiments and theoretical descriptions,” *Phys Med Biol*, vol. 61, no. 21, pp. 7704–7724, 2016, doi: 10.1088/0031-9155/61/21/7704.

[13] A. A. Schoenfeld, S. Wieker, D. Harder, and B. Poppe, “Changes of the optical characteristics of radiochromic films in the transition from EBT3 to EBT-XD films,” *Phys Med Biol*, vol. 61, no. 14, pp. 5426–5442, 2016, doi: 10.1088/0031-9155/61/14/5426.

[14] C. Fiandra *et al.*, “Clinical use of EBT model Gafchromic^{TM} film in radiotherapy,” *Med Phys*, vol. 33, no. 11, pp. 4314–4319, 2006, doi: 10.1118/1.2362876.

[15] B. D. Lynch, J. Kozelka, M. K. Ranade, J. G. Li, W. E. Simon, and J. F. Dempsey, “Important considerations for radiochromic film dosimetry with flatbed CCD scanners and EBT GAFCHROMIC® film,” *Med Phys*, vol. 33, no. 12, pp. 4551–4556, 2006, doi: 10.1118/1.2370505.

[16] L. Menegotti, A. Delana, and A. Martignano, “Radiochromic film dosimetry with flatbed scanners: A fast and accurate method for dose calibration and uniformity correction with single film exposure,” *Med Phys*, vol. 35, no. 7, pp. 3078–3085, 2008, doi: 10.1118/1.2936334.

[17] L. Paelinck, W. De Neve, and C. De Wagter, “Precautions and strategies in using a commercial flatbed scanner for radiochromic film dosimetry,” *Phys Med Biol*, vol. 52, no. 1, pp. 231–242, 2007, doi: 10.1088/0031-9155/52/1/015.

[18] A. Micke, D. F. Lewis, and X. Yu, “Multichannel film dosimetry with nonuniformity correction.pdf,” *Med Phys*, vol. 38, no. 5, pp. 2523–2534, 2011.

[19] E. Butson, H. Alnawaf, P. K. N. Yu, and M. Butson, “Scanner uniformity improvements for radiochromic film analysis with matt reflectance backing,” *Australas Phys Eng Sci Med*, vol. 34, no. 3, pp. 401–407, 2011, doi: 10.1007/s13246-011-0086-0.

[20] D. Poppinga, A. A. Schoenfeld, K. J. Doerner, O. Blanck, D. Harder, and B. Poppe, “A new correction method serving to eliminate the parabola effect of flatbed scanners used in

radiochromic film dosimetry.," *Med Phys*, vol. 41, no. 2, p. 021707, 2014, doi: 10.1118/1.4861098.

[21] A. Rink, "Point-based ionizing radiation dosimetry using radiochromic materials and a fibreoptic readout system," *Methods*, 2008, doi: 10.1017/CBO9781107415324.004.

[22] D. F. Lewis and M. F. Chan, "On Gafchromic EBT-XD film and the lateral response artefact," *Med Phys*, vol. 43, no. 2, pp. 643–649, 2016.

[23] B. S. Hiaso, R. S. Stein, K. Deutscher, and H. H. Winter, "Optical anisotropy of a thermotropic liquid crystalline polymer in transient shear," *Journal of polymer Science*, vol. 28, pp. 1571–1588, 1990.

[24] K. Roozen, T. Kron, A. Haworth, and R. Franich, "Evaluation of EBT radiochromic film using a multiple exposure technique," *Australas Phys Eng Sci Med*, vol. 34, no. 2, pp. 281–289, 2011, doi: 10.1007/s13246-011-0067-3.

[25] A. Rink, I. Alex Vitkin, and D. A. Jaffray, "Characterization and real-time optical measurements of the ionizing radiation dose response for a new radiochromic medium," *Med Phys*, vol. 32, no. 8, pp. 2510–2516, 2005, doi: 10.1118/1.1951447.

[26] T. Shameem, N. Bennie, M. Butson, and D. Thwaites, "A comparison between EPSON V700 and EPSON V800 scanners for film dosimetry," *Phys Eng Sci Med*, vol. 43, no. 1, pp. 205–212, 2020, doi: 10.1007/s13246-019-00837-3.

[27] J. M. Lárraga-Gutiérrez, O. A. García-Garduño, C. Treviño-Palacios, and J. A. Herrera-González, "Evaluation of a LED-based flatbed document scanner for radiochromic film dosimetry in transmission mode," *Physica Medica*, vol. 47, no. December 2017, pp. 86–91, 2018, doi: 10.1016/j.ejmp.2018.02.0

6 Effect of mirror system and scanner bed of a flatbed scanner on lateral response artefact in radiochromic film dosimetry.

This chapter consists of the manuscript

T. Shameem, N. Bennie, M. Butson, and D. Thwaites, "Effect of mirror system and scanner bed of a flatbed scanner on lateral response artefact in radiochromic film dosimetry," *Physical and Engineering Sciences in Medicine*, vol. 47, pp. 1651–1663, 2024

https://doi.org/10.1007/s13246-024-01478-x

Preface: This chapter extends the component-level investigation from lens effects (Chapter 5) to mirror polarization effects and to the physical scanner bed, i.e. this study separates and quantifies contributions from additional scanner components to polarisation and/or LRA and further demonstrates that multiple scanner sub-systems interact with film optical anisotropy to produce the observed artefact. Together with the lens study, it builds a mechanistic picture of scanner-film interactions and provides some initial recommendations on how readout systems might be modified based on physics-focussed principles, thereby reducing overall corrections for LRA and the uncertainties in film dosimetry that arise from them

Authors: *Tarafder Shameem[1,2], Nick Bennie[1], Martin Butson[2,3], David Thwaites[2]

[1]North Coast Cancer Institute, Lismore, NSW, Australia; [2]Institute of Medical Physics, School of Physics, University of Sydney, Sydney, NSW, Australia; [3] EPA, NSW, Australia

Abstract

Radiochromic film, evaluated with flatbed scanners, is used for practical radiotherapy QA dosimetry. Film and scanner component effects contribute to the Lateral Response Artefact (LRA), which is further enhanced by light polarisation from both. This study investigates the scanner bed's contribution to LRA and also polarisation from the mirrors for widely used EPSON scanners, as part of broader investigations of this dosimetry method aiming to improve processes and uncertainties. Alternative scanner bed materials were compared on a modified EPSON V700 scanner. Polarisation effects were investigated for complete scanners (V700, V800, on- and off-axis, and V850 on-axis), for a removed V700 mirror system, and independently using retail-quality single mirror combinations simulating practical scanner arrangements, but with varying numbers (0-5) and angles. Some tests had no film present, whilst others included films (EBT3) irradiated to 6 MV doses of 0-11.3 Gy. For polarisation analysis, images were captured by a Canon 7D camera with 50 mm focal length lens. Different scanner bed materials showed only small effects, within a few percent, indicating that the normal glass bed is a good choice. Polarisation varied with scanner type (7-11%), increasing at 10 cm lateral

off-axis distance by around a further 6%, and also with film dose. The V700 mirror system showed around 2% difference to the complete scanner. Polarization increased with number of mirrors in the single mirror combinations, to 14% for 4 and 5 mirrors, but specific values depend on angles and mirror quality. Novel film measurement methods could reduce LRA effect corrections and associated uncertainties.

Keywords: Radiotherapy dosimetry, Radiochromic Film, GafChromic, EPSON scanner, Film dosimetry, mirror effect, scanner bed effect

6.1 Introduction

Radiochromic film is often used for two-dimensional dose measurement in radiotherapy. Its high spatial resolution, weak energy dependence and near tissue equivalency make it popular for patient-specific quality assurance (QA) of complex radiotherapy treatment techniques (e.g IMRT, VMAT, SABR/SBRT) [1–5]. Digitization of optical density of irradiated films is commonly done using commercial flatbed scanners, as they are inexpensive and can produce very high-resolution images; for practical clinical work, EPSON scanners are commonly used [3,6–9]. However, the dosimetry system of radiochromic film coupled with a commercial flatbed scanner has some drawbacks as for any other dosimetry system. The orientation effect, of film to scanner bed, and the lateral response artefacts (LRA) are the two main issues associated with the system [6–15]. A strict protocol of marking and placing the film in the same orientation throughout the dosimetry process eliminates the orientation effect. The LRA effect is the change of measured optical density from middle to side of the film, orthogonal to the scanner's light source travel direction [12,15–19]. It remains as a major issue which has been investigated widely [15,17–21]. The origin of the LRA effect comes from two different sources, the film itself and various components of the flatbed scanner. The needle-like crystal structure [15,22,23] in the active layer of radiochromic films introduces anisotropic scattering and polarization of light [23]. Upon irradiation, the neighbouring polymers create bonds and turn into even longer rods, which enhances both of these phenomena. The lens system, scanner bed and mirror system of flatbed scanners [7] are the components that contribute towards LRA in different ways. The lens system fails to collect all the light from distant parts of the film [9,14]. The difference of refractive indices of film and scanner bed can cause a path length effect which reduces optical densities at the distant part of the film. The co-efficient of reflection changes with the incident angle of light on the mirror system components [6] and the mirror system introduces light polarization [6,7,12]. The magnitude of light polarization, introduced by the scanner and the film, increases with increasing lateral distance from the centre of the scanner [6]. Other studies also considered light polarization resulting from various films [8] and film-scanner combinations [7,12].

There is little data in the literature on the relative effects from the different scanner components. The lens system was investigated by Shameem et al [9] within the current project. Van Battum

et al [6] investigated the path length effect. They stated that "*The film-induced optical path length variation becomes relevant if its refraction index differs from that of the glass plate of the flatbed scanner*". Schoenfeld et al [7] provided a discussion of the theoretical background of the pathlength effect and the role of mirrors in LRA caused by light incident angle affecting the co-efficient of reflection. Van Battum et al [6] investigated light polarisation caused by some film-scanner combinations, with most experiments reported for an EPSON XL10000 scanner. A schematic diagram of the mirror system used in the EPSON 10000XL is provided in [8] and is redrawn here (Figure 1), showing the light travel path through the mirror system and the positions and angles of the mirrors to each other and to the incident light path. It may be noted that the 10000XL is a bigger scanner (A3) than the A4 scanners often used in practical dosimetry applications and has a five-mirror system, whereas the V700, V800 and V850 scanners considered in the current work are A4 scanners and use four-mirror systems.

The purpose of this work was to investigate the scanner bed path-length effect and also the polarization effect caused by mirrors but using independent novel approaches to those previously reported [6,7] in the literature and for these often-used A4 scanners. The relative path length effect caused by the scanner bed was considered by comparing a range of materials having different refractive indices from that of film or glass. The measurement of the polarisation effect of mirror systems followed two approaches, one considering effects from the complete scanner system, using a method directly comparable to the previous EPSON XL10000 A3 scanner study [6], but here applied to currently-used A4 scanners, and the other independently investigating the polarisation effect from the mirror system alone, separated from the other scanner components to avoid any influence from those. In the latter work, the mirror system from an old EPSON V700 scanner was removed and a Canon 7D camera was used to capture images. In addition, a third set of experiments used retail-grade commercial mirrors to investigate the effect of varying the number of mirrors on the magnitude of polarization, given different model EPSON flatbed scanners use either 4 or 5 mirrors, and considered the effect of varying the angle of one of the mirrors to investigate the impact of different mirror orientations. This work is part of a wider study systematically investigating each component of the scanner system separately, with a view to improving the overall radiochromic film measurement process and reducing uncertainties, including optimising novel scanner designs and procedures for film dosimetry.

6.2 Method

Path Length Effect: The film preparation, handling and irradiation methods for this work were similar to those described in our previous work [9,24]. Full detail can be obtained there, but essential detail is repeated here for completeness. EBT3 films (Ashland Specialty Ingredients, G.P., NJ, USA) were cut into 3cm × 20.3cm strips along the short side of the film. Film was irradiated at 90cm SSD and 10cm depth of plastic water with 10cm backscatter in a phantom

of 30cm × 30cm area presented to large area beams to achieve uniform dose across the film. Film pieces were irradiated on an Elekta Synergy linear accelerator (linac) using a 6MV beam and a 40cm × 40cm field size, giving 0MU, 500MU and 1000MU, which in these conditions delivered doses to the film of 0Gy, 5.64Gy and 11.28Gy respectively.

The scanner bed was removed, and various materials were used as substitute beds one by one. The materials used included a piece of clear acrylic sheet, another piece of unirradiated EBT3 film and a 'no bed' (air only) setup. In addition, a laminating pouch, consisting of two sheets of plastic with dry glue on the inner side, was included as it contains grainy particles in its glue and it was thought this might add information linked to the similar scatter effects expected from the crystals in gafchromic film, i.e to enhance the polarisation. For scanning the films with 'no bed', a hole was cut in the middle of a glass scanner bed, and the film piece was placed over the hole to scan it with no solid bed directly beneath the area of interest. In this study, an EPSON V700 scanner was used, since a non-clinical one was available to dismantle and modify without having any impact on the clinical service. Other flatbed scanners have similar scanner beds and mirror systems, so its use should be representative for a range of units.

Irradiated EBT3 films were left in the box for two hours[25,26] and then scanned using the modified scanner with each of the above 'beds'. Although EBT3 films still darken after two hours, the post irradiation coloration develops much more slowly then. Scanning all the films in this investigation took about 15 to 20mins during which the change of measured LRA due to darkening of the film is expected to be negligible. The light source of the scanner is across the short side of the scanner bed and the longer side of a film strip was positioned on the scanner bed to be parallel to the light source, perpendicular to scan direction. The film piece was taped down to the bed to flatten the curvature. Gloves were used at all times during film handling to avoid any contamination from fingerprint marks. The following settings were used for the scanner

- Mode: Professional
- Document Type: Film (with Film Area Guide); this setting allows transmission scanning
- Film Type: Positive Film
- Image Type: 48-bit colour
- Resolution: 508dpi
- No Colour Correction was applied

The film piece was placed at the central position on the scanner bed and on the other materials used as substitute scanner beds to ensure the whole film piece is in the scanning area. Each film piece was scanned 5 times. The scanned images were saved as *.tiff (tagged image file format) which were read and separated into three colour (RGB) channels, each of which were analysed

separately, in ImageJ V1.49 software. In each case, the film piece was rotated by 180º and the whole process was repeated.

In ImageJ an average profile was generated across each film for each combination using a rectangular ROI cropped 1mm in from the film edge [9,24]. The average profiles for each dose level, each orientation, each bed type and each colour channel were analysed in MS Excel where they were normalised to the mean of the central 100 data points. For each bed type and each dose level there are 10 scans, 5 in initial orientation and 5 in 180º rotation. Averaging these 10 scans eliminated any small asymmetries in profiles resulting from the scanner or from the film itself and its irradiation. Since, the aim of this experiment is only to compare the relatively small effects of different bed materials, symmetrising the profiles in this way does not affect the relative results, whilst helping to clearly visualise these small effects when presented graphically. There is a small beam flatness variation over the films at irradiation in these conditions [9], however the profiles were not corrected for this, since they were only to be compared in a relative way to the standard glass scanner bed material and this small variation would be common to all.

Mirror effect: Firstly, for direct comparison to the findings of van Battum [6] on an EPSON 10000XL scanner, a similar procedure was used in the current work for complete V700, V800 and V850 scanners. For the first part of this, to test the degree of polarisation resulting from the complete scanner system and for all three scanner types to compare to the 10000XL, a 5cm × 5cm piece of a linear polarizer sheet was cut and placed at the centre of the scanner bed. The linear polariser was rotated to 180º using an arc template to guide precise steps of 10º. A 1cm × 1cm pixel area at the centre of rotation was used to measure the optical density. The procedure was repeated at 10cm lateral (right) to the centre. For the second part of this, the variation of polarisation with dose given to the film was investigated, for V700 and V800 scanners only. EBT3 films irradiated to different doses, as described in the previous section, were placed under the polarizer and the whole procedure was repeated.

However other scanner components may influence the results when the system is complete. Therefore, an independent approach was also taken to investigate the mirror system alone, separated from other components for one of the scanners and also the effect of varying the number of mirrors was considered from zero up to five. For these experiments, an EPSON V700 scanner's upper part and the scanner bed were removed to access the light source, which was placed on its side so that it remained vertical, perpendicular to the tabletop. Firstly, the mirror system of an out-of-use V700 scanner was taken out and placed in front of the light source and secondly, sets of single mirrors were arranged in front of the light source to simulate the angles of practical scanner mirror systems (Figure 1).

In each case, a Canon 7D camera with a 50mm lens was positioned along the axis of the reflected light from the last mirror of the mirror assembly to capture images. A sheet of EBT3

film was irradiated by 500MU with the same set up as described above. After two hours, the film was taped on a glass plate, with an arc template attached to the other side. A piece of linear polarizer was taped on the arc template. This combination was placed between the light source and the mirror system with linear polarizer facing the camera. Five images were captured and the process was repeated rotating the linear polarizer by 10º at a time up to 180º. The whole process was repeated after removing the film, leaving the linear polarizer and mirror system and also after removing the mirror system leaving the film and linear polarizer only in between light source and camera. The images were captured as RAW (unprocessed) format, which were converted to *.tiff format using a Canon software, named "Digital Photo Professional", and were read and separated into three colour channels in ImageJ V1.49 software. A rectangular ROI was selected covering only the part of the image illuminated by the V700 light source. The mean pixel values of each colour channel of the selected ROI were measured using ImageJ V1.49 software and recorded in an MS Excel spreadsheet. The pixel values were normalised as a percentage of the average of 0º and 180º polariser sheet angles. Results were plotted as normalised pixel values, normalised to the centre position, against linear polariser angle. The uncertainty was calculated as the standard deviation of pixel values of five images as a percent of mean pixel values.

To investigate the change of polarization caused by varying the number of mirrors, five individual independent mirrors were placed at positions and angles to each other to simulate the arrangement for the 10000XL scanner [14] (Figure 6-1). These are from a retail-grade household mirror, cut into five pieces. They are approximately 1.5mm thick and constructed from silvered (aluminium) glass, whereas the EPSON scanner mirrors were about 5mm thick and of better optical quality. The reflective coating on the retail grade mirror has a coarser texture than the EPSON mirrors. The procedure was repeated with linear polariser only on the glass plate (no film). The mirrors were then taken out one by one, starting from mirror 5 until no mirrors were left and the whole process was repeated, with the camera re-positioned for each mirror arrangement. To check the dependence of mirror polarization on light incident angle, mirror 1 and mirror 2 were used, with mirror 2 rotated around its vertical axis by 30º and 60º anti clockwise from its original position to give angles of 139º and 169º respectively (as compared to Figure 6-1) and the whole process was repeated for each.

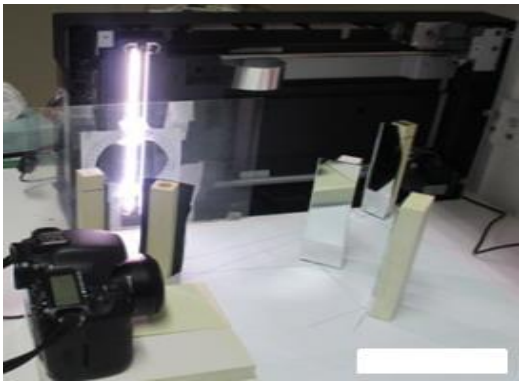

a. Camera and mirror set up

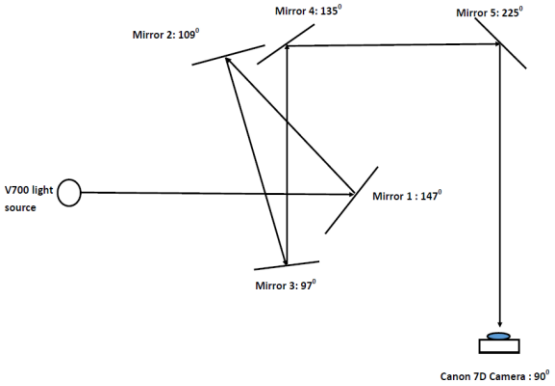

b. Schematic diagram of EPSON 10000XL mirror system

Figure 6-1: Mirror and camera set up for the five-mirror experiment and the schematic diagram of EPSON 10000XL mirror system.

The following experimental setup conditions and camera settings were used

- ISO: 100
- Shutter speed; 1/500
- Aperture: f4.5
- The room light was on
- The distance between camera lens and last mirror or light source (with no mirror set up) always kept at 50cm

No colour correction was applied when converting the RAW image to .tiff image.

6.3 Results:

Path length effect: Figure 6-2 shows the profiles of the red channel for 0MU, 500MU and 1000MU dose level across film pieces with different scanner 'bed' materials below them. The difference between the standard glass bed and no bed at all (or using an acrylic sheet as a substitute bed) was found to be insignificant. The differences found between these and the other substitute bed materials used in this investigation (laminating pouch and a piece of film) were up to approximately 4% and 2% respectively at the extreme lateral positions. Similar differences were found for the other delivered doses and also for all dose levels in the green channel. Uncertainty, as standard deviation of the pixel values of 10 scans, was found to be less than 0.5% at any data point.

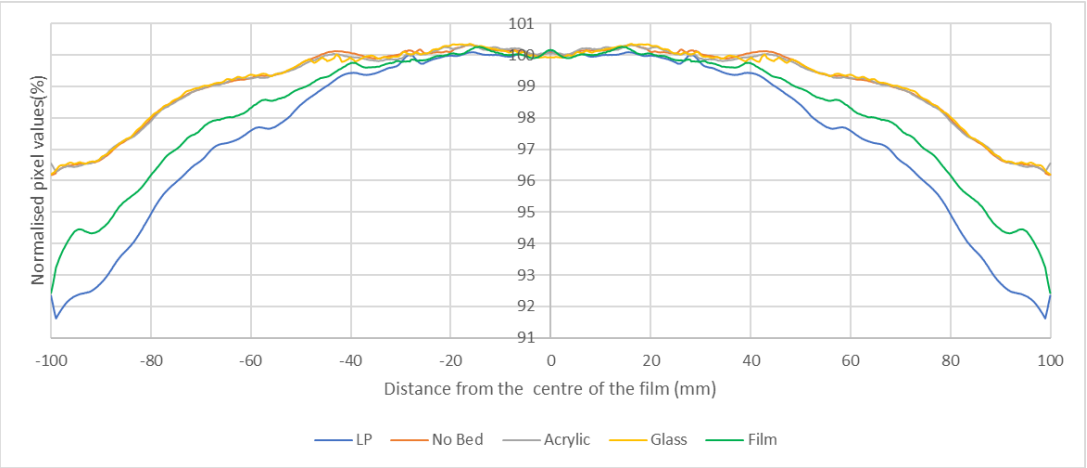

a. 0 MU

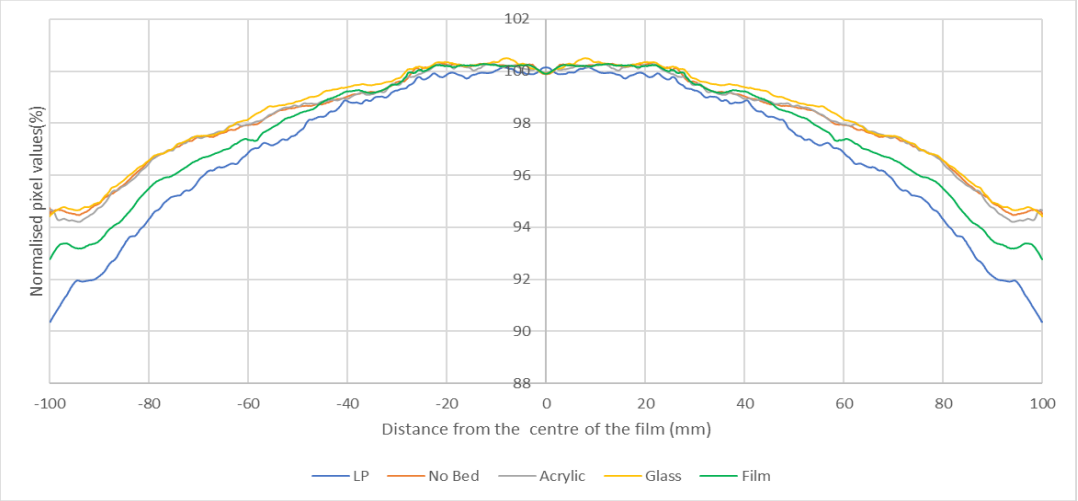

b. 500 MU

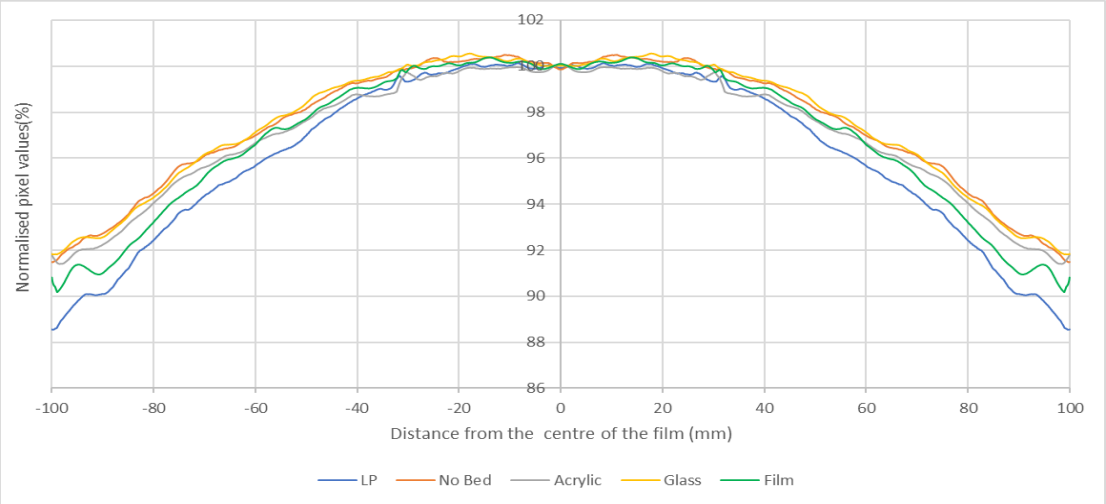

c. 1000 MU

Figure 6-2: Normalised pixel values across the film pieces for different scanner 'beds' for a. 0MU, b.500MU and c.1000MU. LP is the laminating pouch.

Mirror effect: Figure 6-3 shows the change of pixel values with the change of polariser angle, normalised to the average pixel values with polariser angles of 0º and 180º for complete V700, V800 and two V850 scanners (with no film present). The results show that the degree of polarization is different for different models of flatbed scanner. The two examples of the same scanner type (V850) were insignificantly different from each other.

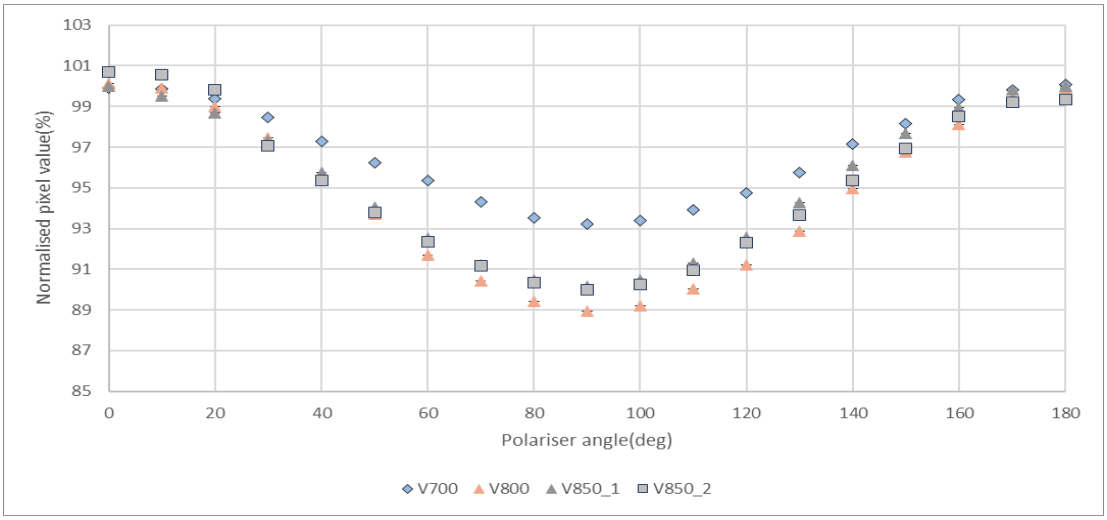

Figure 6-3: Normalised pixel values with respect to polariser angle for complete V700, V800 and two V850 scanners (no film present).

Figure 6-4 shows the increasing degree of polarization with increasing dose given to EBT3 film for a V700 scanner and a V800 scanner. In both scanners the degree of polarization increased with increased dose level. There are small differences of around 1% in polarization between the two (V700 and V800) scanners for the irradiated films.

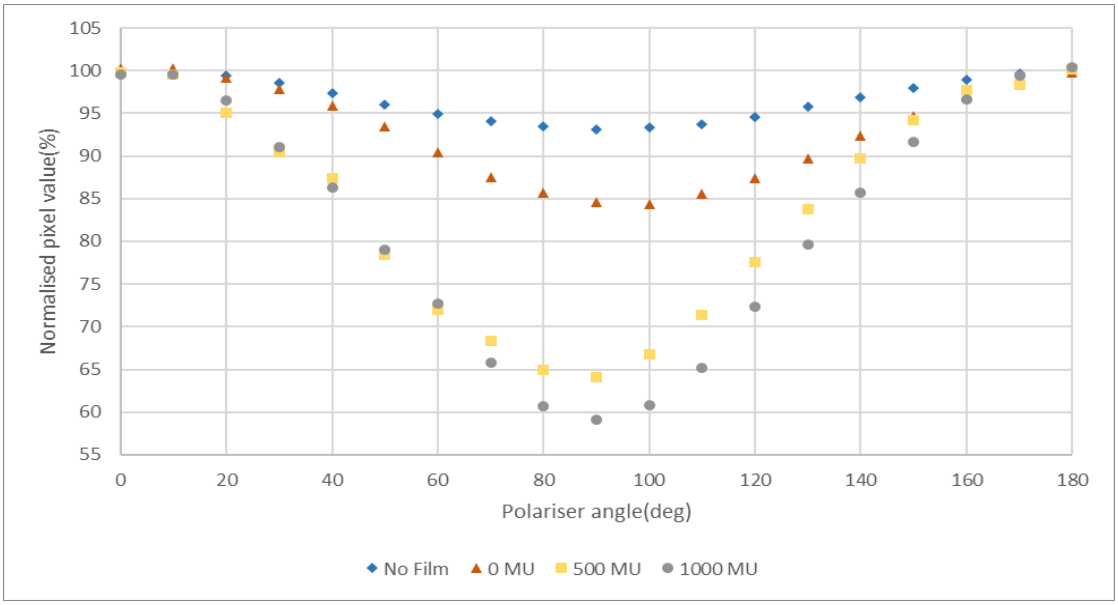

a. V700 scanner

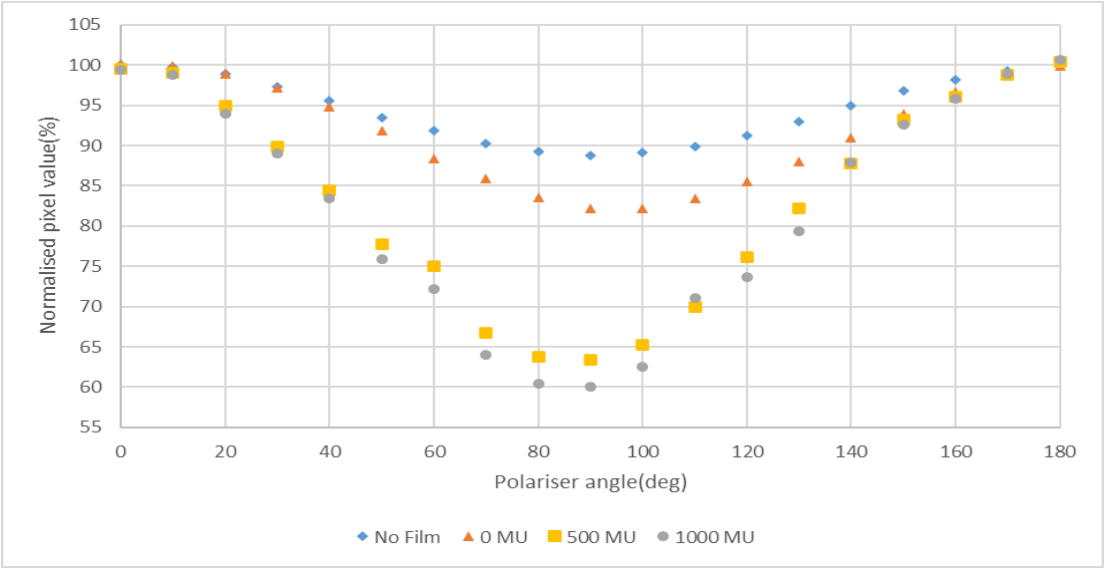

c. V800 scanner

Figure 6-4: Increasing degree of polarization with increasing dose given to the EBT3 film for V700 and V800 scanners.

Figure 6-5 shows the polarization at the centre and 10cm right from the centre of V700 and V800 scanners and with a separate scale the differences. The changes in the degree of polarization at 10cm lateral to the centre are up to 5.7% and 6.9% for V700 and V800 scanners respectively.

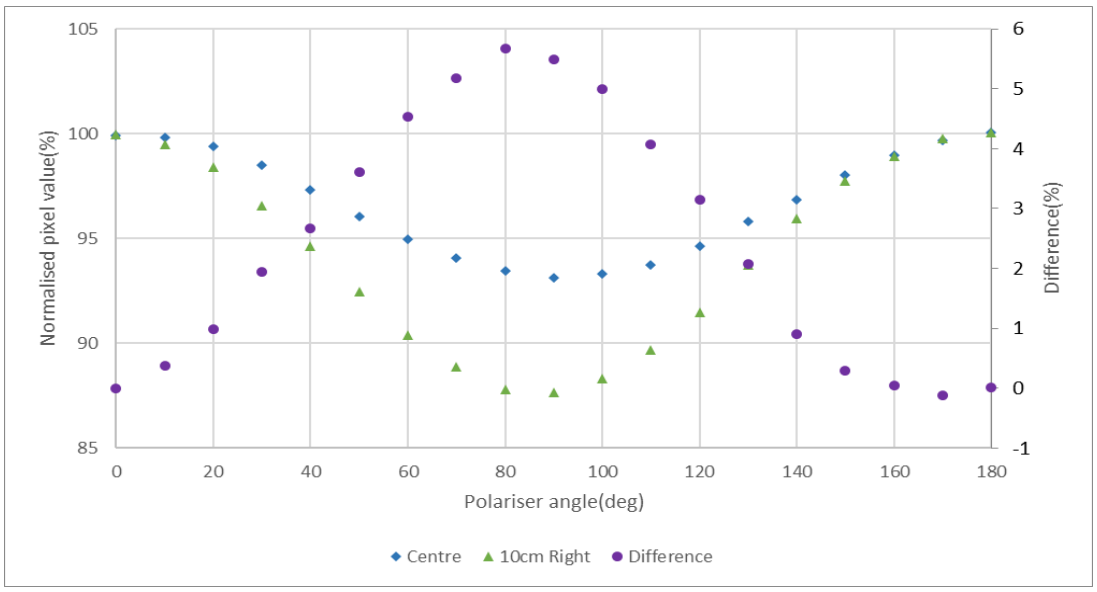

a. V700 scanner

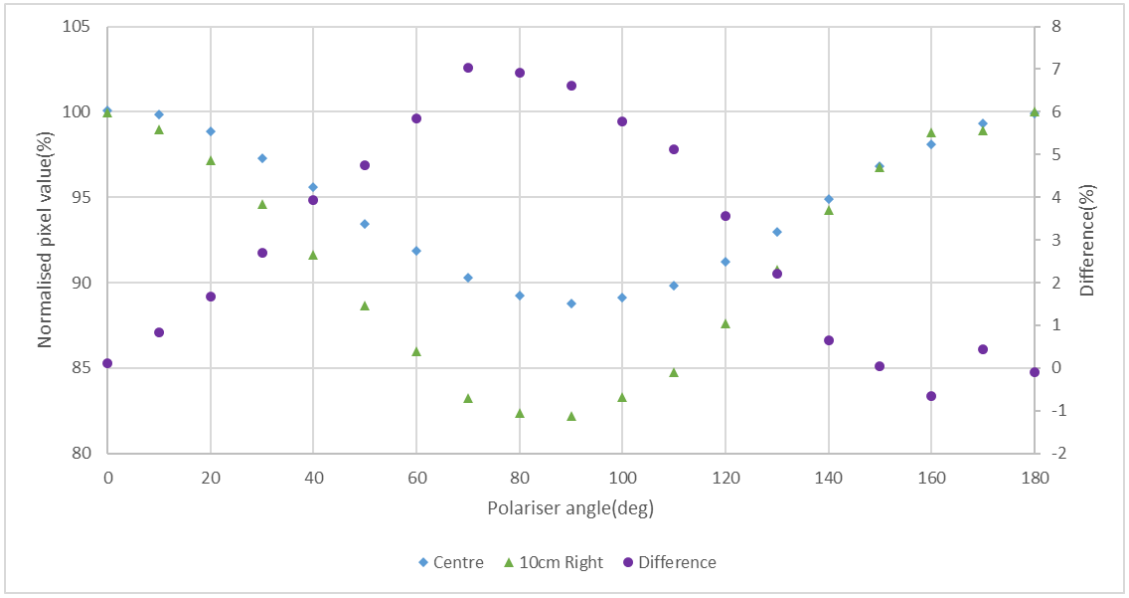

b. V800 scanner

Figure 6-5: Polarization at the centre and 10cm lateral (right) to the centre of V700 and V800 scanner (no film present) and the difference between them.

Figure 6-6 shows the change of pixel values with the change of polariser angle, normalised to the average pixel values with polariser angles of 0º and 180º with only the V700 mirror assembly present, with and without film, and for film only (film irradiated to 500MU). The larger contribution of polarization results from the film.

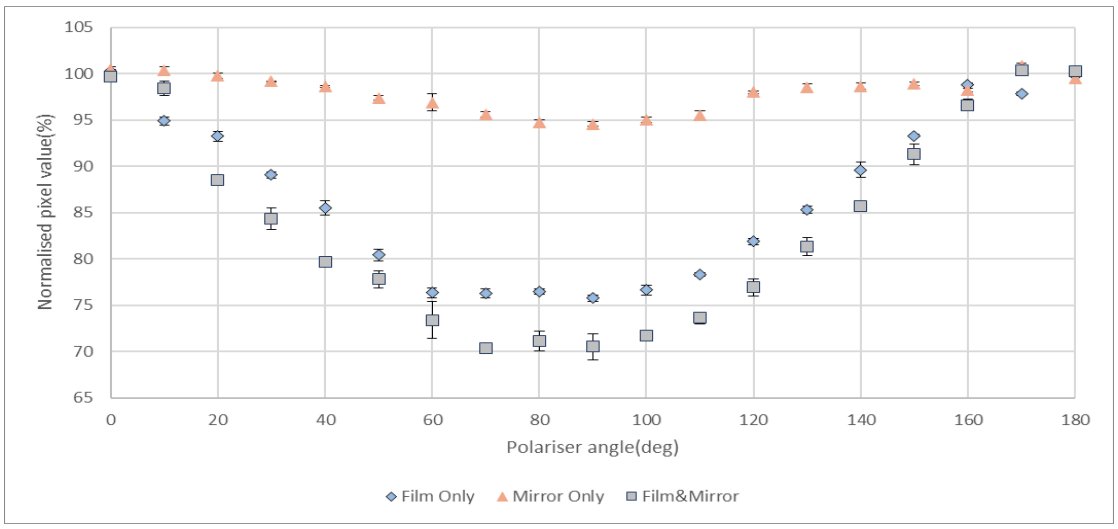

Figure 6-6: Normalised pixel values with respect to polariser angle for V700 mirror system and irradiated (500 MU) EBT3 film.

Figure 6-7 shows the change of pixel values with the change of polariser angle, normalised to the average pixel values with polariser angles of 0º and 180º, using the independent retail-grade mirrors, varying the number of mirrors from 1 to 5, and also without any mirrors present. The pixel values changed by no more than around 1% with polariser angle when there were no mirrors. With the addition of one mirror the results were insignificantly different from the no mirror result. With two and three mirrors the results were almost identical to each other and showed approximately 5% change at the polariser angle of 90º. With the addition of the 4th and 5th mirrors the pixel values changed by approximately 14% at the polariser angle of 90º and were similar for both these numbers of mirrors The results indicate that the mirrors introduce polarisation, and the degree of polarisation depends on the number of mirrors used, but in a pairwise manner.

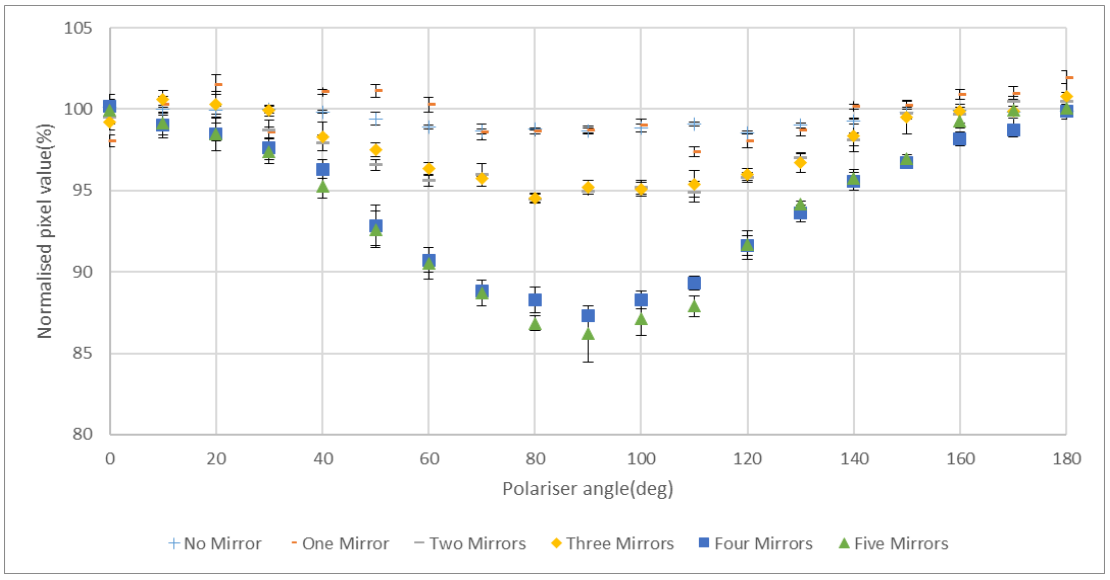

Figure 6-7: Normalised pixel values with respect to polariser angle for varying numbers of mirrors (mirrors only, no film).

Figure 6-8 shows the change of polarization depending on light incident angle on the mirror, rotating mirror 2. With a 30º rotation, polarization remains almost identical to the original orientation but with a 60º rotation, polarization increases significantly.

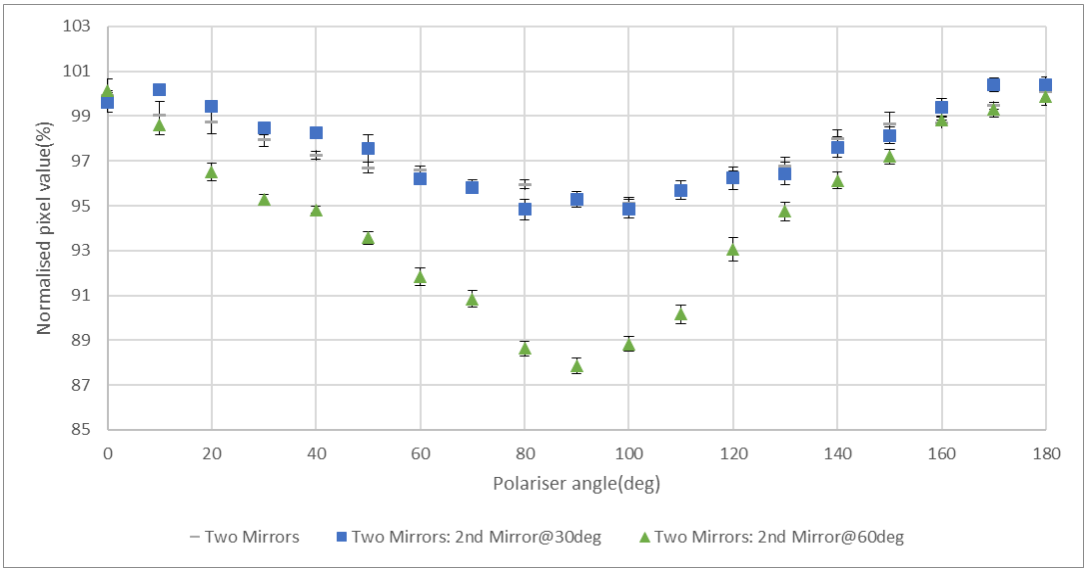

Figure 6-8: Polarization dependence on incident angle of light onto mirror 2 (no film).

6.4 Discussion:

In this study, all the images were separated into three colour channels (RGB) and analysed separately for Red and Green channels. The Blue colour channel was not considered as no previous study was found to recommend it as useful for film dosimetry. All the results reported in this study are for the Red channel as this is the widely used colour channel. All the results of the Green channel followed very similar trends of those for the Red channel and for this reason it was not reported separately.

Path length effect: Figure 2 shows profiles of irradiated film pieces when using different materials as the 'scanner bed' to support the film, including no bed, i.e., equivalent to suspending the film piece in air. A previous study [6] discussed the theory behind a path length effect, which might indicate that any material placed between the light source and imaging system would introduce some degree of path length effect unless the material has similar refractive index to air. So, a piece of film will always have some degree of pathlength effect. The current work aimed to investigate if the scanner bed enhances that effect and whether materials other than the standard glass might change pathlength effects. Profiles were symmetrised, which as explained above does not affect the purpose of this experiment, and compared using different materials as scanner bed to those acquired with the normal glass bed

supplied with the scanner. Differences of up to about 4% were observed using some quite different bed materials. The maximum difference to glass was observed for the laminating pouch, which showed the greatest LRA variation of all the materials tested, at up to 4% difference from glass. Using film as the 'scanner bed' showed differences of up to 2%. The other two alternative materials ('no bed' and acrylic) were observed to be insignificantly different from glass. Since another film piece used as 'bed' has exactly the same refractive index as the experimental film, this may have been expected to show the least variation, or alternatively the 'no bed' option as this introduces nothing else to contribute to the path length effect. The increased LRA, observed for two of the materials (film and laminating pouch), did not result significantly from pathlength effect. The film has rod like crystals and the laminating pouches use EVA glue, which are solid particles at room temperature. In both of these, polarization of light by scattering is a known phenomenon [27,28], which is likely to have occurred here for film or laminating pouch used as substitute beds. The results indicate that using other materials would not improve the scanning system compared to the standard glass scanner bed.

Mirror Effects: Polarization is expected to be caused by the scanner mirror system [6,7,12] and this contributes to the LRA effect. The degree of polarization caused by the different models of flatbed scanners was found to be different. The three models of EPSON flatbed scanners used in this study were found to cause around 7%, 10% and 11% polarization for V700, V850 and V800 scanners respectively (Figure 3). These can be compared to the reported 15% change for a 10000XL scanner [6]. In addition, the polarization was observed to increase with dose to EBT3 film by 20.5% and 25.5% in the V700 scanner and 18.8% and 22.2% in the V800 scanner for 500MU and 1000MU respectively, compared to the 0MU film which itself causes 8.9% in the V700 and 6.6 % in the V800 compared to no film (Figure 4). Increased polarization with dose is in line with the theoretical explanation given by a previous study [26], which explained how active ingredients create bonds with each other upon irradiation, which causes increased polarization and anisotropic scattering. Polarization increases at the 10cm lateral position by 5.5% and 6.6% for V700 and V800 scanners respectively compared to polarization measured at the centre position (Figure 5), with no film present. These increased off-centre values are similar in trend and magnitude with previous work on EPSON 10000XL and EPSON 1680 scanners [6], although not directly quantitatively comparable to the larger scanner and lateral positions used there.

Since the main objective of this study was to investigate the polarization caused by the mirror system only, the mirror assembly of a V700 scanner was taken out and investigated separately using an independent method with the Canon 7D camera for taking images. The result was close to that of the whole V700 scanner (93.1% and 94.6% respectively), indicating that the mirror system makes the greatest contribution to polarization from the complete scanner system. Additionally, the current work considered variable numbers of mirrors from five down to zero,

showing only small polarization with the absence of any mirror system or with only one mirror and increasing polarization as the number of mirrors increased. This supports the potential benefit of having fewer or no mirrors in an optimized measurement system. Light polarization also depends on mirror angle with respect to the light travel path, with large angles contributing more to the effect.

The results show that every scanner type causes a different magnitude of light polarization and that different numbers and angles of mirrors also change the polarization produced. The retail-grade mirrors produced notably greater polarization with four or five mirrors than the complete A4 scanner mirror systems investigated here, although similar to that reported elsewhere for the A3 10000XL scanner [6]. Polarization by reflection from a mirror is complex. When light is reflected from a glass mirror with some coating on one side, light penetrates through the coating to some degree, which means there is refraction involved in the process, which induces some degree of polarization. There are a number of other variables impacting on this, including the birefringence properties of the transparent material, the mirror coating material, thickness and smoothness, the refractive index and also even the presence of dust on the mirror [27–29]. Modelling the polarization by the mirrors used in this investigation is beyond the study's scope. However a possible qualitative explanation of the results of varying the number of mirrors can be proposed. The birefringence property of a transparent material means it works as a waveplate which alters linearly polarised light into circularly/ellipticaly polarised light and vice versa. Light from the original scanner source shows minimal linear polarisation and upon reflection from the first mirror it maintains a similar magnitude of polarization because the glass of the mirror alters the light to circularly/eliptically polarized light which passes through the linear polarizer. The second mirror alters the circularly/elliptically polarized light into linearly polarized light and so on. For these alternate changes, the degree of linear polarization observed would be consistent with the current results, caused by paired mirror groups of no mirror-one mirror, two mirrors-three mirrors and four mirrors-five mirrors. The differences in results between the relatively inexpensive retail grade mirrors (used to test the effect of varying mirror numbers) and the complete scanner mirror systems (4 mirrors) most likely resulted from differences in quality (reflective coating and/or material) of the mirrors.

This study was carried out using an EPSON V700 flatbed scanner as the platform for the scanner bed and mirror-only separate experiments, which might appear as a possible limitation. This was used, as noted, since an older non-clinical V700 scanner was available to be dismantled and modified to enable this work. However, all flatbed scanners have a glass scanner bed and use mirror systems, albeit of varying mirror numbers, to direct the light into a lens system to capture an image. Although this scanner basic platform was used, the mirror numbers and arrangements investigated were representative of other scanners, particularly as different numbers of mirrors were investigated in this work. In addition, for the bed effect measurements, the results are comparative between standard (glass) and modified scanner construction and are

independent of platform. For both sets of investigations and findings, the results are therefore expected to be more generally applicable to other scanner designs.

Based on the outcomes of our previous and current findings, an optimal scanner configuration entails avoiding a lens with a focal length below 50mm [9], maintaining a scanner bed material with a refractive index akin to that of glass (thereby advocating the conventional use of glass due to its additional advantageous attributes for this purpose), and minimizing the presence of mirrors, ideally limiting to none or at most one. If one mirror is used the angle of the mirror with respect to light source has to be equal to or less than 30^{o}. Such a design would minimise LRA effects and the need for LRA corrections and would therefore be expected to increase measurement accuracy. However, adherence to these specifications is also anticipated to result in increased size of a practical scanner design.

6.5 Conclusion:

Two components of flatbed scanners were investigated for their contribution to the LRA effect of a radiochromic film dosimetry system. Scanner bed material can induce further LRA (in addition to the film). The work showed that the conventionally used glass bed is a good choice, comparing LRA considerations against some alternative materials. However, the scanner mirror systems can introduce significant light polarisation which impacts on LRA. The findings clearly indicate that the magnitudes of polarization resulting from different models of EPSON scanners are different and also vary with the number, angles and quality of mirrors used, as well as with dose to the film. Conventionally EPSON flatbed scanners use four or five mirror systems, which were observed to introduce similar magnitudes of light polarisation. With a smaller number of mirrors, smaller effects were observed; a one mirror system had no significant effect on light polarisation. This further supports the conclusions from the work evaluating lens effects in film dosimetry [15], that a re-designed direct imaging system could potentially improve overall film dosimetry by significantly reducing the need for LRA effect corrections and hence associated uncertainties, although this would increase system size. Further work is justified to investigate novel scanner designs and measurement methods.

6.6 References

[1] M. Martišíková, B. Ackermann, O. Jäkel, Analysis of uncertainties in Gafchromic® EBT film dosimetry of photon beams, Phys Med Biol 53 (2008) 7013–7027. https://doi.org/10.1088/0031-9155/53/24/001.

[2] L.J. Van Battum, D. Hoffmans, H. Piersma, S. Heukelom, Accurate dosimetry with GafChromicTM EBT film of a 6 MV photon beam in water: What level is achievable?, Med Phys 35 (2008) 704–716. https://doi.org/10.1118/1.2828196.

[3] B.C. Ferreira, M.C. Lopes, M. Capela, Evaluation of an Epson flatbed scanner to read Gafchromic EBT films for radiation dosimetry, Phys Med Biol 54 (2009) 1073–1085. https://doi.org/10.1088/0031-9155/54/4/017.

[4] T. Kairn, N. Hardcastle, J. Kenny, R. Meldrum, W.A. Tomé, T. Aland, EBT2 radiochromic film for quality assurance of complex IMRT treatments of the prostate: Micro-collimated IMRT, RapidArc, and TomoTherapy, Australas Phys Eng Sci Med 34 (2011) 333–343. https://doi.org/10.1007/s13246-011-0087-z.

[5] M.J. Butson, P.K.N. Yu, T. Cheung, H. Alnawaf, Energy response of the new EBT2 Radiochromic film to X-ray radiation, Radiat Meas 45 (2010) 836–839. https://doi.org/10.1016/j.radmeas.2010.02.016.

[6] L.J. Van Battum, H. Huizenga, R.M. Verdaasdonk, S. Heukelom, How flatbed scanners upset accurate film dosimetry, Phys Med Biol 61 (2015) 625–649. https://doi.org/10.1088/0031-9155/61/2/625.

[7] A.A. Schoenfeld, S. Wieker, D. Harder, B. Poppe, The origin of the flatbed scanner artifacts in radiochromic film dosimetry - Key experiments and theoretical descriptions, Phys Med Biol 61 (2016) 7704–7724. https://doi.org/10.1088/0031-9155/61/21/7704.

[8] A.A. Schoenfeld, S. Wieker, D. Harder, B. Poppe, Changes of the optical characteristics of radiochromic films in the transition from EBT3 to EBT-XD films, Phys Med Biol 61 (2016) 5426–5442. https://doi.org/10.1088/0031-9155/61/14/5426.

[9] T. Shameem, N. Bennie, M. Butson, D. Thwaites, Effect of scanner lens on lateral response artefact in radiochromic film dosimetry, Phys Eng Sci Med (2022). https://doi.org/10.1007/s13246-022-01136-0.

[10] N. Bennie, P. Metcalfe, Practical IMRT QA dosimetry using Gafchromic film: a quick start guide, Australas Phys Eng Sci Med 39 (2016) 533–545. https://doi.org/10.1007/s13246-016-0443-0.

[11] M.J. Butson, T. Cheung, P.K.N. Yu, Scanning orientation effects on Gafchromic EBT film dosimetry, Australas Phys Eng Sci Med 29 (2006) 281–284. https://doi.org/10.1007/BF03178579.

[12] M.J. Butson, T. Cheung, P.K.N. Yu, Evaluation of the magnitude of EBT Gafchromic film polarisation effects.pdf, Australas Phys Eng Sci Med 31 (2009) 21–25.

[13] H. Alnawaf, M.J. Butson, T. Cheung, P.K.N. Yu, Scanning orientation and polarization effects for XRQA radiochromic film, Physica Medica 26 (2010) 216–219. https://doi.org/10.1016/j.ejmp.2010.01.003.

[14] A.A. Schoenfeld, D. Poppinga, D. Harder, K.J. Doerner, B. Poppe, The artefacts of radiochromic film dosimetry with flatbed scanners and their causation by light scattering from radiation-induced polymers, Phys Med Biol 59 (2014) 3575–3597. https://doi.org/10.1088/0031-9155/59/13/3575.

[15] D. Lewis, M.F. Chan, Correcting lateral response artifacts from flatbed scanners for radiochromic film dosimetry, Med Phys 42 (2015) 416–429. https://doi.org/10.1118/1.4903758.

[16] C. Fiandra, U. Ricardi, R. Ragona, S. Anglesio, F. Romana Giglioli, E. Calamia, F. Lucio, Clinical use of EBT model GafchromicTM film in radiotherapy, Med Phys 33 (2006) 4314–4319. https://doi.org/10.1118/1.2362876.

[17] L. Menegotti, A. Delana, A. Martignano, Radiochromic film dosimetry with flatbed scanners: A fast and accurate method for dose calibration and uniformity correction with single film exposure, Med Phys 35 (2008) 3078–3085. https://doi.org/10.1118/1.2936334.

[18] L. Paelinck, W. De Neve, C. De Wagter, Precautions and strategies in using a commercial flatbed scanner for radiochromic film dosimetry, Phys Med Biol 52 (2007) 231–242. https://doi.org/10.1088/0031-9155/52/1/015.

[19] A. Micke, D.F. Lewis, X. Yu, Multichannel film dosimetry with nonuniformity correction.pdf, Med Phys 38 (2011) 2523–2534.

[20] E. Butson, H. Alnawaf, P.K.N. Yu, M. Butson, Scanner uniformity improvements for radiochromic film analysis with matt reflectance backing, Australas Phys Eng Sci Med 34 (2011) 401–407. https://doi.org/10.1007/s13246-011-0086-0.

[21] D. Poppinga, A.A. Schoenfeld, K.J. Doerner, O. Blanck, D. Harder, B. Poppe, A new correction method serving to eliminate the parabola effect of flatbed scanners used in radiochromic film dosimetry., Med Phys 41 (2014) 1–8. https://doi.org/10.1118/1.4861098.

[22] D.F. Lewis, M.F. Chan, On Gafchromic EBT-XD film and the lateral response artefact, Med Phys 43 (2016) 643–649.

[23] B.S. Hiaso, R.S. Stein, K. Deutscher, H.H. Winter, Optical anisotropy of a thermotropic liquid crystalline polymer in transient shear, Journal of Polymer Science 28 (1990) 1571–1588.

[24] T. Shameem, N. Bennie, M. Butson, D. Thwaites, A comparison between EPSON V700 and EPSON V800 scanners for film dosimetry, Phys Eng Sci Med 43 (2020) 205–212. https://doi.org/10.1007/s13246-019-00837-3.

[25] K. Roozen, T. Kron, A. Haworth, R. Franich, Evaluation of EBT radiochromic film using a multiple exposure technique, Australas Phys Eng Sci Med 34 (2011) 281–289. https://doi.org/10.1007/s13246-011-0067-3.

[26] A. Rink, I. Alex Vitkin, D.A. Jaffray, Characterization and real-time optical measurements of the ionizing radiation dose response for a new radiochromic medium, Med Phys 32 (2005) 2510–2516. https://doi.org/10.1118/1.1951447.

[27] G. van Harten, F. Snik, C.U. Keller, Polarization Properties of Real Aluminum Mirrors, I. Influence of the Aluminum Oxide Layer, Publications of the Astronomical Society of the Pacific 121 (2009) 377–383. https://doi.org/10.1086/599043.

[28] E. Hecht, Optics, n.d.

[29] K. Crabtree, Polarization Critical Optical Systems: Important Effects and Design Techniques, 2007.

7 Summary, Conclusions and Future Work

7.1 Summary and conclusion

Radiation therapy is continually incorporating techniques that involve more and more complex treatment methods, with more complex and heterogenous dose distributions and also higher doses per fraction and shorter fractionation. Consequently, the required patient QA needs not only dosimetric accuracy, but also high-resolution geometric accuracy and measurement systems must be 2D and 3D. Radiochromic film dosimetry has the potential of being the dosimetry system of choice, particularly where the measurement situation requires high resolution or flexibility of dosimeter shaping or placement. The most problematic issue with film dosimetry is the lateral response artefact (LRA) (and polarisation which contributes to it), which is systematically investigated here in relation to which parts of flatbed bed scanners contribute to this effect, by how much, and what can be done to minimise it. This in turn could minimise or eliminate the need for LRA corrections and remove the uncertainties in film dosimetry associated with that. Newer and improved films are also compared with existing films to assess their relative performance, including LRA, and to consider how these new films may be better than the older ones for different radiotherapy applications. The work has been published in four papers [1–4], which are reproduced in the thesis as Chapters 3 to 6.

Chapter 3 provides the most popular and widely used radiochromic films for patient QA in radiation therapy are Ashland Gafchromic film products. Chapter 3 provides a comprehensive characterization and comparison of four types of these films, EBT3, EBT4, EBT-XD and MD-V3, two of which are more established and two of which are novel, with little information in the literature. Ashland recommended EBT3 and EBT4 for standard radiotherapy dose ranges, ≤ 10 Gy, and EBT-XD and MD-V3 for higher dose ranges, up to 60 Gy and 100 Gy respectively. EBT4 is the replacement for EBT3, which has been discontinued after introduction of EBT4. As per vendor specification, these two films are identical except EBT4 has better signal to noise ratio (SNR) because of a new type of dye in the active layer. MD-V3 is the newest addition to the Gafchromic family, which has not been extensively studied previously, and whose polymer crystal size and shape is similar to that of EBT-XD. A personal communication from the vendor mentioned that a new type of dye has been used in this film to hinder the bonding process of polymer crystals upon irradiation, which therefore reduces orientation and LRA effects and also reduces LRA increase with dose increase, although the vendor specification/ data sheet does not mention this. From this work's evaluation, EBT4 shows better SNR than that of EBT3, which is expected, as per vendor and other studies which have been carried out during the current work's progress[5–7], but the current work goes further by quantifying this change. Conversely, EBT4 shows larger response change with post-irradiation time than EBT3.

Based on the square shape of provided MD-V3 films and verbal communication from the vendor, there was an assumption that this would show less orientation effect than the other film types. However, this investigation shows that it has a very similar orientation effect to EBT-XD, although these both have much smaller effects than that of EBT3 and EBT4. Until now, all radiochromic films show an increase of LRA with increasing dose. However, MD-V3 is shown to have LRA that does not change with increasing dose, meaning the new dye is effectively suppressing the changing chemical bonding of polymer crystals with dose delivered. At 5 Gy EBT-XD and MD-V3 exhibit identical LRA, which is much smaller than that of EBT3 and EBT4. This stays the same for MD-V3 at other dose levels including 0 Gy (i.e. no dose dependence of LRA for this film type), but changes with dose for all the EBT films. Recommendations from this work include

- EBT4 is a suitable replacement for EBT3 for radiotherapy dosimetry in lower-dose applications, provided that both calibration and clinical timings post-irradiation are kept quite similar, as EBT4 has worse post-irradiation darkening. This latter recommendation is also good practice for all radiochromic film use, i.e. maintain a very similar time gap, between irradiation and scanning, to be applied for all uses of the film, specifically for calibration curve determination and for pre-treatment QA film dosimetry.
- MD-V3 is preferable to EBT-XD for high dose applications, due to its reduced dose dependence of the LRA artifact. MD-V3 and EBT-XD also show more promise for standard radiotherapy dose ranges than the commercial marketing might indicate.

The other contemporaneous studies cited [5–7] above showed that EBT4 has better SNR over EBT3 but did not report on any worse stability of polymerisation in EBT4, which may result in wrong dose calculation if the recommendation made by this work about readout timing is not followed. The current work is also the first investigation on the new feature of MD-V3 film, i.e. of dose independent LRA, which is a clear advantage.

The work presented in Chapter 3 measures key dosimetric properties for these several modern film products, to help clarify how film formulation changes the magnitude and practical significance of LRA and orientation effects and therefore informs the need for film-specific calibration and scanner-film pairing.

Chapter 4 provides comparison of different characteristics of two widely used A4-size flatbed scanner models, EPSON V700 and V800 systems. Both of these scanners use the same lens and mirror system, but with different sensors, being line sensors and matrix sensors for V700 and V800 respectively, and light sources, being white cold cathode fluorescent lamp and white LED for V700 and V800 respectively. Some previous studies compared different type and brands of scanners [8–13] and different scanner size [14,15] from the same vendor, which have different mirror systems and light sources. The two scanners compared here are very similar having the same size, same mirror systems and same lens system and may have been expected to contribute

similarly to the problems of film dosimetry. However, the investigation found differences big enough not to use these scanners interchangeably, even though the lens and mirror systems are the same. The light source and/or sensors have an effect on the responses of the scanners, producing different pixel values in the same colour channels and showing different repeated scan effects, different LRA and different calibration curves. This quantitative comparison of two scanners of quite similar design, but with some specific differences, clearly demonstrates how sensitive the ultimate film dosimetry can be on scanner design and specific components. This strongly indicates that full characterization and commissioning is needed before using an alternative scanner, even if supplied as a direct replacement, and appropriate scanner-specific correction factors need to be obtained.

The work presented in Chapter 4 documents practical, clinically relevant differences between two commonly used Epson flatbed models, quantifies inter-model differences in LRA, orientation dependence, and scanner response, and provides pragmatic guidance for clinical scanner upgrades. It also firmly established the basis for the following investigations of the effects from different specific scanner components.

Chapter 5 provides a quantitative investigation and understanding of the lens effect on LRA. The focal length of the lens system used in the V700 scanner is 38 mm which is quite wide but is necessary in that scanner design to place it close to the mirror system to capture the whole width of the scanner bed. As a result of being so close, it cannot collect all the light from the furthest edges of films. This investigation found that if the lens is kept further away with a lens of larger focal length it can capture more and more light resulting in less and less LRA. The result also shows that if a wider lens is used with smaller focal length the LRA gets bigger. The study concluded that a 50 mm lens would be a reasonable compromise between distance needed and acceptable LRA, as bigger that 50 mm does not improve the LRA much. For example, LRA of an EBT3 film irradiated with 1000 MU is about 8%, in a V700 scanner having 38 mm lens, which reduces to about 2% and 1% for a 50 mm and 100 mm lens respectively. The practical implication of this for re-designed measurement systems would be to use a larger focal length to reduce the LRA effect and hence to reduce the need for (and uncertainties from) making LRA corrections, although this would increase system size. A previous study [16] mentioned that the lens system cannot capture all the light, but it didn't quantify the effect. The current work not only quantifies the effect of the scanner lens system but also recommended a practically suitable lens to be used for minimising the contribution of the lens system to LRA for any future novel design of readout system.

The work presented in Chapter 5 demonstrates that lens optics materially affect lateral non-uniformity, showing that component-level optical design can be a controlling factor in LRA magnitude and shape and thus motivates exploring hardware-informed mitigation strategies to design.

Chapter 6 provides a systematic quantitative investigation on two other components of flatbed scanners, the scanner bed and the mirror system, for their contribution to the LRA effect of a radiochromic film dosimetry system. Scanner bed material can induce further LRA (in addition to the film) if the refractive index is different to that of film. The work showed that the conventionally used glass bed is a good choice, comparing LRA considerations (and practical construction requirements) against some alternative materials. On the other hand, there was a clear indication that mirror systems introduce light polarization, which contributes to LRA. The magnitude of this depends on the number, angles and quality of mirrors used. Conventionally EPSON flatbed scanners use four or five mirror systems, which were observed to introduce similar magnitudes of light polarisation. As the number of mirrors was reduced the magnitude of polarization was reduced. Two previous studies [17,18] mentioned that mirror systems introduce light polarisation. The current work systematically quantifies the light polarisation caused by mirror systems consisting of varying number of mirrors and recommends the optimal number of mirrors that should be used in future novel designs of readout systems to minimise the effect.

The work presented in Chapter 6 extends the component-level analysis from Chapter 5 to polarization effects caused by the scanner mirror system and to the physical scanner bed. This paper separates and quantifies additional scanner contributions to LRA and further demonstrates that multiple scanner subsystems interact with film optical anisotropy to produce the observed artefact. Together with the lens study, it builds a mechanistic picture of scanner-film interactions.

The work presented in Chapters 5 and 6 support investigations of a re-designed direct imaging system, consisting of a lens having focal length of 50 mm or more and with no mirror, (or at most one mirror). This could potentially improve overall film dosimetry by significantly reducing the need for LRA effect corrections and hence associated uncertainties. However, the disadvantage that this would introduce an increase in the size of the imaging system. Further work is justified to investigate novel scanner designs and measurement methods incorporating the findings from these studies.

Overall: The four thesis papers/chapters taken together form a coherent research plan that directly addresses the practical gaps identified in the literature review, as outlined in Section 2.8 (Gap 1 by Chapters 5 and 6; Gap 2 by Chapter 4 and Gap 3 by Chapter 3). They also directly address the research hypotheses laid out in Section 1.8, providing practical data and recommendations on the research questions.

The purpose of this research was to find solutions to help minimize or eliminate LRA in radiochromic film dosimetry for radiotherapy applications, by investigating and evaluating Gafchromic films and relevant scanner components. The research outcomes include recommendations on which currently available films would be optimal for use for different dose

ranges; and which will have less LRA, keeping in consideration other characteristics, e.g. using EBT4 will have better LRA but the user needs to follow a stricter protocol of time gap between irradiation and scanning the film being the same for that used for calibration and QA films. Simply moving to EBT4 from EBT3 with the same protocol could end up with worse results, if that recommendation was not taken into account. This body of work successfully identified the scanner components responsible for the major contributions to LRA and recommended the modifications needed to minimize the contribution in future works on redesigning novel readout systems.

In summary, these studies and their findings form a systematic linked programme to meet the aims and research questions: (a) to provide a clear example quantifying the practical scanner differences clinics will face when they change hardware; (b) to determine which scanner components drive LRA so that corrections and/or new designs can be physically motivated rather than purely empirical; and (c) to re-evaluate how modern film chemistries modify scanner artefacts and together impact on the consequent uncertainty budget in clinical use. This combination of component-level scanner physics plus inter-scanner comparison plus re-characterisation of new film generations supports clinical film dosimetry practice in radiotheray, by better understanding the causes and magnitudes of uncertainties in practical use and by consequent recommendations on ways to improve them.

7.2 Future work:

Though Ashland recommended EBT-XD and MD-V3 for high dose radiation therapy, it appeared from this work that those could be used in the standard dose range as well. Several studies [19–24] found EBT-XD provides better results than EBT3 in patient QA. Further work is needed to compare MD-V3 with EBT-XD and EBT4 for patient QA with different dose ranges. This film (MD-V3) might prove to be very useful, as this work shows the LRA of MD-V3 does not change with increasing dose. In addition, these newer films require further work to test their performance for other radiation modalities and energies. EBT4 keeps darkening over longer periods of time of several days, which could be a problem unless a strict protocol is used to ensure the same time gap between irradiation and scan is used during film calibration and also for patient QA or other clinical measurements. This could be avoided with MD-V3 and EBT-XD, as darkening reaches a plateau after about 10 hours for these films. MD-V3 is a good candidate to be used in radiotherapy patient QA in all dose ranges. Further studies are needed to independently confirm its efficacy in as wide a range of applications as necessary for practical use.

Though V700 and V800 use the same lens and mirror system, those do not show the same characteristics, as the sensor and light source are different. It is not immediately clear how much these two components are responsible separately for these differences. The light sources and sensors along with any other possible differences need to be investigated separately to clarify

this and similar studies could be carried out on other scanners to identify best systems for use in radiotherapy film dosimetry to minimize additional uncertainties and provide guidance when changing between conventional flatbed scanners.

The studies, taken together, indicate that an imaging system could be designed having a 50 mm lens, one or no mirrors and a well-designed sensor and light source combination, which might reduce the LRA effect to low enough to not require significant correction factors. Further work is suggested to develop and test prototype designs to incorporate these recommendations. Combined with a lower LRA film and particularly one that does not have significantly enhanced LRA as dose levels increase, such as MD-V3, which also has shorter darkening plateau times, this would make film dosimetry simpler to use and reduce its uncertainties. This would provide a dependable, easy to use, high resolution, lower uncertainty dosimetry system for fast changing complex radiotherapy patient QA.

7.3 References

[1] T. Shameem, N. Bennie, M. Butson, D. Thwaites, Comparative characterisation of different types of Gafchromic films for radiotherapy use, Phys Eng Sci Med (2025). https://doi.org/10.1007/s13246-025-01596-0.

[2] T. Shameem, N. Bennie, M. Butson, D. Thwaites, A comparison between EPSON V700 and EPSON V800 scanners for film dosimetry, Phys Eng Sci Med 43 (2020) 205–212. https://doi.org/10.1007/s13246-019-00837-3.

[3] T. Shameem, N. Bennie, M. Butson, D. Thwaites, Effect of scanner lens on lateral response artefact in radiochromic film dosimetry, Phys Eng Sci Med (2022). https://doi.org/10.1007/s13246-022-01136-0.

[4] T. Shameem, N. Bennie, M. Butson, D. Thwaites, Effect of mirror system and scanner bed of a flatbed scanner on lateral response artefact in radiochromic film dosimetry, Phys Eng Sci Med (2024) 1651–1663. https://doi.org/10.1007/s13246-024-01478-x.

[5] A.L. Palmer, D. Nash, W. Polak, S. Wilby, Evaluation of a new radiochromic film dosimeter, Gafchomic EBT4, for VMAT, SABR and HDR treatment delivery verification, Phys Med Biol 68 (2023) 0–11. https://doi.org/10.1088/1361-6560/aceb48.

[6] F. Guan, H. Chen, E. Draeger, Y. Li, R. Aydin, C. J.Tien, Z. Chen., Characterization of Gafchromic EBT4 film with clinical kV/MV photons and MeV electrons, Prec Radiat Oncol. 7 (2023) 84–91. https://doi.org/10.1002/pro6.1204.

[7] Y. Akdeniz, Comparative analysis of dosimetric uncertainty using GafchromicTM EBT4 and EBT3 films in radiochromic film dosimetry, Radiation Physics and Chemistry 220 (2024). https://doi.org/10.1016/j.radphyschem.2024.111723.

[8] G.R. Gluckman, L.E. Reinstein, Comparison of three high-resolution digitizers for radiochromic film dosimetry, Med Phys 29 (2002) 1839–1846. https://doi.org/10.1118/1.1485056.

[9] S. Devic, J. Seuntjens, G. Hegyi, E.B. Podgorsak, C.G. Soares, A.S. Kirov, I. Ali, J.F. Williamson, A. Elizondo, Dosimetric properties of improved GafChromic films for seven different digitizers, Med Phys 31 (2004) 2392–2401. https://doi.org/10.1118/1.1776691.

[10] T. Aland, E. Jhala, T. Kairn, J. Trapp, Film dosimetry using a smart device camera: A feasibility study for point dose measurements, Phys Med Biol 62 (2017) N506–N515. https://doi.org/10.1088/1361-6560/aa8b36.

[11] M.A. Piliero, F. Pupillo, S. Presilla, A diffuse reflectance spectrophotometer for radiation dosimetry of EBT3 GAFchromic films, Radiat Meas 154 (2022) 106777. https://doi.org/10.1016/j.radmeas.2022.106777.

[12] B.S. Rosen, C.G. Soares, C.G. Hammer, K.A. Kunugi, L.A. Dewerd, A prototype, glassless densitometer traceable to primary optical standards for quantitative radiochromic film dosimetry, Med Phys 42 (2015) 4055–4068. https://doi.org/10.1118/1.4922134.

[13] M.K. Ranade, J.G. Li, R.S. Dubose, J. Kozelka, W.E. Simon, J.F. Dempsey, A prototype quantitative film scanner for radiochromic film dosimetry, Med Phys 35 (2008) 473–479. https://doi.org/10.1118/1.2828203.

[14] H. Alnawaf, P.K.N. Yu, M. Butson, Comparison of Epson scanner quality for radiochromic film evaluation, J Appl Clin Med Phys 13 (2012) 314–321. https://doi.org/10.1120/jacmp.v13i5.3957.

[15] J.M. Lárraga-Gutiérrez, O.A. García-Garduño, C. Treviño-Palacios, J.A. Herrera-González, Evaluation of a LED-based flatbed document scanner for radiochromic film dosimetry in transmission mode, Physica Medica 47 (2018) 86–91. https://doi.org/10.1016/j.ejmp.2018.02.010.

[16] A.A. Schoenfeld, D. Poppinga, D. Harder, K.J. Doerner, B. Poppe, The artefacts of radiochromic film dosimetry with flatbed scanners and their causation by light scattering from radiation-induced polymers, Phys Med Biol 59 (2014) 3575–3597. https://doi.org/10.1088/0031-9155/59/13/3575.

[17] L.J. Van Battum, H. Huizenga, R.M. Verdaasdonk, S. Heukelom, How flatbed scanners upset accurate film dosimetry, Phys Med Biol 61 (2015) 625–649. https://doi.org/10.1088/0031-9155/61/2/625.

[18] A.A. Schoenfeld, S. Wieker, D. Harder, B. Poppe, The origin of the flatbed scanner artifacts in radiochromic film dosimetry - Key experiments and theoretical descriptions, Phys Med Biol 61 (2016) 7704–7724. https://doi.org/10.1088/0031-9155/61/21/7704.

[19] A.L. Palmer, A. Dimitriadis, A. Nisbet, C.H. Clark, Evaluation of Gafchromic EBT-XD film, with comparison to EBT3 film, and application in high dose radiotherapy verification, Phys Med Biol 60 (2015) 8741–8752. https://doi.org/10.1088/0031-9155/60/22/8741.

[20] M.P. Grams, J.M. Gustafson, K.M. Long, L.E.F. de los Santos, Initial characterization of the new EBT-XD Gafchromic film, Med Phys 42 (2015) 5782–5786.

[21] A.A. Schoenfeld, S. Wieker, D. Harder, B. Poppe, Changes of the optical characteristics of radiochromic films in the transition from EBT3 to EBT-XD films, Phys Med Biol 61 (2016) 5426–5442. https://doi.org/10.1088/0031-9155/61/14/5426.

[22] H. Miura, S. Ozawa, F. Hosono, N. Sumida, T. Okazue, K. Yamada, Y. Nagata, Gafchromic EBT-XD film: Dosimetry characterization in high-dose, volumetric-modulated arc therapy, J Appl Clin Med Phys 17 (2016) 312–322. https://doi.org/10.1120/jacmp.v17i6.6281.

[23] D.F. Lewis, M.F. Chan, On Gafchromic EBT-XD film and the lateral response artefact, Med Phys 43 (2016) 643–649.

[24] S. Khachonkham, R. Dreindl, G. Heilemann, W. Lechner, H. Fuchs, H. Palmans, D. Georg, P. Kuess, Characteristic of EBT-XD and EBT3 radiochromic film dosimetry for photon and proton beams, Phys Med Biol 63 (2018). https://doi.org/10.1088/1361-6560/aab1ee.